IDENTIFICATION AND CHARACTERIZATION OF INTERMEDIATE FILAMENT BINDING PROTEINS IN THE NERVOUS SYSTEM

By

LAURA DIANE ERRANTE

A DISSERTATION PRESENTED TO THE GRADUATE SCHOOL
OF THE UNIVERSITY OF FLORIDA IN PARTIAL FULFILLMENT
OF THE REQUIREMENTS FOR THE DEGREE OF
DOCTOR OF PHILOSOPHY

UNIVERSITY OF FLORIDA

1994

To *my parents*, with whom I realized how much I could accomplish if only I try,
and to *my dearest Gator*, who would never let me lose sight of my dreams.

ACKNOWLEDGEMENTS

Although it is now time to begin anew, I will never forget the people I have met that have made the past six years a learning experience. Foremost I would like to thank Dr. Gerry Shaw, my advisor, who showed me, through his example, that although it may be difficult at times to do bench work, that this is why we become scientists in the first place. In addition, I appreciate his patience, especially in allowing me to develop my own sense of independence. I would like to acknowledge my committee members, Dr. Barabara Battelle, Dr. Kevin Anderson, and Dr. Daniel Purich, for their insight and support on my doctoral work. I would like to credit Dr. Luttge for having the wisdom 5 years ago to let me know that although I was having difficult times, I still had the ability to become a good scientist. I only hope that the present and future graduate students in the department will benefit from his wisdom as I have over these years. It is easiest to remember to thank the people who have had direct input on your research; however, I would like to give special thanks to Dr. Roger Heintz, my undergraduate advisor at SUNY Plattsburgh, for instilling in me the basics of learning techniques, especially column chromatography which has been essential to my dissertation research, and for his encouragement to enter a field of study that can be intimidating at times but is always fascinating and rewarding.

There are a number of graduate students and staff that have made an

indulible impression on me. In particular I will always treasure my friendships with Paul Bao, Michele Davda, Bunnie Powell, and Margaret Tremwel. I would like to acknowledge my family, especially my mom and brother, Wayne, who may not have an understanding of what I have been doing the past six years but have supported me just the same, no matter how infrequently they heard from me.

It has been a long and sometimes twisted road to reach this point, and I am fortuitous to have found a true friend in Rob Friedman. Even when I thought all was lost, his constant and unconditional support as well as critical assessment of my research, enable me to envision the "light at the end of tunnel" and make my dissertation a reality.

This work was supported by a NIH Predoctoral Training Fellowship MH15737 through the Center for Neurobiological Sciences at the University of Florida and NIH NS22695 (to Dr. Gerry Shaw). In addition, I would like to thank the Center for Neurobiological Sciences at the University of Florida for providing funds to attend scientific meetings.

TABLE OF CONTENTS

ACKNOWLEDGEMENTS iii

LIST OF TABLES viii

LIST OF FIGURES ix

LIST OF ABBREVIATIONS xii

ABSTRACT xiv

CHAPTERS

1 INTRODUCTION AND BACKGROUND 1

- Cytoskeleton 1
- Intermediate Filament Family of Proteins 2
- Neurofilament Assembly 8
- NF Phosphorylation 11
- Interactions Between Neurofilaments and Microtubules 18
- Neurofilaments Interact with Other Cellular Components 21
- Relationship of NFs to Axonal Transport and Caliber 26
- NF Expression After Axotomy 30
- Role of NFs in Disease States 32
- Overview of Dissertation 34

2 GENERAL METHODS 36

- Biochemical Techniques 36
  - Protein Assay 36
  - SDS Polyacrylamide Gels 37
  - Electroblotting of Proteins 38
  - Immuno-Blot Analysis 39
  - Protein Cleavage with Cyanogen Bromide 40
- Isolation of Neurofilament Proteins 41
  - Crude Intermediate Filament Preparation 41
  - Neurofilament Preparation 42
  - Purification of Individual Neurofilament Subunits 43

Anatomical Localization Experiments 44
  Dorsal Root Ganglion Cell Cultures 44
  Pheochromocytoma Cells (PC12 Cells) 45
  Immunofluorescent Studies on Fresh Frozen Tissue 46
  Immunocytochemistry on Formaldehyde Fixed Tissue 47

3 THE DISTRIBUTION OF PLECTIN, AN INTERMEDIATE FILAMENT BINDING PROTEIN, IN THE ADULT RAT CENTRAL NERVOUS SYSTEM 49

Introduction 49
Methods 50
Results 52
  Immunoblot Studies 52
  Comparison of Plectin to IFAP-300 56
  Localization Studies 59
Discussion 70
Notes 78

4 CO-LOCALIZATION OF PLECTIN AND INTERMEDIATE FILAMENTS IN THE RAT NERVOUS SYSTEM 79

Introduction 79
Methods 80
Results 82
  Immunoblot Studies 82
  Co-localization in Cultured Cells 82
  Co-localization Studies Along the Rat Neural Axis 90
  Effects of Peripheral Nerve Axotomy 97
Discussion 105
Notes 115

5 IDENTIFICATION OF NF BINDING PROTEINS 116

Introduction 116
Methods 117
  Pig Spinal Cord Cytosolic Preparation 117
  Affinity Column Preparation 117
  Binding of Cytosolic Proteins to Affinity Columns 118
  Production of Polyclonal and Monoclonal Antibodies 121
Results 122
Discussion 138

6 CHARACTERIZATION OF GAPDH BINDING TO NFs 144
Introduction 144
Methods 145
Co-sedimentation Experiments 145
Immunofluorescence Studies 146
Antibodies 146
Results 147
Co-sedimentation Experiments 147
Immunofluorescence Studies in Cultured Cells 154
Discussion 161

7 OVERALL DISCUSSION 165
General Considerations 165
Criteria for Classifying IF Binding Proteins 165
Relationship between Plectin and NF Proteins 166
The Role of GAPDH in the Nervous System 168
Future Direction 170
Conclusions 173

REFERENCES 174

BIOGRAPHICAL SKETCH 191

LIST OF TABLES

Table 1-1 Mammalian intermediate filament protein family based on the classification scheme of Steinert and Roop (1988) 2

Table 1-2 Protein kinases which phosphorylate neurofilaments *in vitro* .. 14

Table 1-3 Interactions of neurofilaments with other cellular components . 22

Table 3-1 The distribution of plectin in different cell types of the adult rat central nervous system 76

Table 4-1 Summary of the distribution of plectin in different cell types of the adult rat nervous system with respect to intermediate filament proteins 111

Table 5-1 Relative molecular weight (kD) of candidate proteins which bound to the five different types of NF affinity columns 123

Table 5-2 Amino acid composition for candidate neurofilament binding proteins with the data represented as nanomole percent 127

Table 5-3 Results from the FINDER program to identity NFL-38 131

Table 5-4 Comparison of NFL-38 to GAPDH with data represented as nanomole percent for each amino acid 132

LIST OF FIGURES

Figure 1-1 Schematic of neural intermediate filament protein sequences . 5

Figure 3-1 Identification of a 300 kD protein in bovine and rat crude IF spinal cord preparations 55

Figure 3-2 Comparison of amino acid composition of plectin and IFAP-300 proteins 58

Figure 3-3 Plectin immunoreactivity (ID8) of astrocytes in white and gray matter of the telencephalon and diencephalon 61

Figure 3-4 Plectin immunoreactivity (ID8) in the rostral hypothalamus surrounding the third ventricle (3V) as visualized with DAB . . 64

Figure 3-5 Plectin immunoreactivity (IA2 and ID8) in the cerebellum . . . 66

Figure 3-6 Plectin immunoreactivity (ID8) in the caudal brainstem 69

Figure 3-7 Plectin immunoreactivity (ID8) in the cervical spinal cord 72

Figure 3-8 Plectin immunoreactivity (p21) in choroid plexus and blood vessels 74

Figure 4-1 Characterization of peripherin polyclonal and monoclonal antibodies 84

Figure 4-2 Co-localization of plectin (p21) and vimentin (V9) in non-neuronal cells from DRG cultures 87

Figure 4-3 Co-localization of plectin (ID8) and NF subunits in DRG cells and PC12 cells 89

Figure 4-4 Co-localization experiment with antibodies to plectin (p21) (A,C,E,G) and vimentin (V9) (B,D,F,H) 93

Figure 4-5 Co-localization experiment with antibodies to plectin (A,C,E) and GFAP (B,D,F) 95

Figure 4-6 Co-localization experiment with antibodies to plectin (ID8) (A,C,E) and NFs (polyclonal) (B,D,F) 99

Figure 4-7 Co-localization experiment with antibodies to plectin (IA2) (A,C) and peripherin (R19) (B,D) 101

Figure 4-8 Effects of a unilateral facial nerve axotomy on plectin immunoreactivity (1A2) 104
Figure 4-9 Co-localization experiment with plectin (IA2) (A,C) and NF-H (R14) (B,D) after a unilateral facial nerve axotomy 107
Figure 4-10 Co-localization experiment with plectin(IA2) (A,C) and peripherin (R20) (B,D) after a unilateral facial nerve axotomy 109
Figure 5-1 Outline of the method used for identifying candidate NF binding proteins 120
Figure 5-2 Comparison of candidate 38 kD NF binding protein to rod domain of IF proteins 126
Figure 5-3 Comparison of amino acid composition data between NFL-38 and IF-38, and to that of the average amino acid composition in Genbank 130
Figure 5-4 Comparison of CNBr cleavage fragments of NFL-38 and GAPDH 135
Figure 5-5 Immunoblot analysis using antibodies to GAPDH to determine if the 38 kD proteins binding to various NF affinity columns is GAPDH 137
Figure 5-6 Graphical representation of the amino acid composition data for NFL-16, and possible matches as determined by the FINDER program 140
Figure 5-7 Graphical representation of the amino acid composition data for NFL-62, and to that of the average amino acid composition in Genbank 142
Figure 6-1 Co-sedimentation experiment with GAPDH and NF subunits 149
Figure 6-2 Co-sedimentation of GAPDH and NF-L with different concentrations of GAPDH 151
Figure 6-3 Co-sedimentation of GAPDH and NF-L with different concentrations of sodium chloride 153
Figure 6-4 Composite of GAPDH antibody labelling (ID4) of a DRG cultured neuron 156
Figure 6-5 Co-localization experiment in DRG cell cultures with antibodies to GAPDH (ID4) (A,C) and NF-H (R14) (B,D) . . . 158

Figure 6-6 Co-localization experiment in differentiated PC12 cell cultures with antibodies to GAPDH (ID4) (A,B) and NF-M (R9) (C) 160

Figure 6-7 Co-localization experiment in DRG cell cultures with antibodies to GAPDH (ID4) (A) and actin (polyclonal) (B) . . 163

LIST OF ABBREVIATIONS

Amino Acids
- ALA or A - alanine
- ARG or R - arginine
- ASN or N - asparagine
- ASP or D - aspartic acid
- ASX or Z - asparagine and/or aspartic acid
- CYS or C - cysteine
- GLN or Q - glutamine
- GLU or E - glutamic acid
- GLX or B - glutamine and/or glutamic acid
- GLY or G - glycine
- HIS or H - histidine
- ILE or I - isoleucine
- LEU or L - leucine
- LYS or K - lysine
- MET or M - methionine
- PHE or F - phenylalanine
- PRO or P - proline
- SER or S - serine
- THR or T - threonine
- TRP or W - tryptophan
- TYR or Y - tyrosine

BBB - blood-brain barrier

BSA - bovine serum albumin

CBB - Coomassie brillant blue R-250

CNBr - cyanogen bromide

CNS - central nervous system

CSF - cerebrospinal fluid

DAB - diaminobenzidine tetrahydrochloride

DRG - dorsal root ganglion

DTT - dithiothreitol

EDTA - ethylenediamine tetraacetic acid

FBS - fetal bovine serum
GAPDH - glyceraldehyde-3-phosphate dehydrogenase
GFAP - glial fibrillary acidic protein
GST - glutathione S-transferase
IF - intermediate filament
IFAP - intermediate filament associated protein
kD - kiloDaltons
MES - 2-(4-morpholino)-ethanesulfonic acid
MT - microtubule
NF - neurofilament
NF-H - neurofilament high molecular weight subunit
NF-M - neurofilament middle molecular weight subunit
NF-L - neurofilament low molecular weight subunit
TBS - tris buffered saline
PBS - phosphate buffered saline
PMSF - phenylmethyl-sulfonyl fluoride
PNS - peripheral nervous system
PVDF - polyvinylidine difluoride
SDS - sodium dodecyl sulfate
TAME - Nα-p-toluenesulfonyl-L-arginine methyl ester

Abstract of Dissertation Presented to the Graduate School
of the University of Florida in Partial Fulfillment of the
Requirements for the Degree of Doctor of Philosophy

IDENTIFICATION AND CHARACTERIZATION OF INTERMEDIATE FILAMENT BINDING PROTEINS IN THE NERVOUS SYSTEM

By

LAURA DIANE ERRANTE

April 1994

Chairperson: Gerard P. J. Shaw
Major Department: Neuroscience

Neurofilaments (NFs), microfilaments (MFs) and microtubules (MTs) are the major structural proteins that form the neuronal cytoskeleton. Much more is understood about the function of MFs and MTs than is known for NFs. This dissertation research characterized, plectin, a known intermediate filament associated protein (IFAP) in the nervous system, and searched for candidate NF binding proteins in order to examine possible roles for NFs.

Plectin distribution was examined throughout the rat CNS. Plectin was localized to non-neuronal cells with particularly strong immunoreactivity in cells forming ventricular and pia barriers. In addition, plectin immunoreactivity was observed in select motoneurons. Double-label studies with plectin and IF proteins demonstrated that plectin's distribution most closely resembled that for vimentin;

however, the staining patterns were not mutually inclusive. In select motoneurons, plectin colocalized with the neural IF proteins, NF triplet proteins and peripherin. Since plectin and NFs co-exist in the same cell, the previously described *in vitro* plectin/NF interactions may be functionally important.

The second part of the dissertation project involved identifying a 38 kD protein which bound to NF affinity columns. Using a computer program, FINDER, and biochemical analysis, this protein was identified as glyceraldehyde-3-phosphate dehydrogenase (GAPDH). The strength of binding between GAPDH and NF-L subunit was shown to be relatively weak with a dramatic decrease in the amount of protein co-pelleting at 0.05 M sodium chloride. The possible *in vivo* interaction between NFs and GAPDH was examined using fluorescent light microscopy which showed that GAPDH was localized throughout the cell body and processes of dorsal root ganglion cells in culture and differentiated PC12 cells. Although GAPDH immunoreactivity colocalized in part with NF antibody labelling, the immunofluorescent labelling patterns were distinct.

A number of proteins were identified which bound with varying specificity to NFs *in vitro* and have a potential of interacting with NFs *in vivo.* Finding that NFs may interact, *in vivo*, in some neurons with plectin and GAPDH suggests that certain NF proteins may act as important structural elements during neuronal injury, and as docking substrates for the localization of glycolytic enzymes.

CHAPTER 1

INTRODUCTION AND BACKGROUND

Cytoskeleton

The cytoskeleton is a three-dimensional network of fibrous proteins found throughout the cytoplasm. The neuronal cytoskeleton is composed of microtubules (MTs), microfilaments (MFs) and neurofilaments (NFs). MTs and MFs have been well characterized in both neuronal and non-neuronal cells, and both have been shown to have a variety of roles in cell structure and motility. In contrast, very little is understood about the functional role of NFs (Fliegner and Liem, 1991; Shaw, 1991). NFs are primarily thought of as static structures ensuring mechanical stability to the neuron and governing the diameter of the axon (Hoffman et al., 1984). However, changes in phosphorylation state of NFs during development and regeneration indicate that NFs may play a more active role in neuronal function. This chapter will describe pertinent information concerning NF structure, assembly, phosphorylation, interactions with other proteins, and NFs involvement in axonal transport and caliber. The last part of this chapter will discuss the effects on NF proteins of axotomy and neuronal diseases which may indicate possible functions for these neural intermediate filaments.

Intermediate Filament Family of Proteins

NFs belong to a family of intermediate filament (IF) proteins which are 10 nm diameter. The IF family is currently grouped into 6 classes of proteins based on protein sequence similarity and intron placement (Table 1-1).

Table 1-1. Mammalian intermediate filament protein family based on the classification scheme of Steinert and Roop (1988).

Class	Name	MW (kD)	Cellular Location
I	Keratin (acidic)	40-60	epithelial cells and epidermal derivatives (eg. nails and hair)
II	Keratin (basic)	50-70	" "
III	Desmin	52	muscle cells
	Vimentin	57	cells of mesenchymal origin
	GFAP[•]	51	astrocytes; some schwann cells
	Peripherin	57	neurons
IV	NF-triplet proteins		
	NF-H[¶]	115	neurons
	NF-M[§]	95	"
	NF-L[¥]	60	"
	α-Internexin	66	"
V	Nuclear Lamins	60-70	nuclear lamina of all cells
IV	Nestin	200	neural epithelial stem cells

[•] GFAP: glial fibrillary acidic protein; [¶] NF-H: NF high molecular weight protein; [§] NF-M: NF middle molecular weight protein; [¥] NF-L: NF low molecular weight protein

A number of IF proteins are localized to neurons. The classical NFs, NF triplet proteins, are found in varying concentration in most nerve cells. (Liem et al., 1978; Yen and Fields, 1981; Shaw et al., 1981). In addition to the NF triplet protein, α-internexin and peripherin are localized to a more select set of neurons and have been shown to co-localize with NF-triplet protein (Kaplan et al., 1990; Parysek et al., 1991). α-Internexin is distributed predominantly in the central nervous system (CNS) (Pachter and Liem, 1985; Chiu et al., 1989). Peripherin is localized mainly in the peripheral nervous system (PNS) (Portier et al., 1984a, 1984b), but is found also in select fiber tracks and perikarya of neurons throughout the CNS (Parysek and Goldman, 1988; Brody et al., 1989). Although vimentin is primarily thought to associate with non-neuronal cells, it is localized in developing neurons and is expressed in mature neurons in the olfactory epithelium (Schwob et al., 1986) and adult retina (Draeger, 1983). Nestin, a newly described protein assigned to class VI, is widely expressed in neuroepithelial stem cells which are the precursors of CNS neurons and glia (Hockfield and McKay, 1985; Frederiksen and McKay, 1988; Lendahl et al., 1990).

IFs, in general, have a fundamental structure comprised of 3 domains: (1) amino-terminal head; (2) central α-helical rod domain; and (3) variable carboxyl-terminal tail (Figure 1.1). The amino-terminal head domain is typically a short globular peptide sequence of 5-7 kD containing numerous basic amino acids (Geisler et al.,1982). However, the amino-terminal domain of nestin is only 11 amino acids long and is slightly acidic (Lendahl et al., 1990). The central rod domain (39 kD) contains a highly conserved heptad repeat of hydrophobic amino acids that allows for the formation of an α-helical coiled-coil structure (Geisler et al., 1982). The distinct primary amino acid sequence of the rod domain is proposed to be the driving force of IF protein self-assembly (Steinert and Roop,

Figure 1-1. Schematic of neural intermediate filament protein sequences.

Intermediate filaments can by divided into 3 domains: (1) amino-terminus head domain; (2) α-helical rod domain; and (3) variable carboxyl-terminus domain. Each of these domains can be divided into regions based on repeated sequence or abundance of a amino acids in that region. These regions are denoted with the single letter code for the amino acids. E: glutamic acid; K: lysine; P: proline.

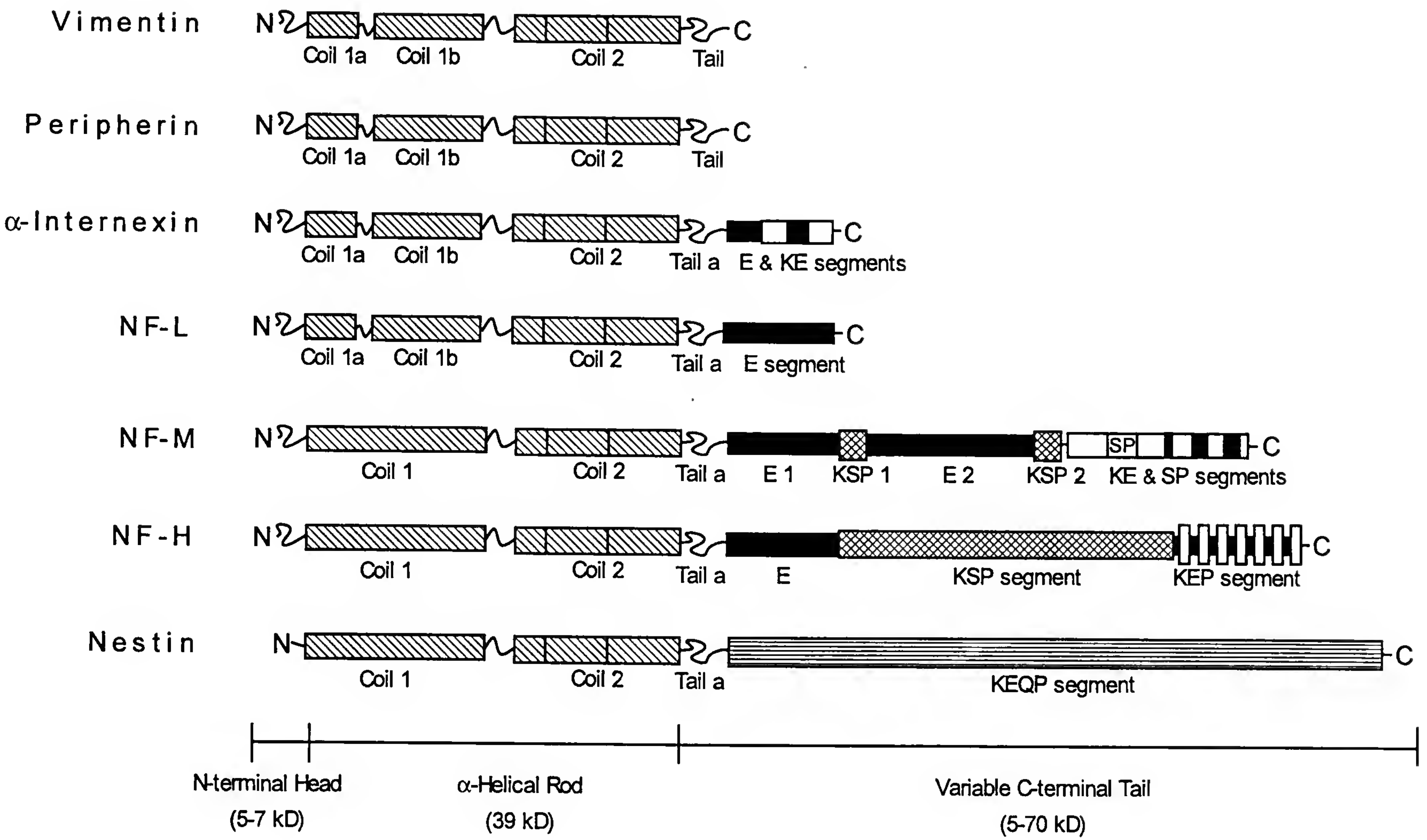
Vimentin
N
Coil 1a
Coil 1b
Coil 2
Tail
C
Peripherin
N
Coil 1a
Coil 1b
Coil 2
Tail
C
α-Internexin
N
Coil 1a
Coil 1b
Coil 2
Tail a
E & KE segments
C
NF-L
N
Coil 1a
Coil 1b
Coil 2
Tail a
E segment
C
NF-M
N
Coil 1
Coil 2
Tail a
E 1
KSP 1
E 2
KSP 2
SP
KE & SP segments
C
NF-H
N
Coil 1
Coil 2
Tail a
E
KSP segment
KEP segment
C
Nestin
N
Coil 1
Coil 2
Tail a
KEQP segment
C
N-terminal Head
(5-7 kD)
α-Helical Rod
(39 kD)
Variable C-terminal Tail
(5-70 kD)

1988). One unifying feature of all IFs is a highly conserved epitope at the end of the rod domain (coil II) which is recognized by the anti-intermediate filament antibody (α-IFA) (Pruss et al., 1981). Most IF subunits, such as vimentin, have a 5-10 kD globular tail sequence at the extreme C-terminus of the molecule. However, the class IV and V IF proteins differ from other IFs in that they have long carboxyl-terminal extensions which contain several distinct types of unusual amino acid sequences.

The NF carboxyl-terminal tails appear to have very little α-helical or ß-sheet structure and are thus thought to consist of largely random coils (Geisler et al., 1985b). The NF tail domain can be divided into 4 regions: (1) tail A; (2) glutamic rich segment (E segment); (3) lysine-serine-proline repeat segment (KSP segment); and (4) lysine and glutamic rich segment (KE or KEP segment). It has yet to be determined if these sequence specific regions are actually functional domains. In contrast to the other IF subunits, nestin's carboxyl-terminal tail domain has a distinct repeat segment (KEQP) which is repeated 35 times (Lendahl et al., 1990). The abundance of glutamic acid residues in the carboxyl-terminal of nestin is the only similarity with the carboxyl-terminal of class IV IF proteins (Fliegner and Liem, 1991).

The latter two segments of NF-M and NF-H carboxyl terminal tails (KSP and KE or KEP) are thought to correspond to the rodlets protruding from the core filament seen in ultra-structural studies (Hisanaga and Hirokawa, 1988). The sequence motif of K-SP or K--SP is also present in microtubule associated proteins tau and MAP2 (Shaw, 1989; Shaw, 1991). The K-SP and K--SP sites in pig NF-M and K--SP site in rat NF-M are phosphorylation sites *in vivo* (Geisler et al., 1987; Xu et al., 1989). At the extreme terminus of NF-M is a highly conserved region known as the KE segment which is rich in lysine and glutamic acid. This highly charged segment may be important in interactions with other neuronal components since it is highly conserved and a closely related sequence is also present in the extreme C-terminus of α-internexin (Shaw, 1991).

NF-H is somewhat similar to NF-M but has a distinct tail domain. In contrast to NF-M, NF-H has a KSP segment that contains far more repeats of the KSP motif. In rat, this KSP motif is repeated 60 times. In addition, the KSP repeat sequences in NF-H are distinct from those found in NF-M (Shaw, 1991). Instead of a KE region at the C-terminus, NF-H has a segment rich in lysine, glutamic acid and proline (KEP) which is evolutionarily more loosely conserved (Shaw, 1991).

Recently, the different tail segments of NF-M and NF-H have been dissected out molecularly and expressed as fusion proteins (Harris, et al., 1991). These specific segments of the high MW NF tail regions can be used to examine the functional significance NF through examining their interactions with NFs, other neuronal components and by using these defined protein segments as substrates for protein kinase assays.

Neurofilament Assembly

The way in which individual NF subunits interact and assemble into NFs is not clearly understood. NF-L appears to be the core structure of assembled 10 nm filaments since urea solubilized NF-L monomers self assemble into homopolymeric structures when urea is removed (Geisler and Weber, 1981). NF-M and NF-H appear to be incapable of forming long 10 nm filaments, however, when NF-L is present, both NF-M and NF-H are readily incorporated into the 10 nm filament (Geisler and Weber, 1981; Liem and Hutchison, 1982). Antibody studies (Willard and Simon, 1981; Hirokawa et al., 1984) and rotary shadowing experiments (Hisanaga and Hirokawa, 1988) support the idea that NF-L is the central core of the filament, and NF-M and NF-H are incorporated into this core by their rod domains where the carboxyl-terminal tail domains of NF-M and NF-H protrude from the central core of the filament. Recently, rotary shadowing experiments with antibodies to the tail domain of NF-M and NF-H confirm that the tail regions of NF-M and NF-H correspond to the protrusions seen ultrastructurally with NFs (Mulligan et al., 1991). A basic question which remains is how individual IF subunits, in general, interact to form 10 nm filaments.

The majority of research on IF assembly has focused on class III IFs, desmin and vimentin, which can form homopolymers *in vivo*. When IFs form dimers it is believed that the hydrophobic portions of the α-helical coil regions of two polypeptide chains interact in a parallel fashion and form a coiled-coil structure (Parry et al., 1982). In addition to satisfying hydrophobic considerations, the coil-

coil type structure allows for favorable charge interactions along the rod domain. The dimers are then thought to form four chain tetramers either in a parallel (Ip, 1988; Hisanaga et al., 1990), anti-parallel (Geisler et al., 1985a) or staggered anti-parallel manner (Stewart et al., 1989). The differences in tetrameric formation may be related to the different IF subunits used or the way in which tetramers interact with the intact filament network (Steinert and Roop, 1988). Higher oligomers are then believed to form by a staggering of the tetramers which then results in the formation of intermediate filaments (Coulombe and Fuchs, 1990; Ip et al., 1985). Eight tetramers are thought to comprise a single 10 nm filament.

Recently the assembly process of NFs was studied using low angle rotary shadowing. These studies showed that the basic building block of IF proteins, NF-L and GFAP, were an eight chain structure formed from two parallel tetramers (Hisanaga et al., 1990), where four octamers were proposed to comprise a single 10 nm filament. Differences were also found in the way in which the filaments were reassembled. Hisanaga et al. (1990) showed that NF-L can assemble into either four chain or eight chain complexes depending on the pH of a low ionic strength buffer. In preceding experiments, alkaline buffer (pH 8.5) produced tetramers (Huiatt et al., 1980; Geisler and Weber, 1982; Ip et al.,1985; Hisanaga et al., 1990); whereas low salt buffer (pH 6.8) favored the formation of octamers (Hisanaga et al., 1990).

Hisanaga and Hirokawa (1990a) also examined how NFs assemble end to end to form long 10nm filaments. They found that in the polymerization of NF-L monomers, sodium ions were important for end-t- end association, whereas magnesium ions were involved in stabilizing lateral associations. When NFs were reassembled using NF-L, NF-M and NF-H, the assembly conditions remained unchanged; however, there was a structural change. With addition of either NF-M or NF-H, rod-like projections were seen emanating from the central core of the filament similar to those previously seen using native NFs (Hisanaga and Hirokawa, 1988).

The domains of individual NF subunits have been examined to determine which portions of NF sequence are necessary for assembly into 10 nm filaments. Genetic deletion of the amino terminal head domain and carboxyl terminal tail domain of the mouse NF-L gene showed that deletions larger than 30% from the head domain and 90% from the tail domain prevented incorporation of these proteins into the intermediate filament network (Gill et al., 1990). In contrast, when deletions were made in NF-M gene, up to 70% of the head domain and 90% of the tail domain could be missing and NF-M would still be incorporated into filaments (Wong and Cleveland, 1990). However, deletions into either amino- or carboxyl-terminal region of the α-helical rod domain of NF-M prevented assembly of this gene product into the filament network. Therefore, the intact rod domain was determined to be critical for NF assembly.

Phosphorylation of NF subunits were found to effect filament assembly. Gonda et al. (1990) demonstrated that protein kinase C phosphorylated a number of serine residues in the N-terminal head domain of NF-L and that an increase in phosphate incorporation decreased the rate of polymerization of NF-L monomer into filaments. In addition, cAMP dependent protein kinase was shown to phosphorylate NF-L and was found to inhibit assembly of NF-L monomers into filaments at phosphorylation levels of 1 mol/mol of protein (Nakamura et al., 1990). Finally, phosphorylation of NF-L filaments resulted in a slow disassembly which took up to 6 hours. Nakamura and co-workers proposed that controlled phosphorylation may modulate the dynamic equilibrium between assembly and disassembly *in vivo.*

Neurofilament Phosphorylation

The NF triplet proteins are phosphorylated *in vivo* and the relative amount of phosphorylation in rat spinal cord was determined by one group to be 3, 6 and 13 moles of phosphate/mole of NF-L, NF-M and NF-H, respectively (Julien and Mushynski, 1981; Julien and Mushynski, 1982; Xu et al., 1990). It is important to note that the relative amount of phosphate associated with NFs is variable and dependent on a number of factors including species, protein preparations, and area of the nervous system examined. What is generally known is that NF-H appears to contain the most phosphate per mole of polypeptide followed by NF-M then NF-L. In the case of NF-H and NF-L the phosphate is associated with serine residues, whereas, NF-M has phosphorylation sites on both serine and threonine residues in the rat (Julien and Mushynski, 1982).

Phosphorylation sites on NF triplet proteins are localized to particular regions on the individual NF subunits. In the case of rat NF-L, phosphorylation sites are found in both the amino head and carboxyl tail domains (Sihag and Nixon, 1989) with the major phosphorylation site located in the middle of carboxyl-terminal tail domain (Xu et al. (1990). In addition, *in vitro* phosphorylation experiments with NF-L and protein kinase C show that there are 3 phosphorylation sites on serine residues in NF-L amino-head domain (Gonda et al., 1990). A detailed study of NF-M phosphorylation sites of rat neurons in tissue culture demonstrated that there are six sites in NF-M carboxyl-terminus, four of which have the KSP motif, one with the K--SP motif, and one motif with a serine residue followed by glutamic acids (Xu et al., 1989). For NF-H the only known phosphorylation sites are in the multiple KSP repeats, though it is likely that other phosphorylation sites exist in other regions of this large molecule (Geisler et al., 1987: Lee et al.,1988).

Three major questions still remain with respect to NF phosphorylation: (1) what kinase activities are phosphorylating these different regions of NF subunits in vivo; (2) are these kinases unique to NFs and/or are they previously characterized protein kinases; and (3) what is the function of NF phosphorylation? A number of laboratories have examined NF phosphorylation (Table 1.2). The research with known kinases has focused primarily on NF-L subunit; whereas, NF-M and NF-H have been utilized to search for novel protein kinase activities responsible for phosphorylating the KSP repeat motif of NFs.

Three classical protein kinases were shown to phosphorylate NFs *in vitro* to various degrees (Table 1-2): (1) calcium/calmodulin protein kinase II (CaM kinase II) (Vallano et al., 1985); (2) cyclic AMP-dependent protein kinase (protein kinase A) (Tanaka, 1984; Dosemeci and Pant, 1992); and (3) protein kinase C (Sihag et al., 1988). *In vivo* phosphorylation experiments examining NF-L and NF-M demonstrated that most of the fragments that are phosphorylated with one of the known protein kinases are located in the amino terminal head domain (Sihag and Nixon, 1989, 1990).

The search for the protein kinase which phosphorylates the KSP repeat motif in NF-M and NF-H has focused on characterizing the protein kinase activities which bind strongly to NFs during crude purification procedures (Table 1-2). These kinase activities are extracted from NF preparations using high salt buffer and have been shown to contain a number of protein kinases: (1) CaM kinase II; (2) nucleotide-dependent kinase; (3) calcium-phosphatidylserine-diglyceride-dependent kinase; and (4) a regulator independent kinase (Dosemeci et al, 1990). The regulator independent kinase phosphorylated all three NF subunits as well as α-casein where the level of phosphate incorporated per mole of protein was in the following order: α-casein > NF-M > NF-H ≈ NF-L. This kinase activity was shown to be related to casein kinase I based on: (1) similarities in specificity of protein kinase inhibitors; (2) the ability of casein kinase I to phosphorylate NFs in a similar manner to the NF-associated kinase; and (3) the molecular weight range for casein

Table 1-2. Protein kinases which phosphorylate neurofilaments *in vitro.*

Protein Kinase	Substrate	MW* (kD)	Reference
cAMP dependent (rat brain)	NF-H, -M, -L	40	Tanaka et al., 1984 Dosemeci and Pant, 1992
Ca^{2+}/Calmodulin dependent (rat)	NF-H, -M, -L	640	Vallano et al., 1985
Protein Kinase C (mouse)	NF-H, -M, -L	77	Sihag et al., 1988
Casein Kinase I	NF-H, -M, -L	30-42	Floyd et al., 1991
cdk1 Kinase	NF-H, -M	34	Hisanaga et al., 1991
nclk Kinase¶	NF-H, -M	33	Lew et al., 1992
NF-Kinase (1983) (rat)	NF-H, -M, -L GFAP, vimentin MAPs, tau	40	Toru-Delbauffe & Pierre, 1983 Toru-Delbauffe et al., 1986
NF-Kinase: 1989 (bovine)	NF-H, -M histone H1	67	Wible et al., 1989
NF-Kinase (1990) (bovine)	NF-H, -M, -L casein	-----	Dosemeci et al., 1990
NF-Kinase (1991) (squid)	NF-H, -M, -L casein	17-44	Floyd et al., 1991

* molecular weight expressed in kiloDaltons

¶ proline directed kinase

kinase I (Hathaway and Traugh, 1982) was comparable to that of NF-associated kinase (Floyd et al., 1991).

Using the salt extraction technique, other laboratories have isolated additional NF protein kinase activities, where their molecular weight and substrate specificity suggest that these NF kinase are distinct from each other. Toru-Delbauffe and Pierre (1983) were able to recover two endogenous protein kinase activities, one which phosphorylated NFs, and the other which phosphorylate casein and was identified as casein kinase I. The NF specific protein kinase was purified by phosphocellulose chromatography and resulted in major band at 40 kD and a minor band at 200 kD on SDS polyacrylamide gels, and appeared to be co-factor independent (Toru-Delbauffe et al., 1986). Wible et al. (1989) partially purified a 67 kD doublet on SDS polyacrylamide gels and, in contrast to the previous kinases, their kinase showed more substrate specificity with a preference for partially dephosphorylated NF-H.

Even though some of the kinases had a preference for the dephosphorylated form of NF-H, phosphorylation by these various NF kinase activities did not result in the expected molecular weight shift if the dephosphorylated NF-H was being phosphorylated in the KSP repeat sequence. Previous work has demonstrated that the two high molecular weight NF subunits, NF-H and NF-M, mobility on SDS polyacrylamide gels is greatly retarded due to the large number of phosphates in the carboxyl-terminal tail domain. Hisanaga and co-workers (1991) demonstrated that the cdc kinase from starfish, $p34^{cdc2}$, phosphorylated both NF-H and NF-M *in vitro.* Furthermore, after phosphorylation of enzymatically dephosphorylated NF-H, NF-H migration on SDS polyacrylamide gels was similar to that observed for the native condition where NF-H is heavily phosphorylated. Similar results were also obtained with a cdc2 kinase, $p34^{cdc2}/p58^{cyclinA}$, isolated from FM3A mouse mammary carcinoma cells (Guan et al., 1992). These findings appear to be significant since cdc kinases are proline directed kinases which specifically phosphorylate the serine residue on the sequence S/T-P making the repeat KSP related sequences in NFs likely substrates. However, cdc kinases are associated with the regulation of cell cycle and have not been localized to neuronal cells which leads one to question the relevance of *in vitro* phosphorylation of NF by cdc2 kinases.

Recently, a proline directed protein kinase was isolated from bovine brain that consisted of two subunits, 33 kD and 25 kD (Lew et al., 1992a). This kinase was shown to phosphorylate NFs, where the 33 kD subunit displayed a high sequence homology to $p34^{cdc2}$ kinase (Lew et al., 1992b). Independent, cloning techniques identified a neuronal cdc2-like kinase (nclk) identical to that isolated by Lew et al. (1992b) which had a 58% homology to mouse $p34^{cdc2}$ kinase (Hellmich et al., 1992). *In situ* hybridization experiments demonstrated that unlike $p34^{cdc2}$ kinase, nclk was expressed in high levels in terminally differentiated neurons (Hellmich et al., 1992).

Complexities in studying NF phosphorylation seems to revolve around the phosphorylation state of the NF subunits. Most of these studies use NFs which are already phosphorylated *in vivo*. When NFs are used in this form, the *in vivo* phosphorylating sites for a specific kinase may already be phosphorylated. In addition, the phosphorylation state of NFs may effect the activity of a NF kinase (Wible et al., 1989). Another problem with complete enzymatic dephosphorylation is that some phosphate groups are more susceptible to a phosphatase than others, thus all of the phosphates may not be removed. And finally, the number of potential phosphorylation sites that exist in NF subunits make it difficult to determine where a specific NF-kinase is acting.

Since NFs are phosphoproteins and seemingly contain a number of potential sites for phosphorylation, the next obvious question is what is the role of NF phosphorylation. The distribution of phosphorylated NFs differs within the neuron. NFs are heavily phosphorylated in the axon, whereas the dendrites and cell body appear to contain little or no phosphorylated NFs (Sternberger and Sternberger, 1983). Even when considering that NF phosphorylation may be involved in calcium buffering during nerve excitation and regulation of NF assembly/disassembly, the functional significance of the phosphorylation differences within the neuron is still not understood.

Ultrastructural difference between NFs found in axons and dendrites was apparent with deep-etch freeze fracture technique (Hirokawa, 1982; Hirokawa et al., 1984). NFs appeared to be spaced farther apart in axons then they were in dendrites. These studies also revealed what appeared to be extensive cross-links between the NFs in axons which were not seen with other intermediate filaments.

Therefore, it was hypothesized that the carboxyl-tail domains of NF-M and NF-H were mediating this cross-linking, and that the length of the cross-links were regulated by the amount of phosphate incorporation in the KSP segments. However, no effect on the structure or length of NF tail projections were observed upon enzymatic dephosphorylation which removed around 90% of the phosphate groups (Hisanaga and Hirokawa, 1989).

In conclusion, there appears to be a diversity of protein kinase activities capable of phosphorylating NFs. At least some of these phosphorylation events are under tight spatial control in the neuron. Since NF subunits contain numerous potential phosphorylation sites, we can expect that different phosphorylation events will have different functional significance in the neuron.

Interactions Between Neurofilaments and Microtubules

Indirect findings suggest an interaction between NFs and MTs. Anatomically, NFs and MTs run parallel to each other in the longitudinal direction in axons and dendrites, and there appears to be morphological cross-bridges between these two structures (Wuerker and Palay, 1969; Burton and Fernandez, 1973; Rice et al., 1980; Hirokawa, 1982; Hirokawa et al., 1984). In addition, biochemical evidence shows that: (1) NFs co-purify with MTs prepared by the polymerization-depolymerization method (Berkowitz et al., 1977); and (2) both NFs and MTs travel in the slowest component of axonal transport (Hoffman and Lasek, 1975).

More direct evidence demonstrating NF-MT interactions showed that NFs inhibit tubulin polymerization. This MT assembly inhibition was found to be the result of NFs binding to high molecular weight microtubule associated proteins (MAPs) which are known to catalyze MT assembly (Leterrier et al., 1982). To further examine this interaction, Aamodt and Williams (1984) compared the ability of NF isolated from brain (NF-Brain) with that of NFs isolated from spinal cord (NF-SC) to form viscous complexes with MTs. They demonstrated that only NF-Brain were able to form viscous complexes with MTs. They hypothesized that NF-SC did not have MAPs bound to them; a suggestion supported by the finding that when purified MAPs were added to NF-SC and MTs, a viscous solution formed. Flynn et al. (1987) went on to show that NFs bound to the carboxyl-terminal thrombin fragment of MAP2 (28 kD) which also is the MT binding site. Solid-phase binding techniques show that NF-L was the only NF protein to bind to MAP2 (Heimann et al., 1985). The 28 kD fragment of MAP2 was also found to bind to purified NF-L (Flynn et al., 1987).

To examine a possible *in vivo* interaction of MAP2 binding to both NF and MT network, ß,ß'-iminodipropionitrile was used to segregate the two cytoskeletal networks in peripheral nerves. Two different monoclonal antibodies to MAP2 demonstrated that one antibody to MAP2 co-localized with the NF network while the other co-localized with MT network, suggesting that MAP2 is acting as a crosslinker between these two fibrous networks (Papasozomenos et al., 1985).

In addition to MAP2 binding to NF-L, another MT associated protein, tau, bound to reassembled NF-L. Competition studies with MAP2 and tau for binding to NF-L demonstrated that these proteins bound to different sites on NF-L. The *in vivo* significance is in question since the affinity of either MAP2 or tau was decreased when NF-M and NF-H were present in the filamentous form as normally is the case *in vivo* (Miyata et al., 1986).

Hisanaga and Hirokawa (1990b) examined the ability of NF subunits to bind directly to polymerized MTs, and showed that dephosphorylated NF-H bound to polymerized MTs *in vitro*. Further work by Hisanaga and co-workers (1993) suggested that the binding of dephosphorylated NF-H to MTs was not dependent on the degree of dephosphorylation but on the removal of a particular group of phosphates. This was demonstrated by using two different phosphatases; alkaline phosphatase and acid phosphatase. Partially dephosphorylated NF-H co-precipitated with MTs in a similar manner even though alkaline phosphatase removed 46 of 51 phosphates on NF-H whereas only 19 phosphates were removed with acid phosphatase. In addition, this binding of dephosphorylated NF-H to MTs is thought to occur at the carboxyl terminal tail region of NF-H.

NFs were shown to promote tubulin assembly *in vitro* (Minami et al., 1982); however, NF preparations used in these initial studies were contaminated with MAPs so that the MAPs may have been a factor promoting tubulin assembly. To clarify these results, Minami and Sakai (1983) demonstrated that highly purified NF preparations retained their ability to promote MT assembly as measured by a gelation assay. Adding purified NF subunits to the assay demonstrated that NF-H was the subunit responsible for promoting tubulin assembly. NF-M was able to induce some MT assembly whereas NF-L had no effect on MT assembly. Negative stain images of MT assembled in the presence or absence of NFs showed that there was an increase in MT assembly in the presence of NFs. When these structures were examined under the electron microscope, there appeared to be no morphological differences between the assembled microtubules. In the electron micrographs, the NFs appeared to make a lateral association with the MTs which resembled a T shaped structure.

The role of NF binding to MTs is not known but it is believed that the tail regions of the high molecular weight NF proteins are involved in some cross-linking function. MAP2 is localized in dendrites and may be mediating some of the interactions between NFs and MTs; whereas, tau is localized in axons where it may be performing a similar function.

Neurofilaments Interact with Other Cellular Components

The interactions of NFs with other components of the neuron is not as well studied as those interactions between NFs and MTs (Table 1-3). The majority of proteins that will be discussed below bind primarily to NF-L.

Brain spectrin (fodrin) is closely associated with the plasma membrane throughout the neuron (Levine and Willard, 1981) and is thought to play an active role in stabilizing the membrane as well as immobilizing certain membrane proteins

Table 1-3. Interactions of neurofilaments with other cellular components.

Component	NF Subunit	Affinity (Kd)	Method	Reference
Microtubules	NF-H	------	gelation of tubulin	Minami & Sakai, 1983
	NF-H (dephos.)	$3.8 \times 10^{-8}M$	co-sedimentation	Hisanaga & Hirokawa, 1990
MAP2	NF	$1.0 \times 10^{-7}M$	co-sedimentation	Leterrier et al., 1982
	NF	------	immunocytochemistry	Papasozomenos et al., 1985
	NF-L	$2.0 \times 10^{-7}M$	solid-phase binding	Heimann et al., 1985
	NF-L	$4.8 \times 10^{-7}M$	co-sedimentation	Miyata et al., 1986
MAP2 (28kD fragment)	NF, NF-L	------	co-sedimentation	Flynn et al., 1987
Tau	NF-L	$1.6 \times 10^{-6}M$	co-sedimentation	Miyata et al., 1986
Brain Spectrin	NF-L	$4.3 \times 10^{-7}M$	solid-phase binding	Frappier et al., 1987
Plectin	NF-H, -M, -L	------	solid-phase binding	Foisner et al., 1988
Synapsin I	NF-L	------	solid-phase binding co-sedimentation	Steiner et al., 1987
NAPA-73	NF	------	ultrastructural analysis	Ciment, 1990
Nucleic Acids				
rRNA	NF-H, -M, -L	preference 18s	co-sedimentation	Traub et al., 1985
dsDNA	NF-H, -M, -L	weakly	"	" "
ssDNA	NF-M, -L	preference for NF-L	"	" "

(Hirokawa, 1989). Frappier and co-workers (1987) demonstrated that brain spectrin associates with NF-L and GFAP reversibly and in a concentration dependent manner using *in vitro* binding assays. Cleavage with BNPS-skatole reagent demonstrated that the binding site for brain spectrin was localized to the 40 kD N-terminal fragment which includes the head domain of brain spectrin and the proximal portion of the rod domain. Further cleavage of the 40 kD N-terminal fragment demonstrated that brain spectrin bound to the 20 kD proximal portion of the rod domain in NF-L (Frappier et al., 1991). The binding of brain spectrin to NF-L may indicate how NFs associate with the plasma membrane.

Plectin is an intermediate filament associated protein of an apparent molecular weight of 300 kD (Wiche and Baker, 1982). Using *in vitro* binding assays, plectin was shown to bind to the α-helical rod domain of all IF proteins examined including the NF triplet protein subunits (Foisner et al., 1988). Plectin has been extensively studied over the past decade in non-neural tissue (Wiche and Baker, 1982; Wiche et al., 1983; Wiche et al., 1984) and is considered to be a widely distributed IF associated protein. Plectin is believed to be important in the interaction between IF proteins, and the association between IF proteins and other components of the cytoskeleton such as the plasma membrane (spectrin), nuclear envelop (lamins) and MTs via MAPs (Herrmann and Wiche, 1987). In addition to these functions, plectin may be important in cell to cell interactions at tight junctions or myotube attachment sites since both light and electron microscopic show it associated with these regions (Wiche, 1989).

Synapsin I is a phosphoprotein located in the synaptic terminal and is involved in neurotransmitter release (Llinas et al., 1985). Synapsin I is thought to act as a cross-linker between synaptic vesicles and the cytoskeleton in synaptic terminals thereby localizing vesicles near release sites in the terminal. It is thought that upon influx of extracellular calcium, synapsin I is phosphorylated by CaM kinase II and released from the cytoskeleton, thereby allowing synaptic vesicles to associate with release sites on the presynaptic membrane (Hirokawa et al., 1989). *In vitro* binding studies by Steiner et al. (1987) have shown that synapsin I binds to NF-L. This interaction between synapsin I and NF-L can be reduced by 60% upon phosphorylation of synapsin I with CaM kinase II. However, since NFs do not appear to exist in polymer form at the synaptic terminal, the binding of NF-L to synapsin I may not be functionally significant.

NAPA-73 is an avian specific 73 kD NF-associated protein that is expressed developmentally in the nervous system and heart (Ciment et al., 1986; Ciment, 1990). In contrast to other NF binding proteins, NAPA-73 appears to associate only with bundles of IFs (not individual subunits) suggesting that NAPA-73 is involved in the bundling of filaments (Ciment, 1990).

NF binding to RNA and DNA was investigated by Traub et al. (1985). They examined the binding of individual NF subunits to rRNA (total rRNA from Ehrlich ascites tumor cells), native DNA (double stranded DNA), and heat-denatured DNA (partially single stranded DNA) using sucrose gradients. NFs had a higher affinity for 18S rRNA than 28S rRNA and this affinity could be abolished in the presence of 6 M urea for NF-M and NF-H. In contrast NF-L interaction with 18S rRNA was resistant to 6 M urea. Native DNA bound very weakly to NF subunits, whereas, heat-denatured DNA bound strongly to NF subunits except in the case of NF-H. The specificity of binding of the different forms of nucleic acids suggested that the association was not solely based on electrostatic interactions (Traub et al., 1985). The relevance of NFs binding to RNA and DNA is not known. However, some researchers speculate that NFs degraded at the axonal terminal by calpain proteases are transported back to the cell body where they could act as a messenger for the events occurring at the nerve terminal (Traub, 1985; Schlaepfer, 1987).

Another characteristic aspect of NFs is the ability to bind calcium. Assembled NFs in both phosphorylated and dephosphorylated states contain high and low affinity binding sites for calcium (Lefebvre and Mushynski, 1987, 1988). The dephosphorylation of NFs results in a 50% decrease in the low affinity calcium binding sites which may be related to the loss of phosphate groups. Coinciding with the decrease in low affinity calcium binding sites is an increase in the number of high affinity binding sites. This increase in the high affinity calcium binding sites is probably reflected by a change in the conformation of NFs after dephosphorylation. Glutamic acid residues are known to constitute calcium binding sites in such proteins as calmodulin (Kilhoffer et al., 1983), thus the glutamic acid rich region in the C-terminus of NF tail regions may be the possible binding site for calcium. Lefebvre and Mushynski (1988) found that the high affinity calcium binding sites are located in the α-helical rod domain and that the low affinity binding sites are located at the carboxyl-terminal region of NF molecule. The functional significance of these calcium binding sites is unknown; however, two possible functions for calcium binding to NFs have been suggested: (1) the ability to regulate the activation of calcium binding proteases (calpain) which degrade NFs in the synaptic terminal (Schlaepfer et al., 1985; Schlaepfer, 1988); and (2) the buffering of calcium during nerve excitation (Abercrombie et al., 1990).

Relationship of NFs to Axonal Transport and Caliber

The transport of material from the cell body along the axon is an essential neural function since the axon does not contain the cellular machinery for protein synthesis. Anterograde axonal transport can be broken down into five components on the basis of their uniform rate: (1) 250-400 mm/day (fast component); (2) 40 mm/day; (3) 15 mm/day; (4) 2-5 mm/day (slow component b); and (5) 0.2-1 mm/day (slow component a) (Willard, 1974). Cytoskeletal elements travel in slow component a and b. Actin with its associated proteins travel in slow component b, whereas, NFs and MTs, travel in the slow component a (Hoffman and Lasek, 1975). In addition, there appears to be a slower second wave of NFs travelling at a non-uniform rate that is 100 fold slower than slow component a (Nixon and Logvineko, 1986). It has been proposed that newly synthesized NFs travel down the axon as assembled NFs, and are incorporated into the stationary cytoskeletal network at random points during transport (Nixon and Logvineko, 1986). During axonal transport, NF's overall charge become increasingly negative which corresponds to an increase in phosphorylation state (Nixon et al., 1986). This phosphorylation of NF-L and NF-M is short-lived; 50-60% and 35-40% of the phosphates are removed in five days, respectively. In contrast, NF-H shows little to no phosphate turnover during the same period (Nixon and Lewis, 1986). Lewis and Nixon (1988) suggest that differential turnover rate of NF phosphorylation may regulate the incorporation of NFs into the stationary NF network, and reflect a dynamic interaction of NFs with other proteins.

Even though NFs are normally perceived as static structures, research examining the role NF density as an intrinsic regulator of axonal caliber suggest a more dynamic function for NFs (Hoffman et al., 1984). During development, the increase in NF synthesis has been correlated to a decrease in NF transport velocity and an increase in radial growth of the axon (Willard and Simon, 1983; Hoffman et al., 1985a). This association of NF number to axonal caliber suggests that regulation of NFs by gene expression and axonal transport largely determines the size of the axon. Conversely, after a sciatic nerve crush, there is a decrease in the number of NF proteins delivered to the axon which coincides temporally with the reduction in axonal caliber proximal to the lesion in comparison to more distal regions (Hoffman et al., 1985b). As the slow component advances at its normal rate, the atrophy also advances (referred to as somatofugal atrophy), and when NF synthesis returns to normal levels the atrophy is reversed (Hoffman et al.,1985b).

Similar results are observed with acrylamide toxicity (Gold et al., 1985), further suggesting that NFs play an vital role in regulating axonal caliber.

In contrast, other research showed that NF density varies considerably along the length of the axon, as well as in different axonal types, implying that a local regulation of axonal cytoskeleton must occur (Berthold, 1982; Nixon and Logvineko, 1986; Price et al., 1988; Szaro et al., 1990). To examine the role of the cytoskeleton in the local modulation of axonal caliber, a dysmyelinating mutant mouse line, Trembler, was used. The peripheral nerves of Trembler were characterized by a reduction in axonal caliber, an increase in density of axonal cytoskeletal elements, and a decrease in slow component axonal transport (Low and McLeod, 1975; Low, 1976a,b; de Waegh and Brady, 1990). De Waegh and co-workers (1992) examined the relationship of axonal caliber and NF phosphorylation in the Trembler mouse and found that along with an increase in NF density, there was a concomitant decrease in NF phosphorylation and axonal caliber. Therefore, the decrease in NF phosphorylation could in turn be related to a decrease in charge repulsion thus allowing the NFs to pack more closely together. In contrast, De Waegh and co-workers (1992) suggested that these alterations were regulated by the amount of myelin surrounding the axon. Grafts of Trembler sciatic nerve placed into normal nerve showed regenerated axons with the Trembler morphology while adjacent axons (control) had normal characteristics.

Recently, transgenic techniques were used to examine the effects of murine NF gene overexpression on neurons and to determine if an increase in NF number in the axon resulted in a concomitant increase in axonal caliber (Monteiro et al., 1990). The transgene mRNA exceeded the endogenous NF-L mRNA by fourfold. This resulted in a corresponding increase of the NF-L protein in the peripheral axons of the trangenic mice. Although there was an increase in density of axonal NFs seen morphologically, this did not result in a change in axonal caliber.

These results with overexpressed murine NF-L gene suggest that either the other two NF subunits may be important in regulating axonal caliber or that the correlation between axonal diameter and NF density may only be valid when there is a decrease in NF synthesis. The latter possibility would lend support to the theory of mechanical stability. Since NF-M and NF-H have unusually large carboxyl terminal domains which protrude as sidearms from the core of the filament and are highly phosphorylated in the axon, it has been proposed that NF-M and NF-H are important in forming or regulating the spacing of NFs whether through actual cross-bridges or charge repulsion from the highly negative carboxyl-terminal domains. Although these data appear to contradict the active role of NF density in controlling axonal caliber, it seems more likely that there are both intrinsic and extrinsic factors involved and that the role of NFs seems to be more prevalent in large myelinated axons (Hoffman et al., 1988).

Research on neuropathologies related to abnormal NF accumulation has focused on deficits in axonal transport. Giant axonal neuropathies are characterized as a focal accumulation of NFs along the axon (Gold et al., 1986) which suggests the occurrence of a local interruption of NF transport resulting in the accumulation of NFs. Two model systems have shown that with normal NF synthesis, a retardation of slow component of axonal transport by ß,ß'-iminodipropionitrile (IDPN) results in proximal axonal swelling and distal axonal atrophy (Griffin et al., 1978; Clark et al., 1980); whereas, after treatment with 2,5-hexanedione NF transport is accelerated, resulting in proximal axonal atrophy and distal axonal swelling (Monaco et al., 1984 and 1989).

NF Expression After Axotomy

Differential changes in cytoskeletal proteins following axotomy of peripheral nerves is observed for both sensory and motor neurons. Overall, the synthesis of both tubulin and actin increases after axotomy whereas the synthesis of NF triplet proteins are down regulated (Hoffman et al., 1987; Wong and Oblinger, 1987; Goldstein et al., 1988; Tetzlaff et al., 1988; Oblinger et al., 1989). This results in a decrease in the amount of newly synthesized NFs transported into the axon (Oblinger and Lasek, 1988). However, based on immunocytochemistry, expression of NF triplet proteins appears to remain unchanged . The time course for changes in synthesis is similar for all cytoskeletal proteins in that the largest effects occur between 7 and 14 days, and in the case of a peripheral nerve crush, the level of synthesis returns to normal between 3 to 8 weeks post injury. If reinnervation is prevented, NF synthesis remains at decreased levels.

Normally, phosphorylated epitopes of the high molecular weight NF subunits are restricted primarily to the axon whereas non-phosphorylated epitopes are localized to the cell body and dendrites. However, after axotomy there is a dramatic and transient increase in phosphorylated epitopes in the cell body that is concurrent with a decrease in expression of NF mRNA (Moss and Lewkowicz, 1983; Dräger and Hofbauer, 1984; Goldstein et al., 1987; Shaw et al., 1988). As labelling for NF phosphorylated dependent epitopes increase in the perikarya, there is a concomitant decrease in labelling for the dephosphorylated dependent epitope which suggests that phosphorylation is occurring at the sites that would normally be recognized by dephosphorylated dependent NF antibodies (Goldstein et al., 1987). In the case where axons do not normally regenerate, phosphorylated epitopes on NF-H remain up to 60 days in the cell body after axotomy (Dräger and Hofbauer, 1984).

In contrast to the NF triplet proteins, peripherin expression is upregulated after sciatic nerve crush in both dorsal root ganglion (DRG) cells and lumbar motoneurons (Oblinger et al, 1989; Wong and Oblinger, 1990). In DRG cells, peripherin is normally expressed in small diameter cells whereas NF triplet proteins are localized primarily to the large diameter cells (Parysek and Goldman, 1988; Parysek et al., 1988: Ferri et al., 1990; Goldstein et al., 1991). After a peripheral nerve crush, the mRNA level for peripherin increases in the large diameter cells (maximizes at 7 to 14 days) but remains unchanged for the small diameter cells. This increase in mRNA levels for peripherin translates into an increase in immunoreactivity in large diameter DRG cells. As expected, NFs show a decrease in mRNA synthesis which is not accompanied by a change in immunoreactivity in the large diameter DRG cells. Similar results are observed in lumbar motoneurons after sciatic nerve crush for peripherin. For peripherin, the mRNA levels increase two fold after 4 days, remain elevated for 6 weeks, and finally recover to normal levels at 8 weeks (Troy et al., 1990).

Role of NFs in Disease States

NFs are thought to be involved in the development of various neuropathologies. The breakdown of the normal NF organization is prevalent in motoneuron disease (Hirano, 1991), neurodegenerative disease (Goldman and Yen, 1986) and toxin-induced neuropathologies (Griffin and Watson, 1988). In amyotrophic lateral sclerosis (ALS) there is selective degeneration of anterior horn motoneurons of the spinal cord. One of the hallmark features of ALS is an abnormal accumulation of NFs in the perikarya, axons and dendrites as well as NF induced swelling in the axons early in the degenerative process. It is yet to be determined whether this increase in expression of NF protein is central to this and other neuropathologies or is a secondary consequence of another cellular disorder.

Recent transgenic technology has resulted in two animal models to study the overexpression of NFs, one that examines the effects of NF-L overexpression and the other that examines NF-H overexpression. Doubly transgenic mice, which resulted in a fourfold increase the murine NF-L gene, produced dramatic phenotypic and morphological changes (Xu et al., 1993). Phenotypically, doubly transgenic mice were one to two-thirds the body weight of age-matched controls, kinetic activity was decreased and death usually occurred within 3 weeks due to widespread skeletal muscle atrophy. In the CNS, murine NF-L expression was restricted to neurons; however, outside the nervous system, the expression OF murine NF-L was observed in different areas including skeletal muscle. Morphometrically, select motoneurons showed chromatolytic features that included a disrupted rough endoplasmic reticulum and a displaced nucleus. The overexpression of murine NF-L resulted in excessive accumulation of NFs in the soma and proximal axons of the anterior horn motoneurons which were undergoing chromatolysis. In addition to the increase in NF density in large caliber axons, the NFs were more closely packed together and were not always observed in the normal parallel array to the long axis of the axon. A few mice lived past three weeks, and after 2 months the axons showed a significant decrease in NF density that were still higher than controls. Additionally, muscle mass returned and a slow return of normal kinetic activity was observed. Near normal phenotype at nine months occurred concomitant with a decrease in NF accumulation which had plateaued at three to four weeks. These results led to the hypothesis that excessive NF-L accumulation can result in motoneuron dysfunction before widespread neuronal loss.

In a similar study, in which transgenic mice were produced with human NF-H, a twofold increase of NF-H expression resulted in a more progressive neuropathology that occurred over a period of three to four months (Côté et al., 1993). In these transgenic mice, the expression of the human NF-H was restricted to neurons. Similar to ALS, progressive abnormal accumulations of NFs were observed in the perikarya and proximal axons of anterior horn motoneurons of the spinal cord.

The excessive accumulations of NFs in the neuronal cell bodies in both types of transgenic mice suggest that it is not one particular NF subunit is critical to prevent normal cellular activity. However, the increase in density and disorganization of NF structure taken together could interfere with normal axonal transport and thus result in inappropriate accumulations of NF subunits throughout the neuron. Thus, deficits in axonal transport appear to be a major component in motoneuron neuropathies. This may be due to indirect effects like an abnormal increase in NF proteins in the soma that blocks normal axonal transport which may be the case with ALS, or may be due to a direct effect of axonal transport, that results in local accumulations of NFs, which may be the case with giant axonal neuropathies.

Overview of Dissertation

Although NFs are one of the most abundant proteins in the nervous system, the dynamics of their function remain undefined. As in the case of other cytoskeletal elements, such as MTs and MFs, one way of understanding or defining function is realized by determining what types of proteins interact with these cytoskeletal elements. In the set of experiments described in this dissertation, I have undertaken this approach to identify candidate NF binding proteins in an attempt to assign functional roles to NF proteins.

One candidate NF binding protein is a 300 kD protein which co-purifies with IF proteins isolated from a crude spinal cord preparation. This protein was identified as plectin, a protein previously characterized in non-neuronal tissue. The relationship of plectin to its potential role in the nervous system, and specifically to neural IF proteins was examined.

Using affinity column chromatography, additional candidate NF binding proteins were identified based on molecular weight. A number of proteins bound to the different NF affinity columns with varying specificity. One protein in particular was identified as glyceraldehyde-3-phosphate dehydrogenase (GAPDH). The *in vitro* binding of GAPDH to NF-L was examined as well as possible *in vivo* interactions at the light and ultrastructural level.

These findings provide an initial framework for studying NF associated proteins. NFs appear to interact with a number of proteins and these associations may be specific to individual subunits as well as to the intact 10 nm filaments. In addition, future studies that identify the other candidate NF associated proteins will lead to a better understanding of NF function. Considering the differential labelling of NFs in neurons, NF associated proteins may also show similar specificity which may lead to important markers for different neuronal cell types along the neural axis.

CHAPTER 2

GENERAL METHODS

This chapter describes the routine biochemical and anatomical techniques that were performed for this dissertation project. Techniques that were specific for a particular chapter or modifications of these routine techniques will be described in that chapter.

Biochemical Techniques

Protein Assay

Lowry protein assay. The method of Lowry et al. (1951) was used for some of the protein assays. Briefly, a standard curve from 0 to 100 µg bovine serum albumin (BSA) to a final volume of 0.5 ml was made. The unknown concentration of the protein solution was determined by diluting the protein solutions so it fell in the range of the standard curve. Five milliliters of a solution containing 0.04% copper sulfate, 0.08% potassium sodium tartrate and 2.94% sodium carbonate was added to the BSA standards and protein samples to be assayed. The solutions were then incubated at room temperature for 10 minutes. Next, 0.5 ml of 50% Folin phenol reagent solution (diluted with deionized water) was added to each tube and then each tube was incubated for 30 minutes at room temperature. The absorbance was measured at 650 nm for each sample and the absorbance of BSA standards was plotted against the known concentrations. The unknown protein concentrations were determined from the linear regression line of the BSA standard data.

Pierce protein assay. Pierce Micro BCA protein assay kit was also used in protein concentration determination because of its reliability and ease of use. Protein concentrations were determined in the range of 0-20 µg/ml using BSA as the standard and following the manufacturers instructions. Pierce Micro BCA protein assay kit uses bicinchoninic acid which is a highly sensitive and selective detection reagent for Cu^{+1}. The protein concentration of the unknown samples were determined using the same methodology as described above.

SDS Polyacrylamide Gels

The sodium dodecyl sulfate (SDS) polyacrylamide gel electrophoresis technique was based on the method of Laemmli (1970) with an acrylamide to bisacrylamide ratio of 37:1 (22.2%:0.6%). The electrophoretic apparatus used was the Bio-Rad mini-protean II electrophoresis cell. Sample buffer containing SDS and ß-mercaptoethanol (12.5% (v/v) 1 M Tris-HCl, pH 6.8, 4% (w/v) SDS, 10% (v/v) glycerol, and 0.006% (v/v) bromophenol blue in ethanol) was added to each sample and then each sample was boiled for 5 minutes before protein separation on SDS polyacrylamide gels. The SDS polyacrylamide gels were run at a constant current of 20 mA per gel. The gels were fixed in 40% methanol and 10% acetic acid for 30 minutes, and then stained with 0.025% Serva Blue G for 1 hour followed by destaining with 10% acetic acid for 1-2 hours. This method of staining and destaining of gels is fast and efficient when compared to staining with Coomassie Brilliant Blue R-250 (CBB) in methanol and acetic acid solution which can take up to 24 hours to properly destain the background. In cyanogen bromide (CNBr) cleavage experiments, CBB was used since the initial staining of the bands is comparatively faster (15 to 20 minutes) and high background did not interfere with accurately excising the gel band of interest.

Electroblotting of Proteins

Proteins were electrophoretically transferred to nitrocellulose or polyvinylidine difluoride (PVDF) membrane using Bio-Rad Mini Trans-Blot Cell. A submerged protein transfer system was used where the gel and membrane were sandwiched between Whatman 3M paper and scrub pads. The transfer buffer used in most situations contained 10 mM 2-[N-morpholino]ethanesufonic acid (MES) pH 6.5, 0.01% SDS. The transfer lasted for 1-2 hours at 90 Volts depending on the protein being transferred. To prevent overheating, the mini trans-blot unit was immersed in an ice bath.

The proteins transferred onto the nitrocellulose membranes were visualized with 0.025% Ponceau S in 40% methanol/10% acetic acid, and were used for Western blots. Proteins transferred onto PVDF membranes were used for amino acid analysis and were treated in a slightly different manner than nitrocellulose membranes. Before proteins were transferred onto PVDF membrane, the membrane was immersed in 100% methanol and then equilibrated in transfer buffer for 20 minutes with two changes of buffer. After the transfer of proteins to the PVDF membrane, the PVDF membrane was washed in deionized water for five minutes, and stained in 0.1% CBB in 50% methanol for 5 minutes. The PVDF membrane was partially destained in 50% methanol and 10% acetic acid for five minutes, followed by a final wash in deionized water for 5 minutes (four changes of water). The PVDF membrane containing the transferred proteins was dried and stored at -20°C until analysis.

Immuno-Blot Analysis

Proteins were separated on SDS polyacrylamide gel and electrophoretically transferred onto nitrocellulose membrane as discussed previously. The membrane was blocked with 3% bovine serum albumin (BSA) or 5% nonfat Carnation instant milk containing 0.1% Tween 20 in Tris buffered saline (TBS: 10 mM Tris-HCl (pH 7.5), 0.9% saline). If the nonfat milk was used to block the nitrocellulose, then the primary and secondary antibody was diluted in this solution, and all but the last wash was done with TBS containing 0.1% Tween 20 in place of TBS. The remaining steps were the same as those described when BSA was used to block the nitrocellulose membrane. The membrane was incubated with the primary antibody containing 0.1% BSA for 1 hour at room temperature followed by three 10 minute washes in TBS. Next, the membrane was incubated with secondary antibody, alkaline phosphatase conjugated anti-mouse or anti-rabbit, for 1 hour at room temperature followed by two 10 minute washes in TBS. A ten minute wash in developing buffer (10 ml 0.1 M Tris-HCl (pH 9.5) containing 5 mM $MgCl_2$ and O.1 M NaCl) followed. The antibody binding was visualized using 33μl 50 mg/ml

5-Bromo-4-chloro-3-indolyl phosphate (BCIP) and 33µl 50 mg/ml Nitro Blue Tetrazolium (NBT) in 10 ml developing buffer.

Protein Cleavage with Cyanogen Bromide

To cleave proteins at methionine residues, the cyanogen bromide (CNBr) cleavage method was used on SDS polyacrylamide gel protein bands (Sokolov et al., 1989). The protein to be cleaved by CNBr was separated on a SDS polyacrylamide gel. The gel was stained with CBB (0.25% coomassie blue R-250 in 45% methanol and 10% acetic acid) and the gel band of interest was excised from the gel. The gel band was dried down using a vacuum evaporator at 60-80°C. The volume to rehydrate the gel band was estimated by measuring the length, height and width of the gel band before it was dehydrated, and that volume was added to the dried protein gel band in the form of 200 mg/ml CNBr in 70% formic acid. The gel band was incubated in the CNBr solution at 37°C for at least 6 hours. The rehydrated gel band was dried down in the vacuum evaporator to remove the remaining CNBr and its by-products. The dried cleaved gel band was rehydrated and neutralized in 50% 2X sample buffer and 50% 1 M Tris for 15 minutes. The cleaved protein gel band was placed on 15% SDS polyacrylamide gel to separate the protein fragments. The protein fragments were visualized using Serva Blue G or silver stain depending on the protein concentration.

Isolation of Neurofilament Proteins

Crude Intermediate Filament Preparation

A crude intermediate filament (IF) preparation was used to obtain primarily neurofilament (NF) proteins *in vitro* while maintaining some of their native characteristics. Fresh spinal cord (specific species used will be discussed in the relevant chapter) was homogenized gently using a Wheaton Dounce Type 40 glass homogenizer for small preparations (≤10 g of tissue) or a Sears blender for larger preparations (>10 g tissue). The tissue was brought up in 5 volumes of Buffer A (0.1 M Tris-HCl (pH 7.5), 0.1 M NaCl, and 1 mM Nα-p-tosyl-L-arginine methyl ester (TAME)), and homogenized with 3 strokes of pestle 'B' followed by 1 to 2 strokes with pestle 'A'. For larger preparations, the tissue was homogenized in blender at low speed (three 5 second pulses) followed by three 5 second pulses at high speed. The homogenate was made up to 10 volumes with Buffer A and centrifuged at 2300xg for 10 minutes at 4°C in a SS34 Sorvall rotor. The pellet was taken up in 10 volumes 1 M sucrose in Buffer A, vortexed gently to break up the pellet, and centrifuged at 2300xg for 20 minutes at 4°C in a SM-24 Sorvall rotor (small preparation) or a SS34 Sorvall rotor (large preparation). The floating myelin layer, containing the NF bundles, was carefully removed and the volume was made up to 5 volumes with Buffer A containing 1 M sucrose and 1% Triton X-100. The myelin homogenate was gently vortexed and triturated to suspension, and then shaken on an orbital shaker for 60 minutes at 4°C. This allowed the Triton X-100 to solubilize the myelin and release the intermediate filament bundles.

The suspension was centrifuged at 150,000xg for 1 hour at 4°C in a Beckman TL-100 rotor (small preparation) or a T865 Sorvall rotor (large preparation) to recover the pelleted intermediate filament bundles. The pellet was composed mainly of NF bundles and glial filaments. The pellet was taken up in the appropriate buffer and stored at -20°C.

Neurofilament Preparation

Partially purified NFs were prepared using the method of Delacourte et al. (1980). Fresh pig spinal cord (250 g) was homogenized in 400 ml of 0.1 M MES (pH 6.5), 1 mM ethylenediamine tetraacetic acid (EDTA), 0.5 nM $MgCl_2$, 1 mM PMSF, and I mM TAME using a Sears blender at 4°C. Initially, the spinal cord was homogenized at low speed using 3 five second pulses followed by 3 five second pulses at high speed. The crude homogenate was centrifuged at 13,500xg for 45 minutes at 4°C in a GSA Sorvall rotor. The supernatant was filtered through 8 ply gauze sponges type VII (Professional Medical Products, Inc.) to remove any large floating debris. Next, the filtered supernatant was centrifuged at 78,000xg for 30 minutes at 4°C in a T865 Sorvall rotor. Glycerol was added to the supernatant to form a final concentration of 20% (v/v) glycerol. The solution was warmed to 37°C for 20 minutes. The supernatant was centrifuged at 78,000xg for 45 min at 30°C in a T865 Sorvall rotor. The pelleted material was combined and homogenized in 50 ml of MES buffer and centrifuged at 147,000xg for 30 minutes at 4°C in a T865 Sorvall rotor. The pelleted material was a pale yellowish gel that contained NFs and glial filaments. The pellet was stored at -20°C.

Purification of Individual Neurofilament Subunits

Individual NF subunits were purified following a modified method of Tokutake (1984). The pellet obtained from the NF Delacourte preparation was homogenized on ice in 10 mM sodium phosphate monobasic (pH 7.0), 6 M urea, 1 mM EDTA, and 1 mM dithiothreitol (DTT) in order to solubilize the NFs into their individual subunits. Insoluble material was removed by high speed centrifugation (150,000xg) for 30 minutes at 4°C using a T865 Sorvall rotor and the supernatant was filtered through a 0.45 μm filter. The soluble material containing the NF subunits was put through a DEAE cellulose column (DE-52) at a flow rate of 25 ml/hour at 4°C. The DE-52 column was washed extensively to remove any unbound proteins and before elution of bound proteins. To make sure no more proteins were being eluted, the optical density at 280 nm of the wash buffer coming through the column was checked. A linear gradient of 10 mM to 400 mM monobasic sodium phosphate (500 ml) was used to elute the bound proteins. Tokutake showed that varying the sodium phosphate concentration instead of using a sodium chloride gradient resulted in a better separation of the individual NF subunits. Fractions of 5 ml were collected during the elution, and 10μl of each even number fraction was separated on 7.5% SDS polyacrylamide gels to determine which fractions contained the NF subunits. The fractions which were purest (those that contained 98% of only one of the subunits) were pooled and dialyzed against the appropriate buffer. The purified NF subunits were assayed for protein concentration (Lowry or Pierce micro assay) and stored at -20°C.

Anatomical Localization Experiments

Dorsal Root Ganglion Cell Cultures

New born rat pups (postnatal day 1) were killed by decapitation and the body was pinned at the extremities to a piece of styrofoam. All instruments were sterilized with 95% ethanol. The skin over the spinal cord was removed and a longitudinal cut, using a scalpel, was made through the dorsal portion of the vertebrae. With scissors the dorsal vertebral column was trimmed and the spinal cord removed. The dorsal root ganglia (DRG) were located between the vertebrae and resembled small white spheres. The DRG were removed one by one with fine forceps from one side of the vertebral column and placed in a sterile microfuge screw cap containing Liebowitz L-15 media (Sigma) with 10 ml/liter penicillin (10,000 Units/ml), streptomycin (10,000 mag/ml) and amphotericin B (25 mag/ml) (Gibco) (L-15 incomplete media). This was repeated for the contralateral side and for the remaining rat pups so that each tube contained approximately 10 to 15 DRG. The ganglia were pelleted in a clinical centrifuge (setting 5) for 30 seconds. To the pelleted ganglia, 240 µl 10X sterile trypsin-EDTA solution (Sigma; 0.5% trypsin, 0.2% EDTA. 0.9% NaCl) was added. The resuspended DRG were then incubated at 37°C for 40 minutes to dissociate the ganglia. Then, the DRG were centrifuged for 30 seconds at setting 5 in the clinical centrifuge, the trypsin containing supernatant was removed, and 6-8 drops of fetal bovine serum (FBS; Gibco) was added. The DRGs were incubated for 10 minutes at 37°C, pelleted as described above, and supernatant removed. DRG were triturated in 100 µl of L-15 incomplete media 15 times using an Eppendorf pipet to resuspend the ganglia into single cells. Before plating, 500 µl of L-15 incomplete media was added to each tube, then cells were plated on 6 acid washed coverslips (100 µl per plate) placed in Petri dishes (35x10 mm). Two milliliters of L-15 complete media (L-15 incomplete media, 10% FBS, 0.6% glucose, 2 mM L-glutamine and 0.3% A4M methylcellulose) was added to each Petri dish. Nerve growth factor (NGF) (Sigma 7S mouse submaxillary gland NGF) was added to result in a final concentration of 200ng/ml. The DRG cells were grown in a non-CO_2 incubator at 37°C for 24 hours.

Pheochromocytoma Cells (PC12 Cells)

A stock solution of PC12 cells was thawed rapidly at 37°C, pelleted in a clinical centrifuge, and resuspended in RPMI media containing 85% RPMI 1640 medium (Gibco); 10% heat inactivated horse serum, 5% FBS and 10 ml/liter of penicillin (10,000 Units/ml), streptomycin (10,000 mag/ml) and amphotericin B (25 mag/ml) (Gibco). PC12 cells were plated on a collagen coated Petri dish (60x10 mm), grown at 37°C in a water-saturated atmosphere containing 8.1% CO_2, and fed with new media every 2-3 days. When the cultures reached confluence, they were subcultured at a ratio of 1:3 to 1:4. To generate neurite-bearing PC12 cells, 50 ng/ml 7S-NGF was added to each culture and the total serum concentration was reduced to 1.5% from 15%. PC12 cells were feed every two days with RPMI media containing 1.5% serum and 50 ng NGF. After about a week in culture, PC12 cells produced neurites and were ready to be replated on collagen coated coverslips for immunocytochemistry. The PC12 cells were removed from the Petri dish by trituration with a Pasteur pipette and pelleted in clinical centrifuge at low speed where the supernatant was discarded (contains cellular debris including detached neurites). The pelleted cells were resuspended in RPMI media (1.5% serum) with 50 ng NGF, and plated onto coverslips. The PC12 cells produced neurites within 8 to 16 hours and by 2 to 3 days the PC12 cells have formed extensive neuritic processes.

Immunofluorescent Studies on Fresh Frozen Tissue

Adult rats, either Sprauge Dawley or Long Evans Hooded strains, were anesthetized with 0.5 ml pentobarbital i.p. and sacrificed by decapitation. Nervous system tissue was dissected out, frozen on dry ice for 1 hour or quickly frozen in isopentane cooled with liquid nitrogen, and stored at -70°C until sectioning. The tissue of interest was cut at a thickness of 6 to 10 μm using a cryostat, placed on petroleum ether cleaned glass slides, and stored at -20°C until they were labelled with antibodies. Prior to incubation with primary antibodies, the tissue was fixed in acetone (-20°C) for ten minutes. Tissue sections were air dried 10 to 15 minutes and encircled with a PAP pen (The Binding Site) to make a well for the antibodies. The two primary antibodies, one polyclonal and the other monoclonal, were mixed together in buffer to obtain the appropriate final concentration for each antibody and then were placed on the section. The tissue sections were then incubated at 37°C for 30 minutes or 4°C for 24 hours, followed by three 10 minute washes in PBS. Following primary antibody, sections were incubated for 30 minutes at 37°C or 24 hours at 4°C with secondary antibodies, FITC-conjugated goat anti-mouse (1:40) and Texas Red conjugated donkey anti-rabbit (1:200). After three 10 minute washes in PBS, the sections were coverslipped with anti-bleaching agent (1.0 mg/ml para-phenylenediamine (Sigma) in 20 mM Tris-HCl pH 7.9, 90% glycerol). For tissue culture immunofluorescence, the DRG and PC12 cells were fixed in cold methanol (-20°C) for 5 minutes. The remaining antibody steps were as described above. The fluorescently labelled tissue sections were visualized and photographed using a Zeiss Axiophot microscope system.

Immunohistochemistry on Formaldehyde Fixed Tissue

Adult rats, either Sprauge Dawley or Long Evans Hooded strains, were anesthetized with either 0.5 ml pentobarbital or 80 mg/kg ketamine and 10 mg/kg xylazine, and perfused with saline (0.9% NaCl) containing 0.05% (v/v) heparin and 0.05% (w/v) sodium nitroprusside followed by a fixative solution of 4% paraformaldehyde in Sörensen's Buffer, pH 7.4 (19 mM monobasic sodium phosphate, 81 mM dibasic sodium phosphate). The rat nervous system was dissected out and placed in the above fixative solution overnight or PBS depending on how well the tissue was fixed. Before sectioning, the tissue was blocked and placed in phosphate buffered saline for at least 4 hours before being cut in 30 to 50 μm sections using a vibratome.

For immunocytochemistry, the tissue sections were incubated at in 0.3% hydrogen peroxide in PBS for 30 minutes at room temperature to remove any endogenous peroxidase activity. The tissue sections were washed three times for

10 minutes and mounted on chrome-alum coated slides and allowed to air dry for at least one hour before beginning antibody staining procedure. Vectastain elite ABC kit (KIT) was used to visualize the labelling of the primary antibody. The tissue sections were blocked for 20 minutes in dilute normal serum (KIT) at 37°C. Excess blocking serum was shaken off and the primary antibody in 0.25% Triton-X-100 was placed on the tissue section and incubated for 30 minutes at 37°C or 24 hours at 4°C. The tissue sections were washed three times for 10 minutes followed by incubation with biotinylated secondary antibody (KIT) for 30 minutes at 37°C or 24 hours at 4°C. The tissue sections were washed 3 times for ten minutes followed by incubation with the avidin/biotin reagent (KIT) for 30 minutes at 37°C or 4 hours at room temperature. The tissue sections were washed 3 times for ten minutes in PBS before being developed with freshly prepared diaminobenzidine tetrahydrochloride (DAB) solution (0.05% DAB (Sigma), containing 0.01% hydrogen peroxide in 0.1 M Tris, pH 7.2). The reaction was monitored using an inverted microscope in order to determine when to stop the reaction. The reaction was stopped by placing the tissue sections in tap water for five minutes. The tissue sections were dehydrated using ascending alcohol concentrations: 70%, 90%, 95%, 100%, 100%; and cleared in xylene and coverslipped with permount.

CHAPTER 3

THE DISTRIBUTION OF PLECTIN, AN INTERMEDIATE FILAMENT BINDING PROTEIN, IN THE ADULT RAT CENTRAL NERVOUS SYSTEM

Introduction

Although intermediate filament proteins (IFs) are found with various polypeptides known as intermediate filament associated proteins (IFAPs), IFAPs remain much less characterized than microtubule and microfilament associated proteins. At present only a few proteins are known to be specific IF-binding proteins, (Foisner and Wiche, 1991) such as plectin (Wiche, 1989), IFAP-300 (Yang et al., 1985; Lieska et al., 1985), NAPA-73 (Ciment et al., 1986), filensin (Merdes et al., 1991), and filaggrins (Haydock and Dale, 1990).

One protein in particular, plectin, has been studied extensively in non-neural tissue. Immunofluorescence studies of various non-neuronal tissues demonstrated that plectin was localized to a number of different cell types, and has a cytoplasmic distribution within the cell with a distinct tendency to be concentrated at the cellular periphery near the plasma membrane (Wiche et al., 1983). Later work demonstrated that plectin bound to immobilized IF proteins *in vitro*, including the NF triplet proteins (Foisner et al., 1988). This interaction was found to involve the α-helical rod domain in IFs and the α-helical rod domain of plectin (Foisner et al., 1988; 1991). Originally, plectin was identified from rat glioma C6 cells as a major component of Triton X-100 extracts with an apparent molecular weight of 300 kD as determined from mobility on SDS-polyacrylamide gels (Pytela and Wiche, 1980).

Recent cloning and sequencing of rat plectin has shown that the actual molecular weight of plectin is 527 kD (Wiche et al., 1991). Portions of plectin's primary sequence are related to desmoplakin and the bullous-pemphigoid antigen, both of which are found in association with IFs at the plasma membrane (Wiche et al., 1991). Overall, plectin is postulated to function as a crosslinking protein, mediating interactions between IF proteins and other components of the cell (Foisner and Wiche, 1991) such as the plasma membrane via spectrin, the nuclear envelope via nuclear lamins and microtubules via microtubule-associated proteins (Koszka et al., 1985; Herrmann and Wiche, 1987).

As discussed earlier, previous research on plectin has focused on non-neural tissue, and although plectin binds NF subunits *in vitro*, the *in vivo* significance of this observation is not clear. This chapter focuses on demonstrating that plectin is present in crude insoluble IF extracts from neural tissue and showing the localization of plectin in the adult rat central nervous system.

Methods

Experimental Tissue

A crude intermediate filament (IF) preparation from bovine and rat spinal cord was obtained using a modified axonal floatation technique, details of this method were described in Chapter 2 (Shelanski et al., 1971; Shaw and Hou, 1990). Bovine spinal cord (50 g) was obtained from the slaughter house ~1 hour postmortem and prepared using the large preparation method. Rat spinal cord (~0.2 g) was obtained rapidly (>5 minutes) after decapitation and processed using the small preparation method.

Partial purification of the 300 kD protein was accomplished using a Sephacryl S-400 (Bio-Rad) column (1.5 cm x 100 cm). Bovine IF pellet was resuspended in Buffer B (6 M Urea, 10 mM sodium phosphate (monobasic, pH 7.5), 1 mM EDTA, 1 mM TAME), and centrifuged at 150,000xg in a Sorvall T865 rotor for 45 minutes at 4°C to remove any insoluble material. The supernatant was filtered through a 0.8 µm filter followed by a 0.45 µm filter, then placed in a dialysis bag and concentrated to a final volume of 2 ml by placing dry Sephadex G-50 around the dialysis bag. The concentrated bovine IF material was separated on a Sephacryl S-400 column which was equilibrated with Buffer B containing 5 mM DTT. The flow rate was 15 ml per hour and 4 ml fractions were collected. Five µl from the even number fractions were separated on 6% SDS polyacrylamide gels.

Immuno-Blot Analysis

Proteins were separated on SDS polyacrylamide gel and transferred to nitrocellulose using 10 mM MES (pH 6.8) and 0.01% SDS for 2 hours at 90 volts (constant). For the crude IF preparation from rat spinal cord, approximately 3% of final preparation was used per lane. A detailed description for the methods used here were given in Chapter 2.

Antibodies

Monoclonal antibodies to plectin (1D8 and 1A2) and polyclonal serum to plectin (p21) were previously characterized (Wiche and Baker, 1982; Foisner et al., 1991). Monoclonal antibodies were from tissue culture supernatant and were used either undiluted or diluted 1:2. The polyclonal serum, p21, was used at 1:50. Alkaline phosphatase conjugated anti-mouse IgG secondary antibody was purchased from Sigma and used at 1:1000 dilution. Biotinylated secondary antibodies were obtained from Vector Laboratories and diluted according to the manufacturers directions. Fluorescent secondary antibodies were obtained from Jackson Laboratories and used at 1:100 dilution.

Anatomical Procedures

Both paraformaldehyde fixed and fresh frozen acetone fixed rat neural tissue were used in this study. Plectin was localized in the paraformaldehyde fixed tissue using the Vectastain Elite ABC kit. For fresh frozen acetone fixed tissue, plectin was localized using the indirect immunofluorescence procedure. Both of these anatomical methods were described in detail in Anatomical Localization section in Chapter 2.

Results

Immunoblot Studies

Besides the major IF proteins bands in a crude IF preparation from spinal cord, there were a number of proteins that copurify with IFs (Figure 3-1a, b lanes

1). Since these proteins were present after salt and detergent extractions, it was hypothesized that these proteins may functionally interact with IFs.

In particular, one high MW protein band at 300 kD on SDS polyacrylamide gel, a relatively minor component in this IF preparation, was proposed to correspond to plectin, a known 300 kD protein that interacts with IFs *in vitro* (Foisner et al., 1988). The 300 kD protein from crude IF preparation of bovine spinal cord was partially purified using Sephacryl S-400 column. Figure 3-1a shows the crude bovine IF preparation (lane 1) and Sephacryl S-400 column fractions 16-28 (lanes 2-8, respectively) in which lane 2 contains the 300 kD protein. Immunoblot of fraction 16 (Figure 3-1a, lane 9) demonstrated that the plectin monoclonal antibody ID8 labelled a 300 kD protein.

Since rat neural tissue was to be utilized in the immunocytochemical localization of plectin in the CNS, I investigated whether plectin was present in rat neural tissue and whether the plectin antibody cross-reacted with any of the other proteins present in the crude IF preparation. Immunoblot of crude rat IF preparation demonstrated that plectin was present in rat spinal cord, and the antibody did not cross-react with any of the other proteins present in the rat preparation (Figure 3-1b). The weak smearing just below the major plectin band which did not correspond to any protein band in the protein stained gel (Figure 3-1b, lane 1) was probably a degradation product of plectin (Wiche, 1989). The relatively low amount of plectin immunoreactivity detected may reflect a difficulty in electrophoretically transferring plectin as a result of plectin's very high molecular

Figure 3-1. Identification of a 300 kD protein in bovine and rat crude IF spinal cord preparations.

(A) Partial purification of 300 kD protein (arrow) from crude IF preparation from bovine spinal cord. Lane 1 is a 7.5% SDS polyacrylamide gel showing the IF preparation before purification on a Sephacryl S-400 gel filtration column. Lanes 2-8 represent even number fractions (16-28) from the gel filtration column in which fraction 16 contained the partially purified 300 kD protein. Lane 9 is an immunoblot of fraction 16 labelled with monoclonal antibody to plectin (1D8). (H: NF-H; M: NF-M; L: NF-L; G: GFAP).

(B) Immunoblot of rat spinal cord IF preparation showing plectin antibody staining. Lane 1 is a 6% SDS polyacrylamide gel of a spinal cord cytoskeletal extract stained with Serva Blue G. Lane 2 is an immunoblot strip labelled with plectin ID8 showing that the monoclonal antibody labels a 300 kD protein.

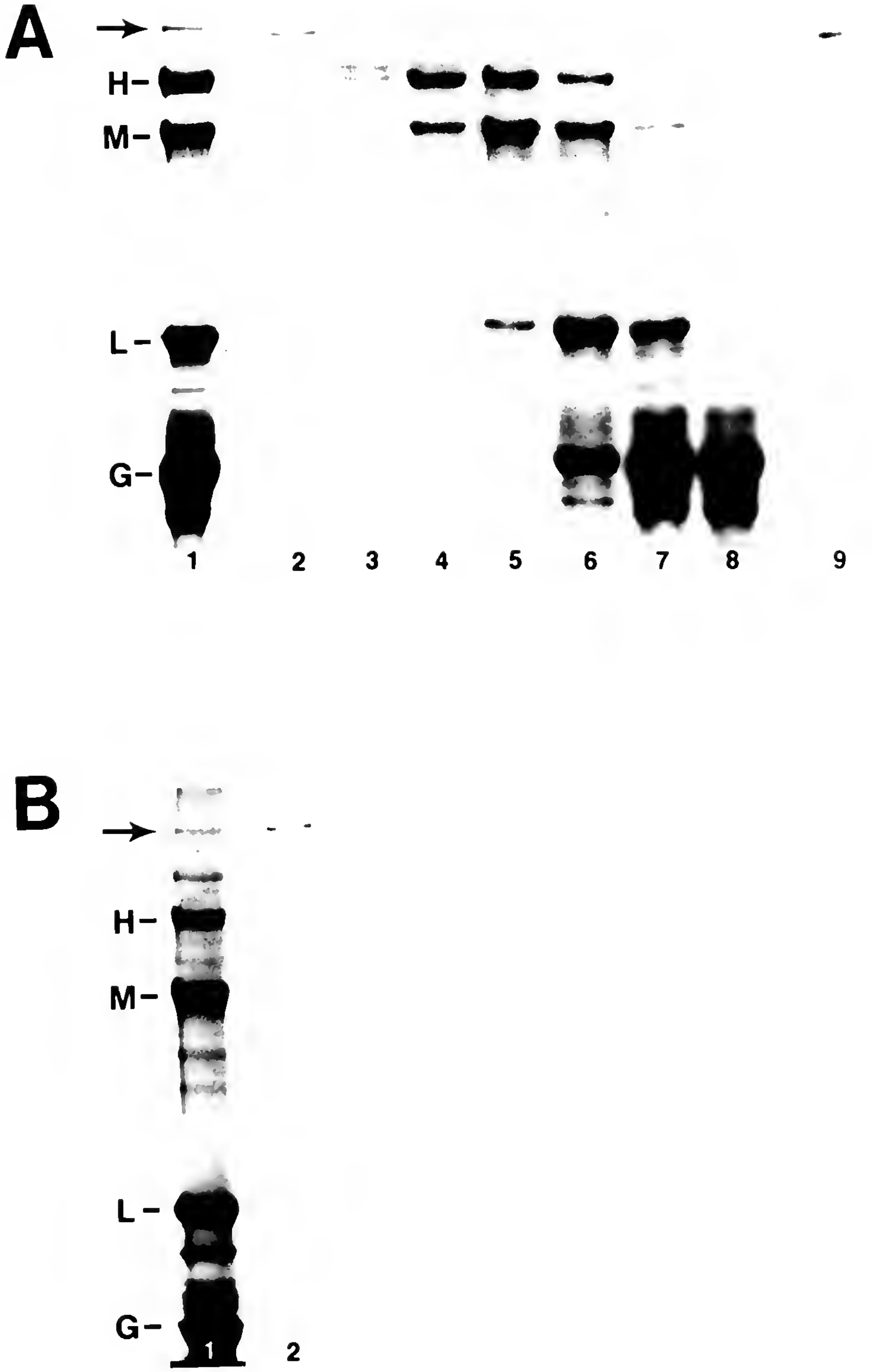
A
→
H–
M–
L–
G–
1
2
3
4
5
6
7
8
9
B
→
H–
M–
L–
G–
1
2

weight, at 527 kD. Even under optimal transfer conditions, when most of the other high molecular weight proteins were transferred completely, a substantial portion of the 300 kD protein band remained in the gel after electroblotting (data not shown). In addition, it was possible that the fairly prominent 300 kD band seen in SDS-PAGE contained other proteins (Lieska et al., 1985; Goldman and Yen, 1986) besides plectin since ion exchange chromatography demonstrates that proteins with a relative molecular weight of 300 kD are eluted off a DEAE ion exchange column at different salt concentrations (data not shown).

Comparison of Plectin to IFAP-300

In addition to plectin, there was another IFAP identified which has similar mobility on SDS polyacrylamide gel known as IFAP-300 (Lieska et al., 1985; Goldman and Yen, 1986). It was of interest to compare the amino acid analysis of these two proteins, since both plectin and IFAP-300 have similar mobilities on SDS polyacrylamide gels (300 kD), staining distribution in non-neuronal cells, and both bind to IF network. IFAP-300 amino acid composition data were taken from Lieska et al. (1985) and the plectin amino acid composition was determined from the published sequence (accession #S21876) and are presented in both table and graphical form (Shaw, 1992) in Figure 3-2. Superficially, these two proteins appear similar; however, differences were observed in the percent composition of a number of amino acids Although these two proteins do not appear to be closely related in amino acid composition, these results do not exclude the possibility that there may be some sequence similarities, and since these two proteins have

Figure 3-2. Comparison of amino acid composition of plectin and IFAP-300 proteins.

A) The percent nanomole (% nmole) for plectin and IFAP-300 is listed. Plectin amino acid composition was determined from the published sequence (Wiche et al., 1991). The amino acid composition for IFAP-300 was obtained from published paper (Lieska et al., 1985) and the values were corrected for quantitation errors using a correction factor (Shaw, 1991).

B) The amino acid composition data are represented graphically using the Star program (Shaw, 1991).

A Amino Acid Composition (% nmole)

Amino Acid	Plectin	IFAP-300
ASX	5.36	9.81
THR	5.21	5.59
SER	6.68	7.19
GLX	19.53	17.08
PRO	3.29	6.57
GLY	6.44	8.99
ALA	11.08	9.87
VAL	5.33	3.82
MET	1.35	1.29
ILE	3.32	1.97
LEU	11.38	9.11
TYR	2.24	2.43
PHE	1.79	2.69
HIS	1.57	1.91
LYS	5.53	5.20
ARG	9.90	6.48

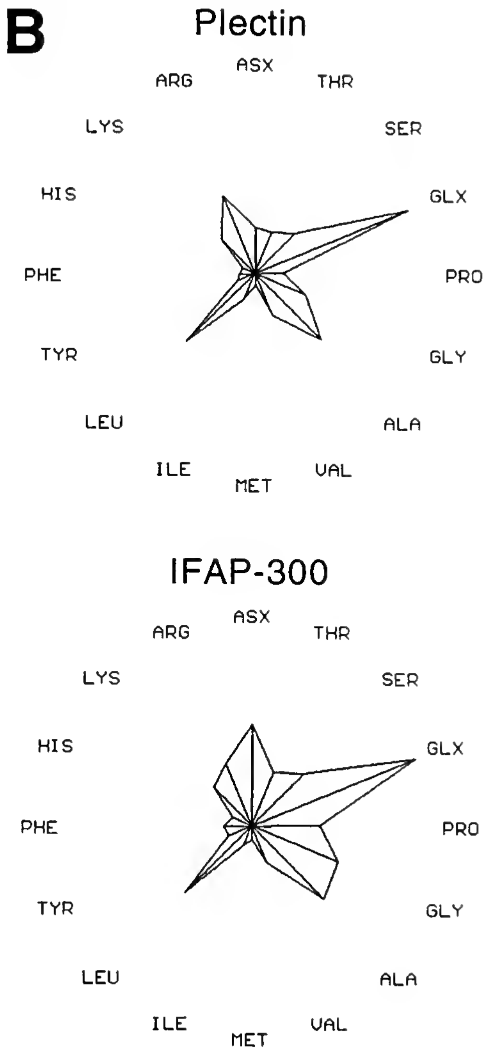

similar molecular weights, binding and tissue localization characteristics, plectin and IFAP-300 may belong to a family of high molecular weight IFAP similar to that observed with the high molecular weight microtubule associated proteins.

Localization Studies

Overall, plectin immunoreactivity in the adult rat central nervous system was predominantly associated with non-neuronal cells. In addition, plectin antibody staining was present in a subset of neurons in the brainstem and spinal cord. Immunoreactivity was generally strongest at the periphery of cells.

Telencephalon and diencephalon. Plectin immunoreactivity was absent in neurons of the telencephalon and diencephalon. The only cells which labelled with the plectin antibody in the cortical gray matter of the telencephalon were astrocytes located in the ventromedial portion of the temporal cortex near the pial surface. The density of astrocytic labelling with plectin antibodies decreased rapidly away from the pial surface (Figure 3-3a). Although this labelling pattern may be attributed to edge effect, a similar staining pattern was not observed in any other cortical regions near the pia mater.

In the diencephalon, plectin positive astrocytes were observed at the ventrolateral portion of the hypothalamus (Figure 3-3b). Plectin immunoreactivity was found prominently in astrocytes throughout the white matter fiber tracts including the optic tract (Figure 3-3c), corpus callosum, internal capsule, fornix, and stria medullaris. Pronounced plectin immunoreactivity was observed in the hypothalamus surrounding the third ventricle. Both ependymal cells lining the

Figure 3-3. Plectin immunoreactivity (ID8) of astrocytes in white and gray matter of the telencephalon and diencephalon.

(A) The ventro-medial portion of the temporal cortex was the only cerebral cortical area where plectin positive astrocytes were localized as visualized with DAB (arrows). Scale bar: 25 µm.

(B) The ventro-lateral portion of the hypothalamus showed diffuse plectin immunoreactivity of astrocytes(open arrow). Scale bar: 25 µm.

(C) White matter regions in the rat nervous system demonstrated plectin antibody labelling of astrocytes as shown in the optic tract as visualized with immunoflurescent secondary antibodies (open arrow). Scale bar: 25 µm.

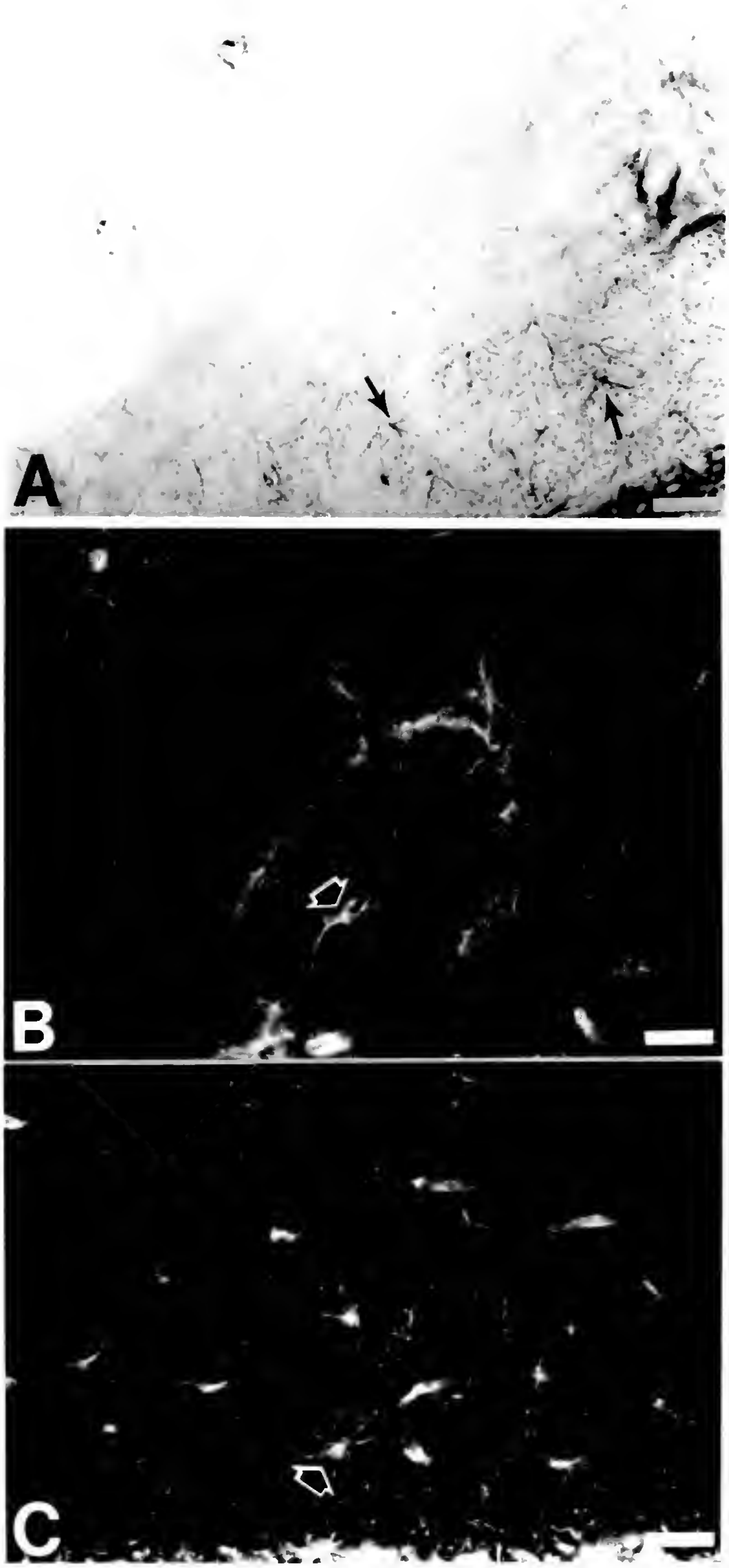
A
B
C

dorsal portion and tanycytes, specialized ependymal cells, lining the ventral portion of the third ventricle were plectin positive (Figure 3-4a). The plectin antibody labelling of ependymal cells showed strong staining at the plasma membrane, diffuse staining throughout the cytoplasm, and dense staining between the ependymal cells (Figure 3-4b). The ependymal labelling pattern was observed in all ventricles. A network of astrocytic fibers labelled with plectin antibodies was seen in the subependymal layer (Figure 3-4b). In tanycytes, plectin immunoreactivity was associated with the periphery of the cell body as well as with the fibrous process (Figure 3-4c).

Cerebellum. Plectin immunoreactivity in the cerebellum was observed in Bergmann glial fibers in the molecular layer, and in astrocytes in the granular cell layer and white fiber tract layer (Figure 3-5a). The entire extent of Bergmann glial processes were labelled with plectin antibodies; however, the strongest staining was associated with Bergmann fibers terminal endings at the pial surface. The relative intensity difference between the knob-like endings and processes of Bergmann glia fibers was observed distinctly in a immunofluorescent higher power view of molecular layer of cerebellum (Figure 3-5b). With respect to the terminal endings of the Bergmann fibers which forms the external glial limiting membrane in the cerebellum, it was difficult to determine whether these subpial structures which were plectin positive formed conical and/or foot type endings (Palay and Chan-Palay, 1974). The staining pattern once again showed strong labelling at the periphery of the cells.

Figure 3-4. Plectin immunoreactivity (ID8) in the rostral hypothalamus surrounding the third ventricle as visualized with DAB (3V).

(A) Cells lining the third ventricle are plectin positive and are of two types: ependymal cells in the dorsal portion and tanycytes in the ventral portion. Scale bar: 100 μm

(B) High power view of ependymal cells which demonstrates plectin antibody staining throughout the cytoplasm with highest density of labelling at the cell membrane (arrowheads). Light astrocytic staining is observed in the subependymal cell layer just lateral to the ependymal cells. Scale bar: 25 μm.

(C) High power view of tanycytes which shows plectin immunoreactivity solely around the plasma membrane (arrowheads) and radial process of the tanycyte (arrows). Scale bar: 25 μm.

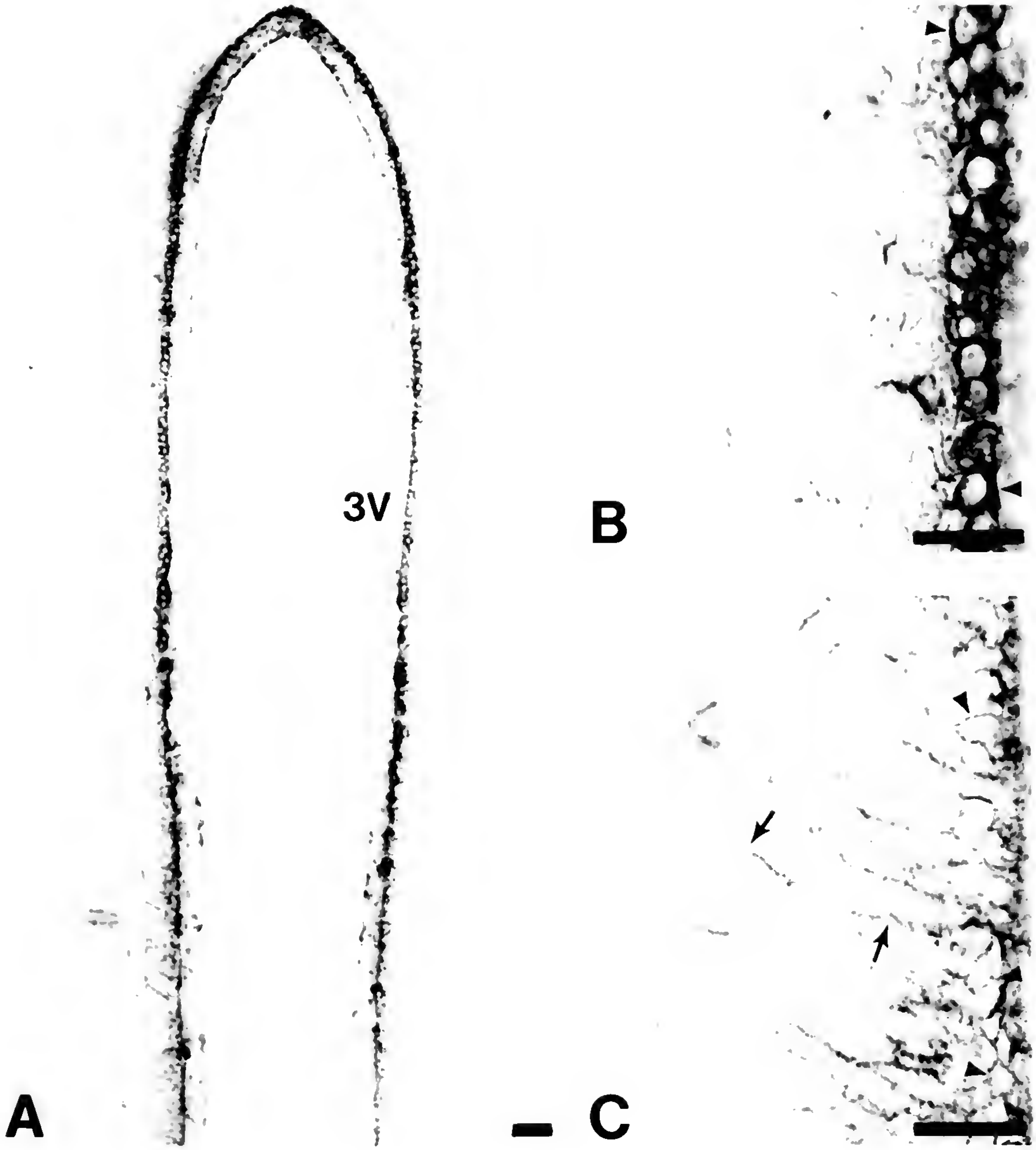
3V
A
B
C

Figure 3-5. Plectin immunoreactivity (IA2 and ID8) in the cerebellum.

(A) In the cerebellum plectin antibody (IA2) labels the full extent of the Bergmann glia process (arrow) in the molecular layer (ml) with pronounced labelling at the pia surface (arrowhead) as visualized with DAB. Weak plectin immunoreactivity is present in the granular cell layer (gcl) and appears to correspond to astocytic processes. Note the absence of plectin antibody staining in the purkinje cell layer (pcl). Scale bar: 100 μm.

(B) Higher power view of the cerebellum molecular layer showing the prominent fluorescent labelling of the Bergmann glia terminal processes using ID8 antibody (arrows) as visualized with immunoflurescent secondary antibodies. In comparison the Bergmann glia fibers are weakly labelled with plectin antibody (open arrows). Scale bar: 25 μm.

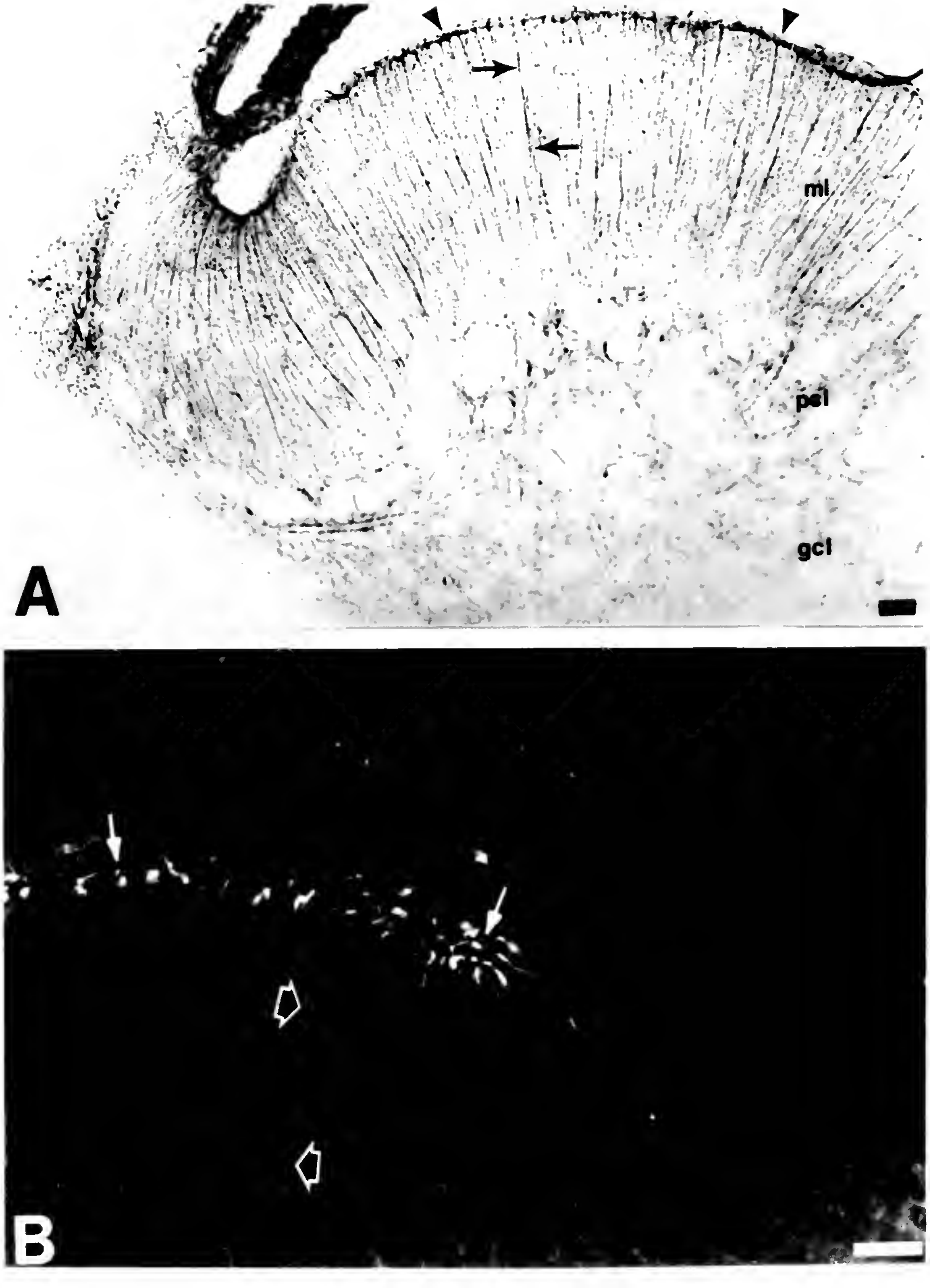
ml
pcl
gcl
A
B

Brainstem and spinal cord. The general pattern of the plectin antibody staining pattern in the brainstem and spinal cord localized plectin primarily to non-neuronal cells in the white matter tracts and to a subset of motoneurons. At low magnification of the brainstem at the caudal medulla, plectin antibody labelling was localized to astrocytes in the periphery and motoneurons in the nucleus ambiguus (Figure 3-6a). A high magnification view of the ventrolateral aspect showed plectin immunoreactivity in the inferior cerebellar peduncle and in the spinal tract of cranial nerve V (Figure 3-6b). Plectin antibody labelling was pronounced at the outer boundary of the inferior cerebellar peduncle as well as in glial fibers traversing the inferior cerebellar peduncle. Throughout this region plectin positive astrocytes were observed. Plectin staining was not observed in neurons associated with the spinal nucleus of cranial nerve V (Figure 3-6b). In contrast, intense plectin immunoreactivity was observed in motoneurons of nucleus ambiguus (Figure 3-6c). However, there appeared to be a gradient in plectin antibody staining in motoneurons such that some motoneurons labelled strongly while others stained lightly (Figure 3-6c). This selective type of motoneuron staining was also observed in the facial nucleus. In the pyramidal tract, plectin positive astrocytes were seen as a network of fibers located adjacent to the pial surface (Figure 3-6d).

In the spinal cord, plectin immunoreactivity was observed at all levels with a similar distribution. Plectin antibody labelling was observed in ependymal cells lining the central canal, in astrocytes in the dorsal columns, in glial fibers transversing the white matter, and in motoneurons in the ventral horn (Figure 3-

Figure 3-6. Plectin immunoreactivity (ID8) in the caudal brainstem.

(A) Ventrolateral quadrant of the medulla shows plectin antibody labelling both neurons and glia. Arrow is pointing to the nucleus ambiguus.(spt: spinal tract trigeminal nerve; icp: inferior cerebellar peduncle; pt: pyramidal tract). Scale bar: 100 µm.

(B) Spinal tract of V and inferior cerebellar peduncle (icp) labelled with the plectin antibody. Prevalent plectin immunoreactivity is observed at the outer boundary of icp and in glial fibers transversing icp (arrows). Scale bar: 50 µm.

(C) Motoneurons in nucleus ambiguus label with plectin antibody. There appears to be a gradient of staining with some motoneurons staining strongly (arrows) while others stain lightly (arrowhead). Around motoneuron cell bodies there is a dense particulate staining. Scale bar: 50 µm.

(D) At the periphery of the pyramidal tracts (pt), a network of plectin positive astrocytes are concentrated near the ventral boundary (arrowheads). Scale bar: 50 µm.

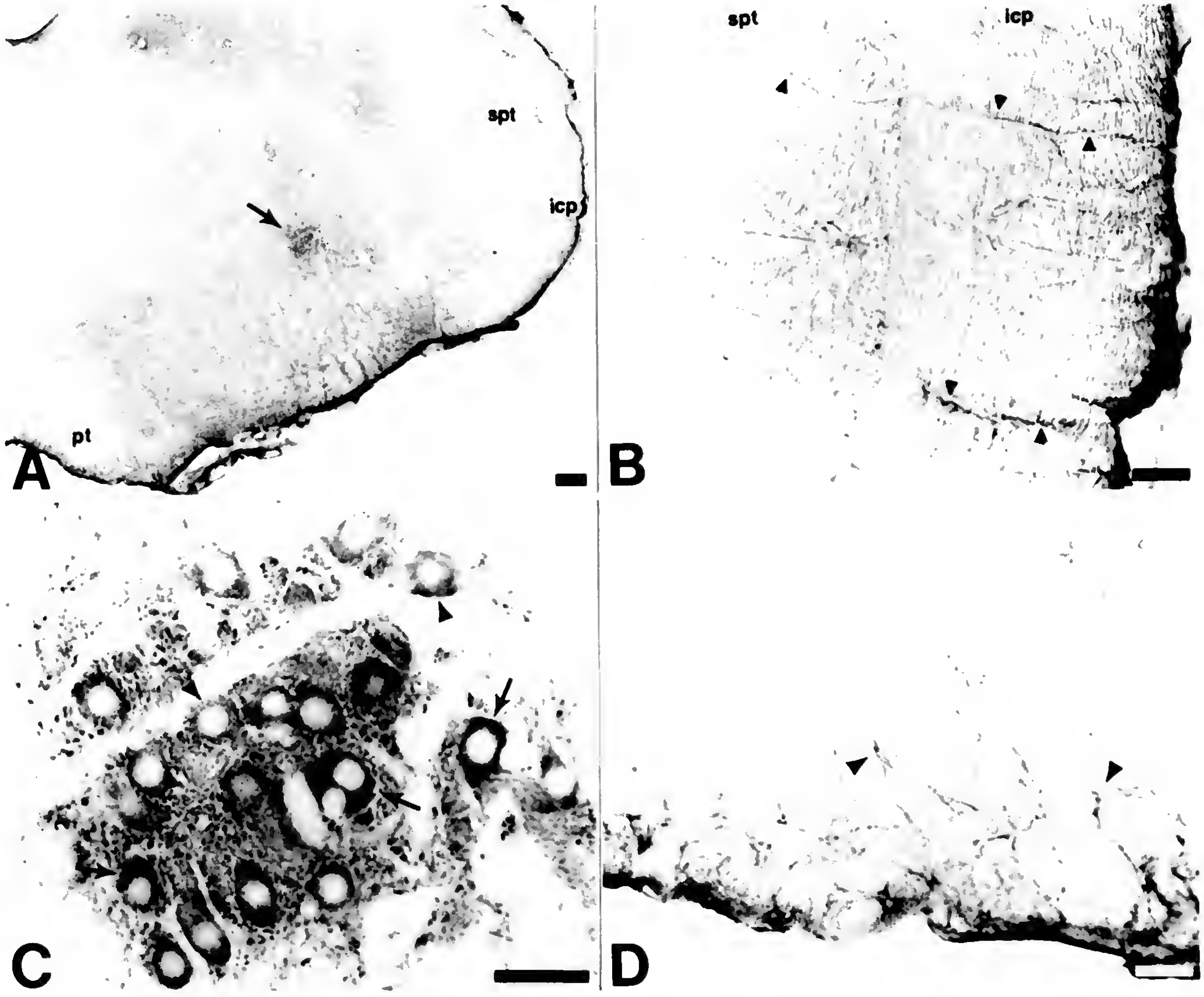
spt
icp
pt
A
spt
icp
B
C
D

7a). At a higher magnification, the ventral white matter showed plectin antibody staining of glia cells which radially span from the pial surface to the gray matter (Figure 3-7b). A closer examination of motoneurons in lamina IX of the spinal cord gray matter showed that plectin immunoreactivity was associated with the cell body and dendrites in a subpopulation of motoneurons (Figure 3-7c). Plectin staining appeared to be excluded from the nucleus. In the vicinity of plectin positive motoneurons, particulate staining was observed which may be cross-sections of dendrites (Figure 3-7c.).

Choroid plexus and blood vessels. Choroidal epithelial cells showed prominent plectin immunoreactivity (Figure 3-8a). Labelling with plectin antibodies was observed throughout the cytoplasm with particularly intense staining at the periphery and at points of contact between adjacent cells Differential plectin antibody staining patterns were observed with blood vessels. Plectin immunoreactivity was predominantly associated with endothelial cells of large blood vessels (Figure 3-8b) but also was observed sporadically with smaller blood vessels (Figure 3-8c).

Discussion

These experiments were initiated in an attempt to identify a salt and detergent resistant 300 kD protein band found in spinal cord cytoskeleton preparations which could represent a NF binding protein. Biochemically, plectin was at least a constituent of this 300 kD protein band, and was found in crude IF preparation of

Figure 3-7. Plectin immunoreactivity (ID8) in the cervical spinal cord.

(A) Low magnification view of the cervical spinal cord that demonstrates plectin antibody labelling of astrocytes in the dorsal columns (dc), radially oriented glia in white matter (wm) and motoneurons in the ventral horn (vh). Scale bar: 100 μm

(B) High magnification view of lateral white matter in which the intensity of plectin antibody staining is graded. The strongest labelling is near the periphery (arrows). Scale bar: 50 μm.

(C) High magnification view of motoneurons in lamina IX showing that plectin immunoreactivity is associated with the cell body and processes of motoneurons in the ventral horn. Particulate staining is observed in the vicinity of motoneurons (arrowheads). Scale bar: 50 μm.

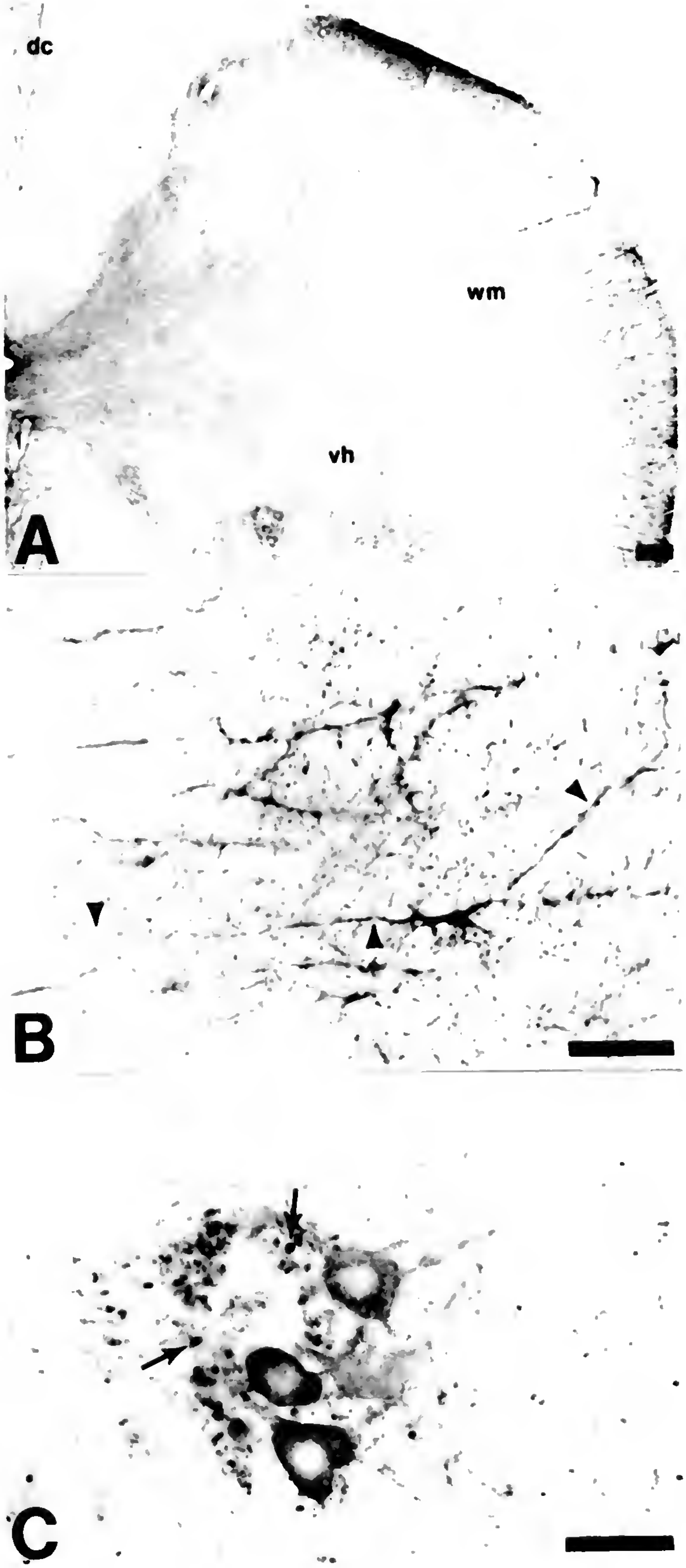
dc
wm
vh
A
B
C

Figure 3-8. Plectin immunoreactivity (p21) in choroid plexus and blood vessels.

(A) Choroidal epithelial cells show diffuse plectin antibody staining throughout the cytoplasm and concentrated staining at the periphery of the cell (arrow). Scale bar: 25 µm.

(B) Pericollosal artery labels strongly with the plectin antibody. Staining is localized predominantly to the inner membrane of endothelial cells (open arrow). Scale bar: 25 µm.

(C) A smaller blood vessel in the temporal cortex labels positive with plectin antibody. Note the astrocytic processes surrounding the blood vessel are labelled with the plectin antibody. Scale bar: 25 µm.

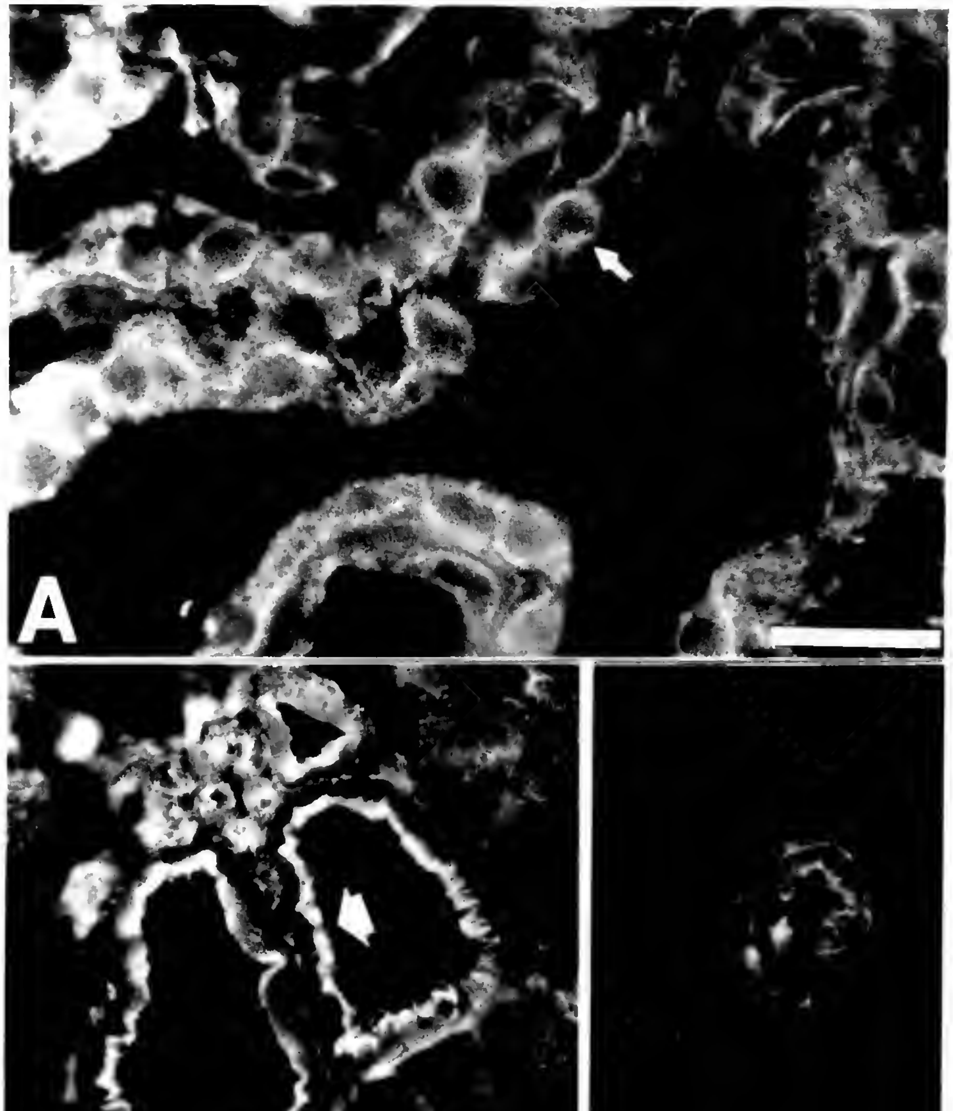
A
B
C

the central nervous system.

One approach to begin to understand the role of a particular protein in the nervous system is to examine the cellular distribution. Plectin immunoreactivity was observed in a number of different cell types in the central nervous system with varying staining intensities (Table 5-1). To summarize these data, prominent plectin antibody staining was localized to the periphery of ependymal cells lining the ventricles, to tanycytes, to choroidal epithelial cells, to endothelial cells and to pia mater cells. In addition, dense plectin immunoreactivity was observed at junctions between choroidal epithelial cells which may be related to tight junctions forming part of the barrier between the blood and cerebral spinal fluid (CSF) (Peters et al., 1991). Previous research by Wiche and co-workers (1989) demonstrated that plectin was associated to various types of junctional zones. An interesting and rather unexpected finding was that plectin antibodies labelled the perikarya of a few neurons in the central nervous system. Generally, the staining pattern of the plectin antibodies in non-neuronal cells of the nervous system coincided well with previous work on the distribution of plectin outside the nervous system (Wiche, 1989) and was similar to the vimentin staining pattern in the central nervous system (Shaw et al., 1981; Pixley et al., 1981; Yen and Fields, 1981). The previous studies of plectin concluded that plectin was widely but not ubiquitously distributed with the peripheral regions of cells, with some overlap with the IF pattern and submembraneous component. The cellular distribution of plectin in the CNS appeared to be similar to that observed in non-neural tissue in that

Table 3-1. The distribution of plectin in different cell types of the adult rat central nervous system.

Cell Type	Staining
Neuronal Cells	
cortical pyramidal	-
cortical interneurons	-
cerebellar granule	-
cerebellar Purkinje	-
brain stem motoneurons	+++/++/+/-
spinal cord motoneurons	+++/++/+/-
Ependyma	
choroid plexus	+++
columnar epithelia	+++
tanycytes	+++
subependyma	++
Glial Cells	
astrocytes (white matter)	+++
astrocytes (gray matter)	+/-
Bergmann fibers	++
Other	
endothelial linings	+++/++/+/-

+: indicates that plectin was localized in these cells, and number of + reflects intensity of staining; -: indicates that plectin was not observed in these cells plectin immunoreactivity was usually associated with the plasma membrane of the cells.

A relationship of plectin with the blood-brain barrier (BBB) is suggested by a tendency for plectin to be concentrated at all three of the elements of the BBB, namely the pia, the walls of blood vessels and the linings of ventricles. However, plectin immunoreactivity was not associated with all blood vessels and was only infrequently associated with glial endfeet surrounding blood vessels. The BBB, therefore, is not invariably associated with plectin immunoreactivity. Consequently one can conclude that plectin is not absolutely required in all parts of this barrier. In contrast, there is a consistent and strong layer of plectin immunoreactivity associated with the ependymal layer including the choroid plexus, suggesting that plectin may mechanically stabilize the submembraneous cytoskeleton and IF components to form the three-dimension structure of the choroid plexus. In line with this idea, previous ultrastructural studies have demonstrated a tendency for plectin to be localized at interfaces between different tissues and especially between tissues and fluid filled cavities. For example plectin is heavily concentrated at the surfaces of kidney glomeruli, liver bile canaliculi, bladder urothelium and gut villi (Wiche et al., 1983).

The selective staining pattern of plectin to subsets of motoneurons in the brainstem and spinal cord is intriguing. One possible explanation for this unique finding is that plectin may be associating with a particular NF subunit. Of the five specific NF subunits, peripherin appears to be the best candidate. Peripherin has a more selective distribution than the NF-triplet proteins and in contrast to cortical localization of α-internexin, peripherin is localized to motoneurons of the spinal cord and brainstem (Portier et al., 1984; Parysek and Goldman, 1988; Greene, 1989; Goldstein et al., 1991).

A common theme in this distinct plectin staining pattern is that plectin may be associating with class 3 IF proteins (based on Steinert and Roop classification scheme, 1988). Since peripherin and vimentin are similar in structure, it is likely unlikely that plectin could be interacting at a similar site present in both proteins. To shed some light on the selective cellular interactions of plectin in the nervous system, Chapter 6 focuses on examining the distribution of plectin with IFs found in the neural tissue.

Notes

Portions of this chapter are from a paper entitled "The Distribution of Plectin, an Intermediate Filament Associated Protein, in the Adult Rat Central Nervous System" by L.D. Errante, G. Wiche, G. Shaw. Journal of Neuroscience Research 37: 515-528. Copyrighted © 1994 by Wiley-Liss. Text is used with the permission of Wiley-Liss, a division of John Wiley & Sons, Inc.

CHAPTER 4

CO-LOCALIZATION OF PLECTIN AND INTERMEDIATE FILAMENTS IN THE RAT NERVOUS SYSTEM

Introduction

Intermediate filaments (IFs) are a family of fibrous proteins found in most eukaryotic cells and comprise a major component of the cytoskeletal network. In addition to being organized into 6 classes based on sequence analysis (Steinert and Roop, 1988), IFs can be categorized based on the types of cells they are localized to. The strict cell-type specific expression of IFs, coupled with their high abundance has permitted the extensive use of IF antibodies as convenient cell-type specific markers. For example, in the nervous system, NF-triplet proteins, α-internexin and peripherin are localized exclusively to neurons, and different neuron types tend to have distinctly different IF composition (Shaw et al., 1981; Yen and Fields, 1981; Portier et al., 1984; Pachter and Liem, 1985; Parysek and Goldman, 1988; Chiu et al., 1989). GFAP is localized to specific glia cell types (Yen and Fields, 1981; Shaw et al., 1981) while vimentin can be found in subsets of glia, ependyma and endothelia as well as some unusual neurons (Yen and Fields, 1981; Shaw et al., 1981; Draeger, 1983; Shaw et al., 1983; Schwob et al., 1986).

IF proteins are similar to the other major cytoskeletal proteins, microtubules and actin, in that IFs have a number a polypeptides associated with them. Unlike microtubule- and microfilament-associated protein, intermediate filament associated proteins (IFAPs) are not well characterized especially in neural tissue. Due to the lack of function associated with IFs in general, proteins have been classified as specific IFAPs based on minimal criteria such that only one of the following conditions need to be satisfied: (1) co-purification with IFs *in vitro*; (2) cellular co-distribution with IFs; (3) binding to IFs or subunit proteins *in vitro*; and (4) have an effect on filament organization or assembly (Foisner and Wiche, 1991).

Plectin is one of the few IFAP to have satisfied more than one of these criteria including solid phase binding to all IF proteins examined and co-localization with vimentin (Wiche, 1989). In the nervous system, plectin has been shown to co-purify with crude IF preparations and to be localized in specific cell types that contain IF proteins (Chapter 3). To address possible *in vivo* interactions between plectin and IF proteins in the nervous system, we examined the co-distribution of plectin with NF triplet proteins, peripherin, vimentin, and GFAP.

Methods

Experimental Tissue and Immunocytochemistry

For immunofluorescent studies, adult rats were sacrificed by decapitation. Neural tissue was dissected out immediately, quickly frozen and stored at -70°C. Immunofluorescent procedures were described in Chapter 2.

For facial nerve axotomy, adult rats were anesthetized with methoxyflurane. An incision was made just behind the right ear, the major branch of the facial nerve was cut, and the incision was closed with surgical staples. Six to seven days post-lesion rats were anesthetized with pentobarbital, and animals were killed by decapitation or after intracardial perfusion with 4% paraformaldehyde as described in detail in Chapter 2. In the case of the paraformaldehyde fix tissue, the brainstem was blocked, immersed in 30% sucrose in PBS until it sunk and then frozen on dry ice for 1 hour. Tissue was cut at 10 µm and placed in PBS and treated in the same manner as previously described for paraformaldehyde tissue (Chapter 2).

Antibodies

Plectin monoclonal antibodies, clones 1D8 and IA2 (diluted 1:2), and rabbit polyclonal serum, p21 (diluted 1:50), were previously characterized (Wiche and Baker, 1982; Foisner et al., 1991). NF-M rabbit polyclonal sera, R9 (diluted 1:200), to the KE (lysine-glutamic acid) region of NF-M was made using NF fusion protein RM:677-845. NF-H rabbit polyclonal antibody, R14 (diluted 1:200), to the KSP (lysine-serine-proline) region of NF-H was made using NF fusion protein RH:559-794 (Harris et al., 1991). Monoclonal antibodies against glial fibrillary acidic protein (GFAP), clone GA5 (diluted 1:1000) and vimentin, clone V9 (diluted 1:200), were purchased from Sigma (Debus et al., 1983; Osborn et al., 1984). Rabbit polyclonal antibody to GFAP (diliuted 1:1000) was a gift from Dr. P. J. Reier. Peripherin rabbit polyclonal sera, R19 and R20 (diluted 1:200) and mouse monoclonal antibody, 8G2 (undiluted), were produced in our laboratory using a trp-E fusion protein construct in the pATH expression vector which was a gift of Dr. Edward Ziff (see Gorham et al., 1990). The fusion protein was expressed in *Escherichia coli* in bulk and purified from inclusion body preparations by DEAE-cellulose ion exchange chromatography as recently described for other trp-E fusion proteins (Harris et al., 1991). The purified fusion protein was injected into rabbits and mice to raise polyclonal and monoclonal antibodies using standard procedures (see Chapter 2).

Results

Immunoblot Studies

Initial characterization of peripherin antibodies were performed on crude IF preparations from rat spinal cord to make sure that the antibody was not cross-reacting with any other cytoskeletal proteins. Both peripherin monoclonal antibody (8G2) and polyclonal antibody (R20) labelled, cleanly and specifically, a single protein band at ~57 kD. The peripherin protein band migrated at a slightly higher apparent molecular weight than vimentin in crude IF spinal cord preparation (Figure 4-1, lanes 2-4, respectively). Peripherin polyclonal antibody R19 also showed the same labelling of a single band at 57 kD (data not shown).

Co-localization in Cultured Cells

Dorsal Root Ganglion (DRG) Cells. Plectin antibodies labelled most of the cell types in DRG cultures isolated from postnatal day 1 rat pups. The non-neuronal cells or satellite cells consisted of two basic types; flat ameboid shaped and spindle shaped which are illustrated in Figure 4-2. Plectin immunoreactivity was localized throughout the cell body and the processes of the spindle shaped

Figure 4-1. Characterization of peripherin polyclonal and monoclonal antibodies.

Lane 1 shows a serva blue stained 6% SDS polyacrylamide gel of crude IF preparation for rat spinal cord. Lanes 2 and 3 are immunoblots of this material labelled with 8G2 and R20, respectively. These results show that both the monoclonal and polyclonal antibodies to peripherin labelled a single protein band at ~57 kD. Lane 4 is an immunoblot of the same material labelled with vimentin monoclonal antibody (V9) which demonstrates that the vimentin protein band is located just below peripherin on a 6% SDS polyacrylamide gel.

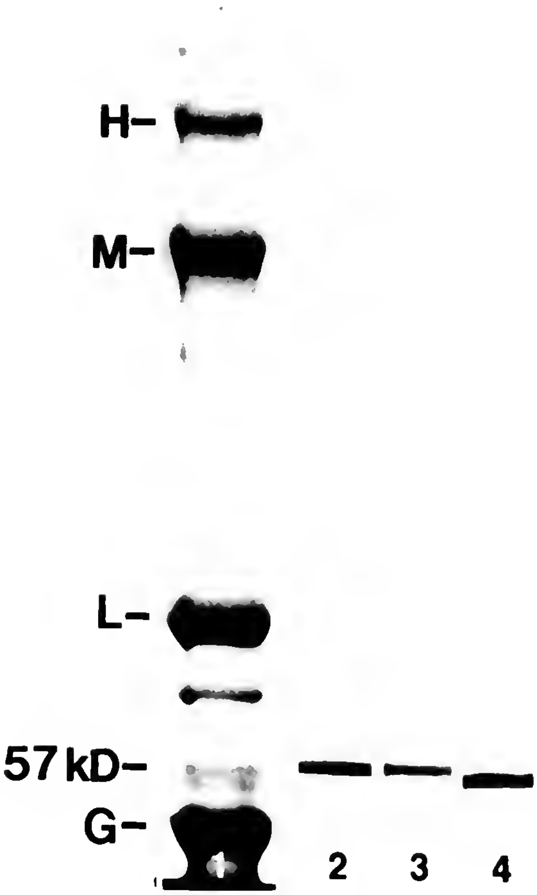
H–
M–
L–
57 kD–
G–
1
2
3
4

cells (Figure 4-2a, right side). In contrast the larger, flatter cells showed particularly strong plectin immunoreactivity surrounding the nuclei and this labelling intensity decreased dramatically at the peripheral regions of the cell (Figure 4-2a, left side). Double labelling of these cells with vimentin revealed that plectin immunoreactivity (Figure 4-2a) was localized discontinuously along vimentin filamentous network (Figure 4-2b).

Plectin immunoreactivity in DRG neurons was similar to that observed for the non-neuronal cells in tissue culture. Plectin antibodies strongly labelled the cell body of DRG cells and weakly labelled the neuritic processes (Figure 4-3a); whereas, peripherin labelled the cell body and neurites with similar intensity. The peripherin antibody labelling pattern was consistent to that observed with NF triplet protein antibodies in DRG (Shaw and Weber, 1981).

Phenocytoma (PC12) Cells. The distribution of plectin was compared to NFs in both undifferentiated and differentiated PC12 cells. In undifferentiated PC12 cells NF antibody labelling was found adjacent to the nucleus and in a tight ball (Figure 4-3d), whereas plectin immunoreactivity was found diffusely throughout the cell and with some overlap with the NF staining pattern (Figure 4-3c). After exposure to nerve growth factor (NGF), PC12 cells stop dividing and differentiate which results in the formation of neuritic-like processes as well as acquiring similar properties as sympathetic neurons. In differentiated PC12 cells, plectin antibodies labelled the cell body strongly with weak labelling in the processes that was similar to that observed in the DRG cultures (Figure 4-3e). Additionally, plectin

Figure 4-2. Co-localization of plectin (p21) and vimentin (V9) in non-neuronal cells from DRG cultures.

(A-B) Plectin immunoreactivity (A) is localized primarily in the cell body of both types of non-neuronal cells; however, there is some labelling in the periphery of the flat cell and in the processes of the spindle-shaped cells. Vimentin antibody labelling (B) demonstrates a filamentous network throughout the cells with selective overlap with the plectin staining pattern. Scale bar: 25 μm.

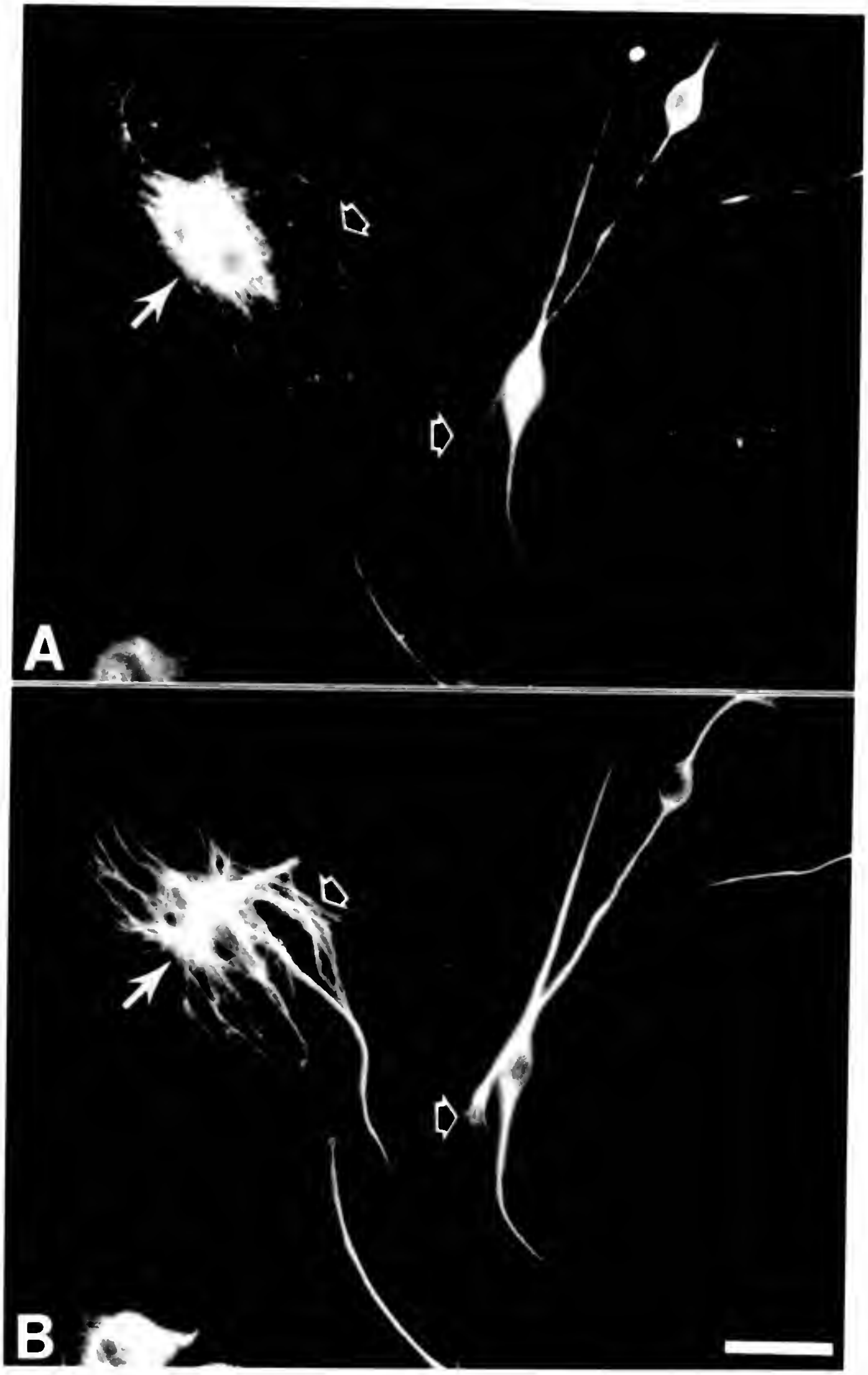
A
B

Figure 4-3. Co-localization of plectin (ID8) and NF subunits in DRG cells and PC12 cells.

(A-B) In DRG cells plectin immunoreactivity (A) was almost exclusively localized to the cell body (arrow) with only weak labelling in the neuritic processes, whereas, peripherin antibody (R20) labelled the cell body as well as the neuritic processes with similar intensity (B). Scale bar: 25 µm.

(C-D) In undifferentiated PC12 cells, plectin antibody labelling (C) was observed diffusely throughout the cytoplasm with some areas of the cell body staining more intensely than others (arrows). Double-labelling with NF antibody (D) demonstrated that there was some overlap with the plectin labelling pattern. Scale bar: 25 µm.

(E-F) In NGF differentiated PC12 cells the pattern of plectin (E) and NF (F) antibody labelling was somewhat similar in the cell body (large arrow); however, NF labelling was more intense in the proximal neurite (small arrow) and plectin immunoreactivity was more intense along certain points of the neurite (arrowhead). Scale bar: 25 µm.

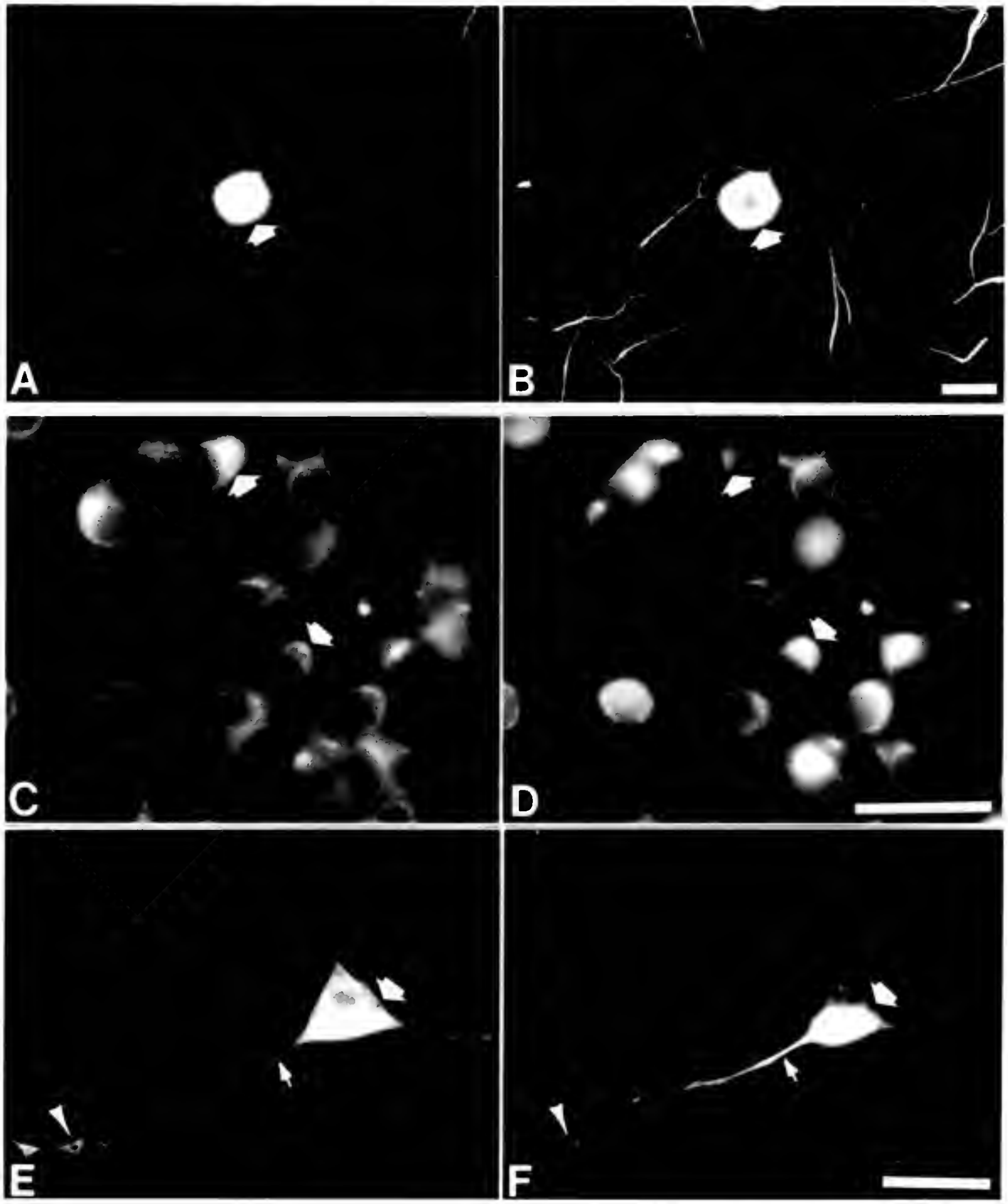
A
B
C
D
E
F

immunoreactivity was strong at particular points along the neuritic process (Figure 4-3e, arrowhead). In contrast, NF immunoreactivity was localized to the cell body and in the initial segment of the neurite-like process (Figure 4-3f).

Co-Localization Studies Along the Rat Neural Axis

Plectin and Vimentin. Prior research localized vimentin primarily to non-neuronal cell: astrocytes, radial glial cells, ependymal cells, meninges and blood vessels in the nervous system (Pixley et al., 1981; Shaw et al., 1981; Yen and Fields, 1981). Plectin distribution in the nervous system most closely corresponded to that of vimentin, when compared to all of the known IF subunits, although differences in the staining pattern appear in the extent and type of labelling within cells. A diffuse plectin antibody staining pattern was evident in white matter astrocytes and choroidal epithelial cells in contrast to the well defined filamentous pattern of vimentin within the same cells (Figure 4-2). A striking difference between antibody labelling patterns was visualized in the Bergmann glial fibers of the cerebellum (Figure 4-4 a-d). Plectin immunoreactivity was associated predominantly with the distal tips of Bergmann glia cell process at the pial surface whereas vimentin immunoreactivity was equally distributed throughout the process and appears to be diminished or absent from the terminal endings. Although plectin was localized to some blood vessels shown previously in Chapter 3 as well as in Figure 4-4 a, it was absent from the blood vessels in certain CNS areas such as in the diencephalon. A section through the thalamus-fornix junction double-stained with vimentin and plectin antibodies showed that both antibodies labelled the astrocytes in the fornix; however, only the vimentin antibody labelled the blood vessels located in the thalamus (Figure 4-4 e,f). Plectin immunoreactivity appeared to be more strongly associated with larger vessels or vessels located at the pial surface such as the pericallosal artery (Chapter 3). In addition, plectin did not completely co-localize with vimentin in the sciatic nerve. Both plectin and vimentin immunoreactivities overlapped in labelling the outer portion of the myelin sheath surrounding the axon; however, plectin polyclonal serum additionally intensely labelled the inner portion of the myelin sheath (Figure 4-4 g,h).

Plectin and GFAP. GFAP was previously shown to be localized to astrocytes and certain radial glial cells in the nervous system (Shaw et al., 1981; Yen and Fields, 1981). As described above, plectin immunoreactivity was localized to the ependymal cells and choroid plexus cells with pronounced staining at the plasma membrane (Figure 4-5 a). In contrast, GFAP antibody staining was found predominantly in astrocytic fibers surrounding the ventricle (Figure 4-5 b). Frequently GFAP positive cells did not label with plectin antibodies (Figure 4-5 c,d), although the white matter astrocytes which are vimentin positive in rat are also plectin and GFAP positive (Figure 4-5 a,b,g,h). The plectin antibody showed punctate staining around the axonal bundles in the caudate nucleus which was similar to that seen in the thalamus; however, there was no distinct cellular staining except for a few lightly stained astrocytes (Figure 4-5 c). In contrast, GFAP immunoreactivity was observed throughout the caudate nucleus especially surrounding the axonal bundles (Figure 4-5 d). Small diameter blood vessels in

Figure 4-4. Co-localization experiment with antibodies to plectin (p21) (A,C,E,G) and vimentin (V9) (B,D,F,H).

(A-B) In cerebellar molecular layer, plectin immunoreactivity (A) is localized to the Bergman glia processes with the strongest staining at the terminal endings just beneath the pia surface. In contrast, vimentin antibody (B) uniformly labels the entire extent of the Bergmann glia process. A blood vessel is labelled with antibodies to both plectin and vimentin (arrowhead). ml: molecular layer; pcl: purkinje cell layer. Scale bar: 50 μm.

(C-D) A high magnification view of A and B showing the terminal endings of the Bergman glia fibers. Plectin immunoreactivity (C) was observed most intensely at the terminal endings in which some of these endings were double-labelled with vimentin (open arrow) whereas others were not (arrowhead). Scale bar: 25 μm.

(E-F) At the thalamus and fornix junction, plectin antibody (E) labels astrocytes in white matter which corresponds to vimentin immunoreactivity (F) in the fornix. In contrast, plectin immunoreactivity (E) is completely absent from blood vessels in the thalamus which label with vimentin antibody (arrows) (F). Scale bar: 25 μm.

(G-H) In a cross-section of sciatic nerve, similar labelling pattern is observed for plectin (G) and vimentin (H) in the sciatic nerve outer myelin sheath layer (arrows); however, plectin antibody also labelled the myelin membrane surrounding the axon (arrowheads). Scale bar: 25 μm.

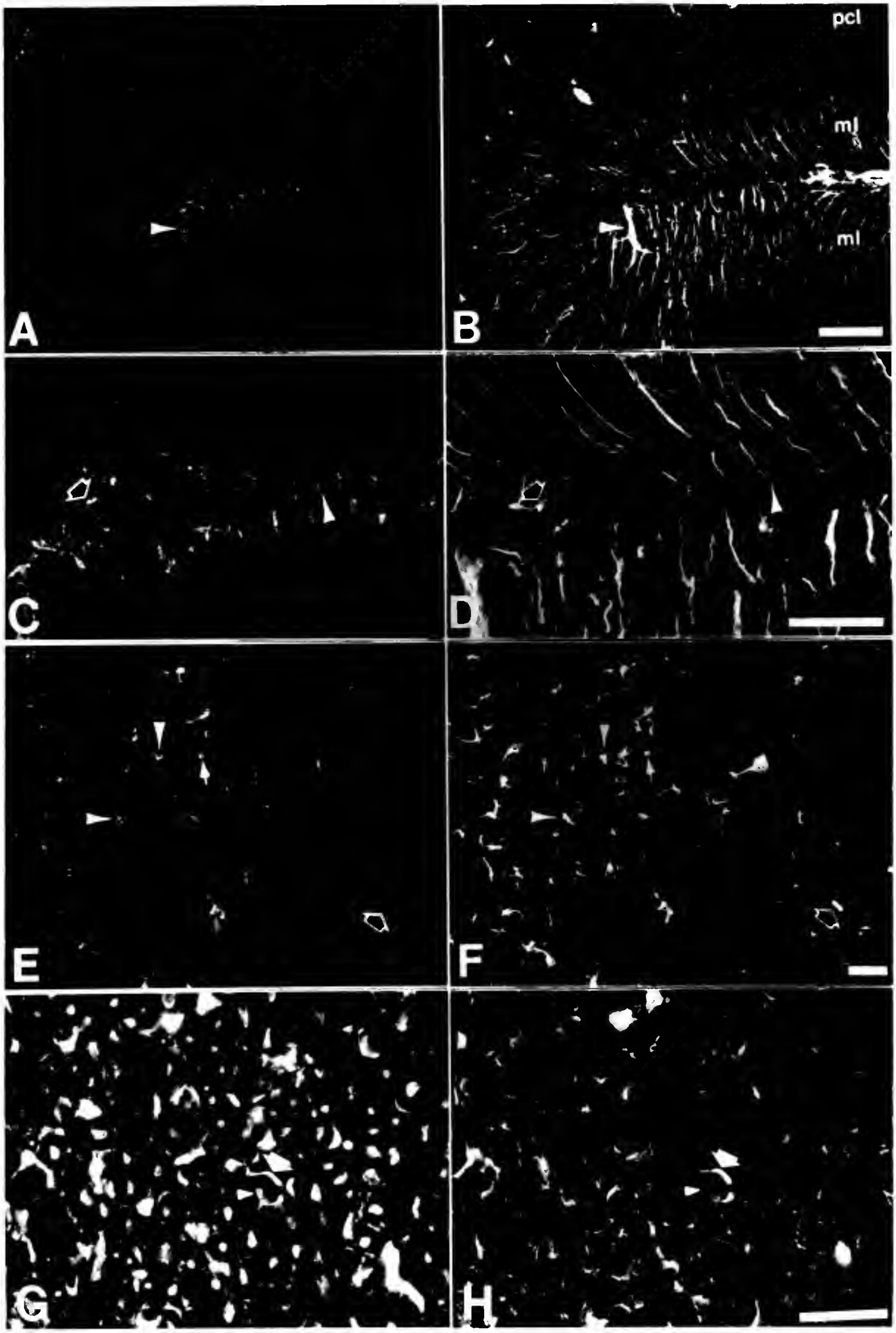
A
B
pcl
ml
ml
C
D
E
F
G
H

Figure 4-5. Co-localization experiment with antibodies to plectin (A,C,E) and GFAP (B,D,F).

(A-B) In lateral ventricle, plectin immunoreactivity (p21) is confined primarily to ependymal (e) and choroid plexus epithelial cells (cp) with weak labelling of astrocytes (arrow) near the ventricle (A). In contrast, GFAP antibody (GA5) labels predominantly the astrocytes around the ventricle (arrow, B). Scale bar: 50 μm.

(C-D) In caudate nucleus, plectin antibody (p21) labels the caudate with indistinguishable punctate particles (C). The area where little to no plectin immunoreactivity represents the fascicles of fiber tracts coursing through the caudate. In contrast GFAP immunoreactivity (GA5) is localized to astrocytes (arrows) throughout the caudate (D). Both plectin and GFAP antibodies label a blood vessel in gray matter (arrowheads); however, the labelling patterns are distinct and plectin antibody does not label all blood vessels (arrowhead). Scale bar: 50 μm.

(E-F) In pyramidal tracts, both plectin (IA2) and GFAP (polyclonal) antibodies label the astrocytes near the pia surface (arrows). Scale bar: 50 μm.

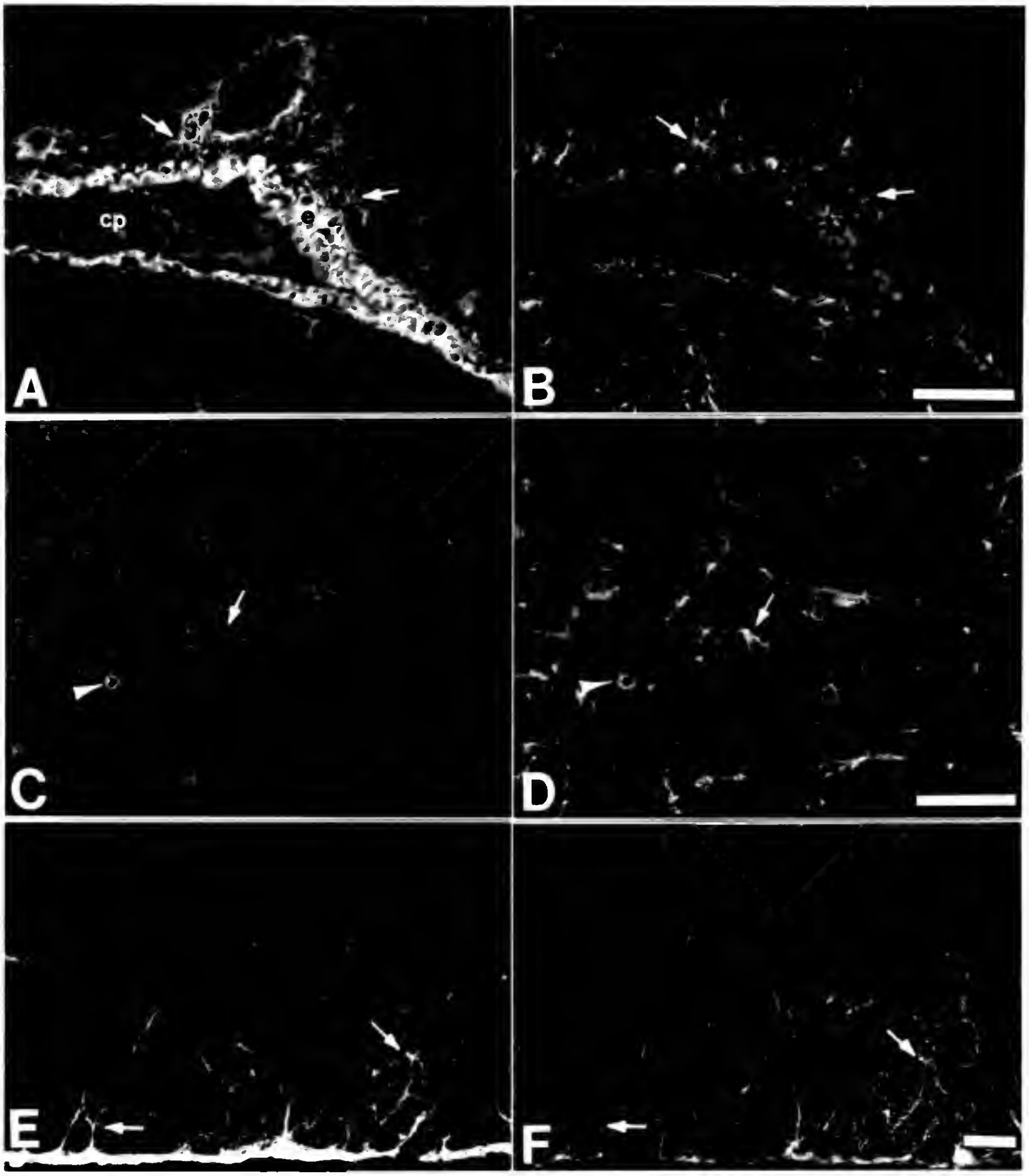
cp
A
B
C
D
E
F

the gray matter of the caudate were labelled with both plectin and GFAP antibodies (Figure 4-5 c,d); however, the staining pattern was distinct in that plectin antibody appeared to be directly labelling the blood vessel whereas GFAP antibody seemed to be associated with the astrocytic end feet around the blood vessel. In the pyramidal tracts, plectin colocalized with GFAP in the astrocyte network near the pial surface (Figure 4-5 e,f).

Plectin and NF triplet proteins. NF triplet proteins are localized exclusively to neurons, although the level and pattern of expression is quite variable between different neuronal cell types (e.g. Yen and Fields 1981, Shaw et al., 1981, Portier et al. 1984, Brody et al. 1989, Pachter and Liem 1985, Chiu et al. 1989, Kaplan et al. 1990). Given that plectin has an ability to cross-link NFs *in vitro*, it is possible that the limited plectin expression seen in certain neurons may reflect a co-distribution with one of the NF subunits.

As expected, NF immunoreactivity was much more extensive and therefore, for the most part, did not overlap with plectin immunoreactivity. However, plectin colocalized with NFs in motoneurons in the brainstem and spinal cord although not all NF positive motoneurons showed plectin antibody staining (Figure 4-6 a,b). In rostral brainstem nuclei, mesencephalic nucleus, plectin immunoreactivity was weak and diffuse throughout the cytoplasm, with strikingly intense labelling at or around the plasma membrane (Figure 4-6 c,d). At higher magnification, the dense labelling of plectin antibody of the plasma membrane between two adjacent cell bodies (arrow) did not exactly correspond to NF-H antibody labelling (Figure 4-6 e,f), but showed some overlap. In a fiber bundle, a distinct staining pattern of plectin immunoreactivity was evident as shown in a cross-section of adult rat sciatic nerve (Figure 4-6 g). Plectin antibodies labelled the Schwann cells surrounding the myelin sheath and the inner membrane surrounding the axon. In addition the axon itself weakly labelled with the plectin antibody, whereas NF antibodies labelled only the axon and not the Schwann cells (Figure 4-6 h).

Plectin and Peripherin. Peripherin is a NF subunit originally identified in the peripheral nervous system (Portier et al., 1984) but is also localized to certain neurons and nerve fibers in the central nervous system (Brody et al., 1989). Like NF-H, plectin co-localized with peripherin in specific motoneurons in the brainstem (Figure 4-7 a-d) and spinal cord. However, some peripherin positive neurons were not labelled with plectin antibodies, indicating that the expression of peripherin in neurons was clearly independent of that of plectin (Figure 4-7 e,f). Plectin immunoreactivity in CNS fiber tracts was similar to that observed in the sciatic nerve (Figure 4-4 g; 4-6 g). Plectin was most closely associated with the outer axon sheath whereas peripherin labelled the axons themselves (Figure 4-7 g,h).

Effects of Peripheral Nerve Axotomy

After peripheral nerve axotomy, expression of the major cytoskeletal proteins are effected differentially. In the case of microtubules and actin, the mRNA for these proteins are dramatically increased over a period of 7 to 14 days, whereas, the NF triplet proteins show a significant decrease in mRNA expressed over the same period of time (Hoffman et al., 1987; Wong and Oblinger, 1987; Goldstein

Figure 4-6. Co-localization experiment with antibodies to plectin (ID8) (A,C,E) and NFs (polyclonal) (B,D,F).

(A-B) In cervical spinal cord motoneurons, plectin antibody (A) only labelled two of the three motoneurons (arrows) which labelled with NFH-KSP polyclonal serum (B). Scale bar: 50 µm.

(C-D) Low magnification view of mesencephalic nucleus of V double-labelled with plectin (C) and NFH-KSP (D) showing that plectin immunoreactivity is concentrated at the periphery of these neurons; whereas, NF antibody labelling is found throughout the cytoplasm. Scale bar: 50 µm.

(E-F) In a higher magnification view of the mesencephalic nucleus of V, plectin antibody (E) labelled most intensely at the periphery of the neurons (arrowhead) while NFH-KSP antibody (F) labelling was the strongest in the cytoplasm and decrease dramatically at the periphery of the neurons (arrowhead). Scale bar: 50 µm.

(G-H) In sciatic nerve, plectin antibody (E) staining is associated with the outermost (open arrow) and innermost (arrowhead) plasma membrane of the Schwann cell process. Diffuse plectin immunoreactivity is also observed within the axon. In contrast polyclonal antibody, NFM-KE, labels only the axons (arrowhead). Scale bar: 25 µm.

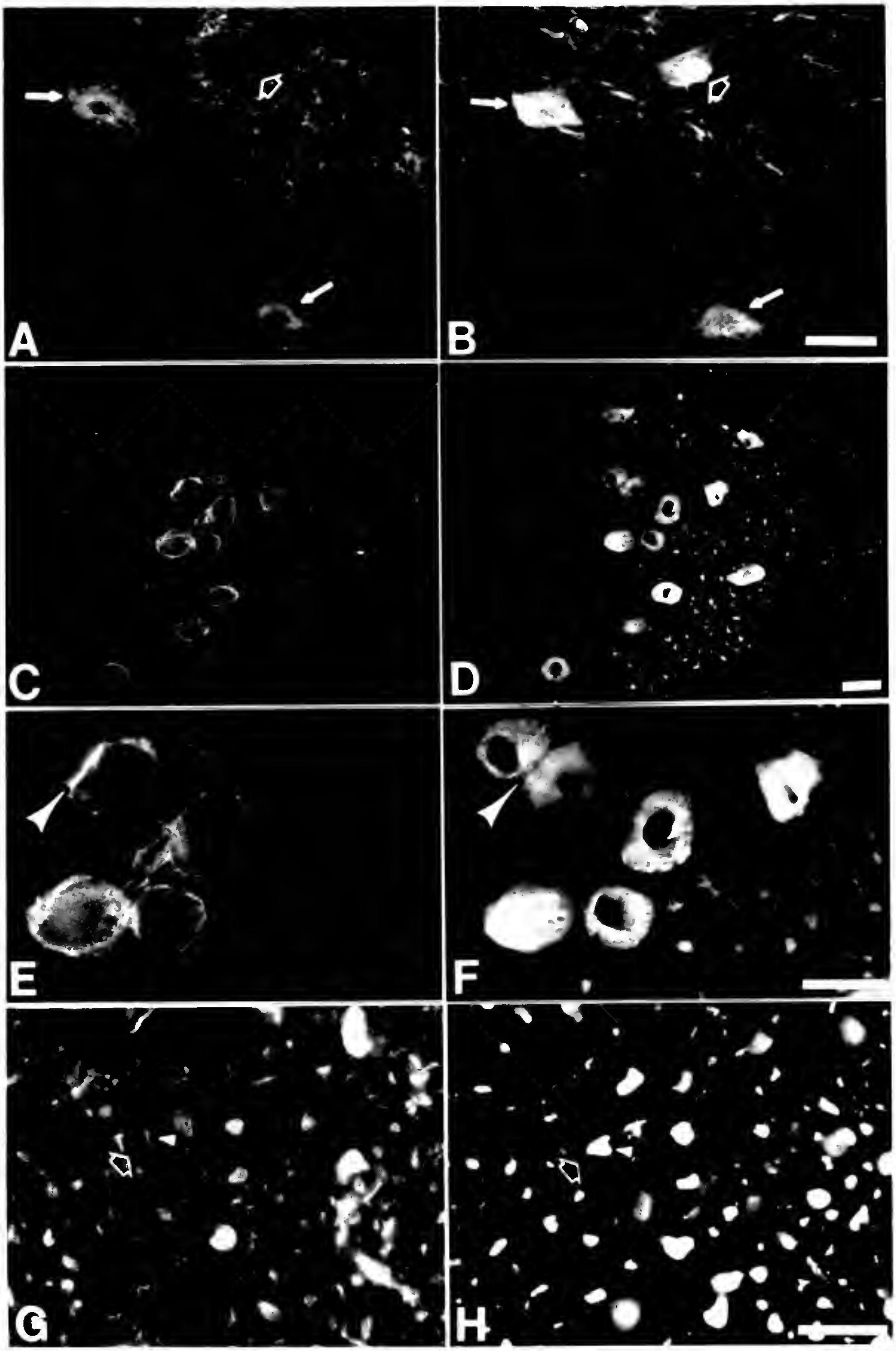
A
B
C
D
E
F
G
H

Figure 4-7. Co-localization experiment with antibodies to plectin (IA2) (A,C) and peripherin (R19) (B,D).

(A-B) In the nucleus ambiguus, plectin (A) and peripherin (B) had similar labelling distribution in the neurons with some slight differences in intensity of labelling. Scale bar: 50 μm.

(C-D) In brainstem (medulla), plectin (C) and peripherin (D) had similar labelling pattern in motoneurons. Scale bar: 50 μm.

(E-F) Although the lateral tegmental nucleus showed strong peripherin immunoreactivity (F), this rostral brainstem nuclei lacked plectin immunoreactivity (E) in the neurons. Scale bar: 50 μm.

(G-H) In a CNS white fiber tract in the spinal cord, plectin immunoreactivity (G) is confined predominantly to the outer portion of the axon (open arrow); whereas, peripherin immunoreactivity labels the axon bundles in cross-section (open arrow). Scale bar: 25 μm.

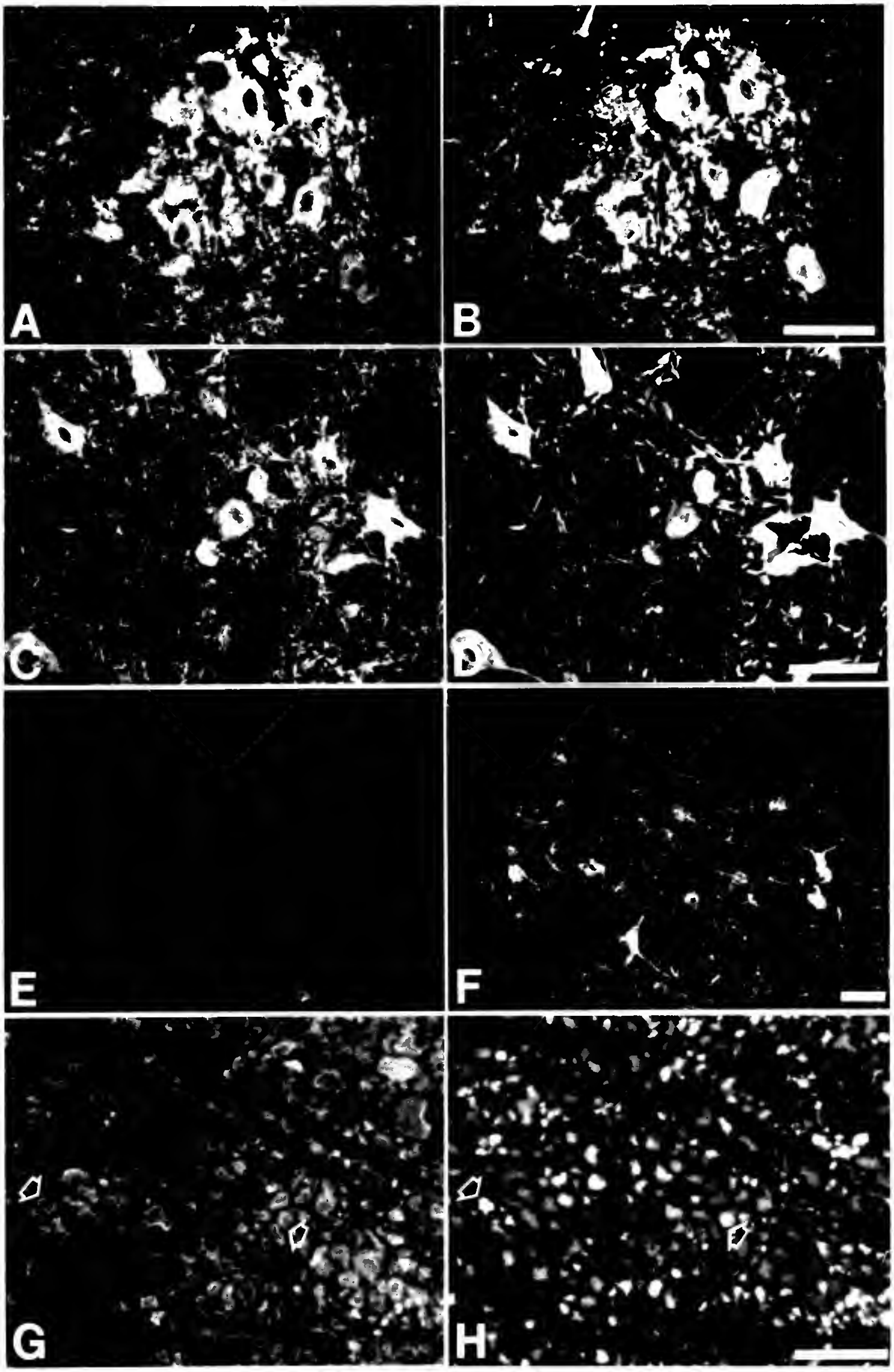
A
B
C
D
E
F
G
H

et al., 1988; Tetzlaff et al., 1988; Oblinger et al., 1989). In contrast to NF-triplet proteins, peripherin mRNA and protein expression is dramatically increased after sciatic nerve axotomy in both the dorsal root ganglion cells and ventral motoneurons (Oblinger et al, 1989; Wong and Oblinger, 1990). Since plectin's neuronal distribution is limited to motoneurons in the brainstem and spinal cord, and one of the primary roles of plectin appears to be related to the structure of the cell (Wiche, 1989), it was of interest to determine if plectin's protein expression would be altered after peripheral nerve lesion.

The facial nerve axotomy model is a popular model based upon the ease of making the lesion and the ability to determine the location of the facial nucleus both externally as well as in cross-section (Kreutzberg et al., 1990). Axotomy of the facial nerve affects musculature ipsilateral to the side of the lesion, most profoundly affecting the rat's whiskers. Figure 4-8 (a,b) shows a low power view of the left and right ventral quadrant of the brainstem labelled with plectin antibody after the facial nerve was transected on the right side. The facial nucleus is outlined with arrowheads. In the control side (Figure 4-8a), the facial motoneurons are weakly labelled with plectin antibodies which is visualized better under high power (Figure 4-8c). On the lesion side, the facial motoneurons show a dramatic increase in plectin immunoreactivity throughout the cell body (Figure 4-8b). Another difference was observed in the extent of labelling. On the control side, plectin immunoreactivity is diffuse with a small area of dense labelling (Figure 4-8c, arrows) similar to that seen previous in nucleus ambiguus and ventral horn

Figure 4-8. Effects of a unilateral facial nerve axotomy on plectin immunoreactivity (1A2).

(A-B) A low magnification view of the of the left (A) and right (B) ventral quadrant of the brainstem labelled with plectin antibody 7 days after the facial nerve was transected on the right side. The facial nucleus is outlined in arrowheads. On the control side (A), the facial motoneurons are weakly labelled with peripherin antibody. On the lesion side (B), there is a dramatic increase in plectin immunoreactivity. Scale bar: 100 μm.

(C-D) A higher magnification view of the facial nucleus shows differences in the extent of plectin antibody labelling within the cell body. On the control side (C), plectin immunoreactivity is weak throughout the cell body with some areas of intense labelling (arrows). In contrast, on the lesion side (D), plectin immunoreactivity is strong throughout the cell body. Scale bar: 50 μm.

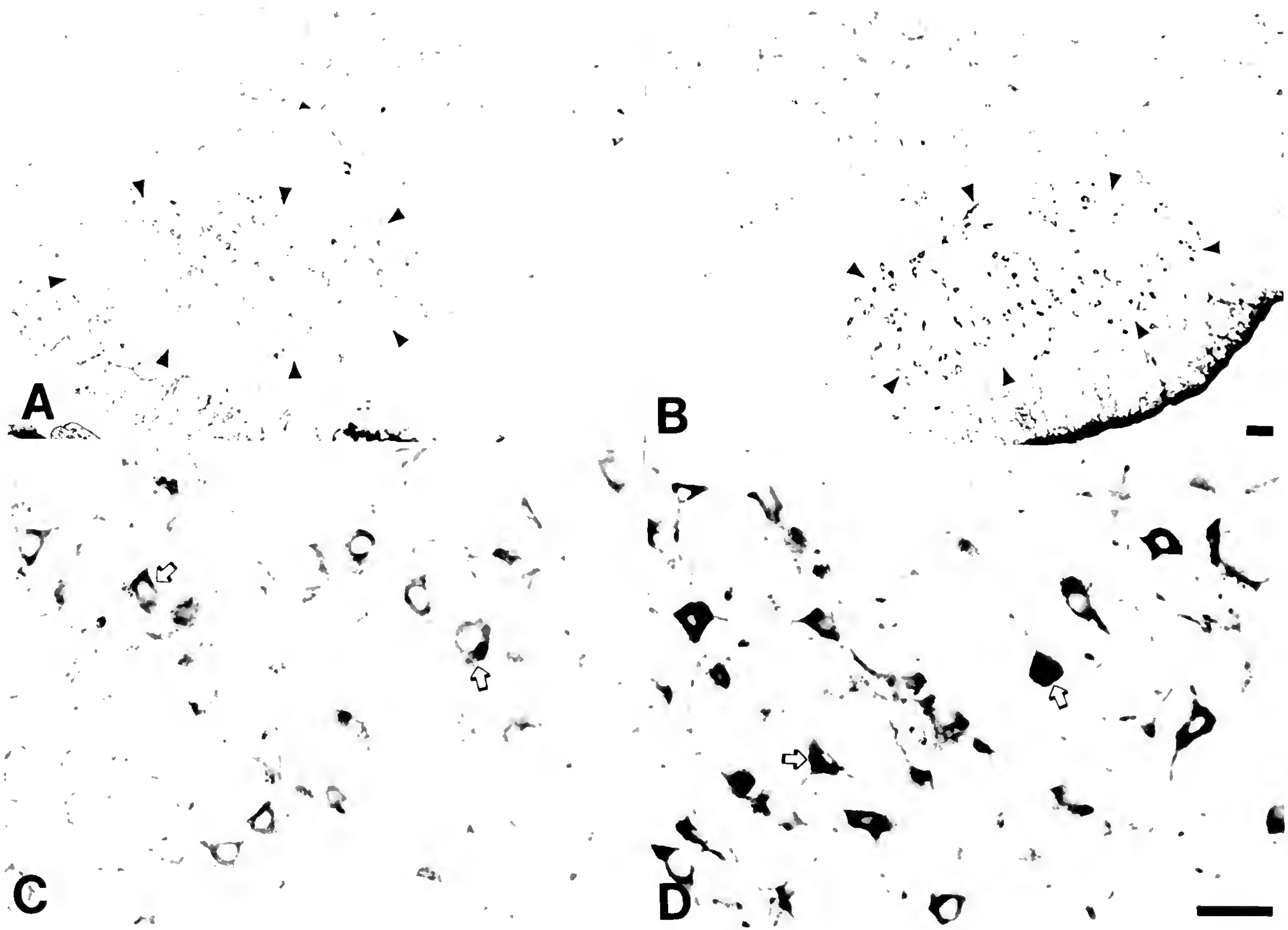
A
B
C
D

motoneurons (Chapter 3). After facial nerve axotomy, the entire facial motoneuron cell bodies labelled densely with plectin antibodies whereas the processes remained weakly labelled similar to the control side (Figure 4-8d).

Immunofluorescent double-label experiments with plectin and NF triplet proteins and with plectin and peripherin were conducted to obtain a better understanding of the relationship between plectin and the different NF subunits after axotomy. As discussed earlier, the mRNA expression for NF triplet proteins decreases after facial nerve axotomy while the protein expression remained unchanged (Tetzlaff et al., 1988). On the control side only a few of the facial motoneurons were double-labelled with both plectin and NF triplet antibodies (Figure 4-9a,c, respectively); however, plectin immunoreactivity was extremely weak. On the lesion side, the majority of the facial motoneurons labelled with both plectin and NF triplet antibodies in a similar manner (Figure 4-9b,d). In the case of peripherin, it was expected that facial motoneurons would express more peripherin protein on the side of the lesion since that was what was observed after axotomy of sciatic nerve. Figure 4-10 showed that there was a prominent increase of both plectin and peripherin protein expression on the lesion side with only weak labelling of motoneurons on the control side.

Discussion

The distribution of plectin in different cell types of the adult nervous system with respect to neural IF proteins is summarized in Table 4-1. Previously, plectin has been shown to bind to several different types of IF *in vitro* (Foisner et al.,

Figure 4-9. Co-localization experiment with plectin (1A2) (A,C) and NF-H (R14) (B,D) after unilateral facial nerve axotomy.

(A-C) Light micrographs showing double-labelling of the facial nucleus on the control side. Plectin antibody (A) only labels a few cells in the facial nucleus weakly (thick arrows) whereas NF-H immunoreactivity (B) is localized in numerous cells in the facial nucleus. Scale bar: 50 µm.

(B-D) Light micrographs showing double-labelling of the facial nucleus on the lesion side. Plectin antibody (B) labelling is stronger on the lesion side (arrows) in comparison to the control side and labels the motoneurons with similar intensity as NF-H antibody (D; arrows). Scale bar: 50 µm.

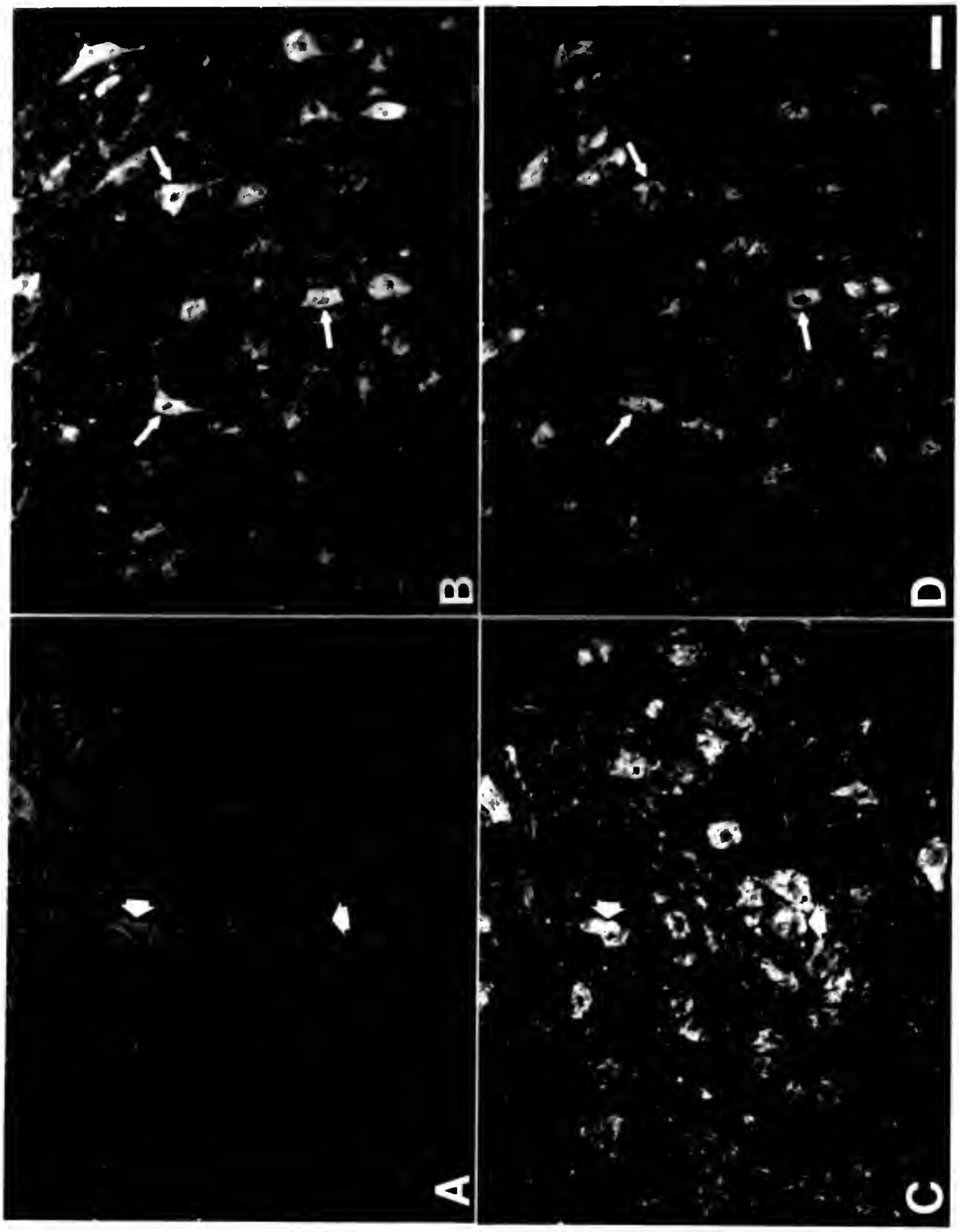
A
B
C
D

Figure 4-10. Co-localization experiment with plectin (1A2) (A,C) and peripherin (R20) (B,D) after unilateral facial nerve axotomy.

(A-C) Light micrographs showing double-labelling of the facial nucleus on the control side. Plectin antibody (A) only labels a few cells in the facial nucleus weakly (thick arrow) which coincides with the weak labelling of the same motoneurons with peripherin antibody (C).Scale bar: 50 µm.

(B-D) Light micrographs showing double-labelling of the facial nucleus on the lesion side. Plectin antibody (B) labelling is stronger on the lesion side (arrows) in comparison to the control side (A, thick arrow) and labels the motoneurons with similar intensity as peripherin antibody (D). Scale bar: 50 µm.

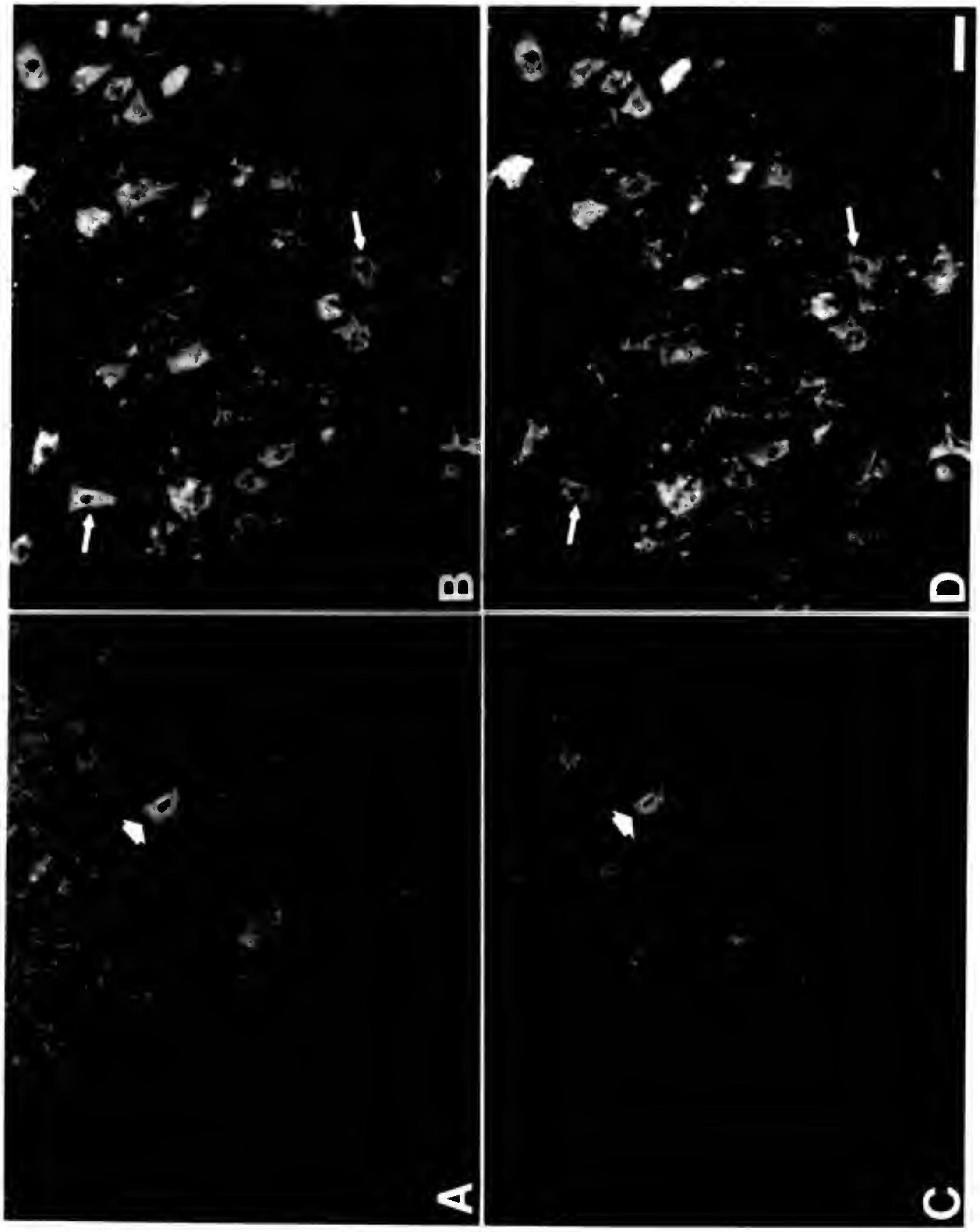
A
B
C
D

1988) and to co-localize with vimentin in non-neuronal tissue (Wiche, 1989). In line with these findings, plectin has similar distribution to that previously reported for vimentin in the central nervous system (Pixley et al., 1981; Shaw et al., 1981; Yen and Fields, 1981). Little plectin immunoreactivity is observed in gray matter astrocytes, which, in rat at least, contain very little vimentin immunoreactivity (Shaw et al., 1981; Yen and Fields, 1981). Similarly, more marked plectin immunoreactivity is found in white matter astrocytes which, in rat, stain strongly for vimentin (Shaw et al., 1981; Yen and Fields, 1981). Double-label experiments with plectin and vimentin antibodies in non-neuronal cells in DRG cultures demonstrate that plectin can be localized along the vimentin's filamentous network; however, the labelling is discontinuous along the vimentin filament bundles. Overall, three major difference exist between plectin and vimentin labelling patterns: (1) the lack of small blood vessel labelling by plectin antibodies in gray matter; (2) the distribution of labelling in the Bergmann glia processes; and (3) the presence of plectin immunoreactivity in motoneurons in the brainstem and spinal cord. The few regions in which plectin antibody labelling overlap with GFAP immunoreactivity coincide with those found previous by for vimentin and GFAP antigen distribution (Shaw et al., 1981; Pixley et al., 1984).

An interesting finding was plectin immunoreactivity in neurons. In DRG cells and PC12 cells, plectin antibody staining was localized predominantly in the cell body; however, there was some weak immunoreactivity in the neuritic processes. Although plectin was found in postnatal day 1 DRG cultures, plectin

Table 4-1. Summary of the distribution of plectin in different cell types of the adult rat nervous system with respect to intermediate filament proteins.

Cell Type	Plectin	NF-triplet	Peripherin	Vimentin	GFAP
Ependyma					
choroid plexus	++	---	---	++	---
ependymal	++	---	---	++	+\-
subependyma	++	---	---	++	++
tanycytes	++	---	---	++	---
Glial Cells					
astrocytes (white matter)	++	---	---	++	++
astrocytes (gray matter)	+/-	---	---	---	++
Bergmann fibers	++	---	---	++	++
Schwann cells	++	---	---	++	+\-
Neuronal Cells					
cortical neurons	---	+/-	+\-	---	---
cerebellar granule	---	++	---	---	---
cerebellar Purkinje	---	++	---	---	---
motoneurons	+/-	++	+\-	---	---
axons	---	++	+\-	---	---
Other					
endothelial cells	+/-	---	---	++	---
pia mater	++	---	---	++	---

++: indicates that the protein was localized in the majority of this cell type; +/-: indicates that the protein labelled a subpopulation of this cell typle; ---: indicates that the protein was not observed to these cells.

immunoreactivity was not found in adult rat DRG cells (data not shown). Whether plectin antibody labelling of the DRG culture cells was related to a developmental progression or was an artifact of tissue culture remains to be determined. In the adult rat nervous system, plectin immunoreactivity was associated with motoneurons in the brainstem and spinal cord. Colocalization experiments with plectin and different NF subunits revealed that plectin positive motoneurons also contained NF triplet proteins and peripherin. The presence of plectin in cells containing the NF triplet proteins also showed that an *in vitro* interaction between plectin and the NF triplet proteins may reflect a meaningful *in vivo* interaction (Foisner et al. 1988).

The relationship between plectin and peripherin was examined since plectin was localized only to a small number of neuron in comparison to the large number of types of neurons that express NF triplet proteins. Previous research as well as this present study showed that subsets of brainstem and spinal cord neurons labelled with peripherin antibodies (Portier et al., 1984; Parysek and Goldman, 1988; Brody et al., 1989). As shown here, plectin positive neurons all expressed peripherin so that peripherin, which is quite similar to vimentin in primary sequence and biochemical properties, may in some functional sense replace vimentin in these cells. In addition, we noted that although plectin positive motoneurons were always peripherin positive, the converse was not true, indicating that while plectin was expressed in consort with peripherin or vimentin in the nervous system, not all cells expressing these two proteins expressed detectable amounts of plectin.

To further study the relationship between plectin and neural IF proteins in motoneurons, the expression of plectin, peripherin, and NF-H, was examined immunocytochemically after a unilateral lesion to the facial nerve. Previous research has investigated the effects on cytoskeletal elements after a nerve axotomy and found that tubulin, actin and peripherin mRNA were upregulated, whereas NF triplet proteins mRNA were down regulated with maximum effects occurring at 7-14 days depending on the model system used (Hoffman et al., 1987; Wong and Oblinger, 1987; Goldstein et al., 1988; Tetzlaff et al., 1988; Oblinger et al., 1989). In addition, peripherin immunoreactivity was shown to increase in ventral horn motoneurons on the lesion side and NF triplet protein antibody labelling appeared to remain unchanged when using a phosphate insensitive antibody. After facial nerve lesion, plectin immunoreactivity in the facial nucleus on the lesion side dramatically increased in comparison to the control side. The number of motoneurons that labelled with plectin did not appear significantly different; however, the extent of labelling within the cytoplasm was dramatic. On the control side there was diffuse plectin immunoreactivity with only some small areas of intense immunoreactivity. The increase in plectin immunoreactivity that was localized throughout the cytoplasm, suggested that plectin may be performing a stabilizing function after injury to the cell. Another possibility is that the transport of plectin into the axons may decrease resulting in an increase in plectin in the accummultation in the cell body. However, since plectin does not appear to localize to axons in renders this hypothesis rather unlikely. In comparing plectin's expression to NF-H, plectin was weakly localized to some of the NF-H positive motoneurons on the nonlesion side, whereas, on the lesion side the same neurons expressed both plectin and NF-H with similar intensities. Double-label experiments with plectin and peripherin antibodies showed that plectin and peripherin were localized to the same motoneurons on both the non-lesion and lesion sides, and that the intensity of staining was similar for both of the antigens.

The submembraneous labelling of neurons in the brain stem and spinal cord suggests that plectin may stabilize the submembraneous cytoskeleton in these cells, and also may act as a cross-linker between the plasma membrane and cytoskeleton network, as appears to be the case in non-neuronal cells (Wiche et al., 1983; Hermann and Wiche, 1987; Wiche, 1989). The reorganization within the motoneuons after a peripheral nerve axotomy is extensive. In particular there is both an up-regulation and down-regulation of mRNA for cytoskeletal proteins. The increase in plectin immunoreactivity after peripheral nerve axotomy suggests that plectin may function to stabilize the cytoskeleton during injury state since plectin is known to interact with cytoskeletal elements. Future studies examining the time course of the increase in plectin immunoreactivity, including immunoelectron microscopy studies to determine the ultrastructural distribution of plectin in motoneurons after peripheral nerve axotomy, should result in a better understanding of the function of plectin.

Notes

Portions of this chapter are from a paper entitled "The Distribution of Plectin, an Intermediate Filament Associated Protein, in the Adult Rat Central Nervous System" by L.D. Errante, G. Wiche, G. Shaw. Journal of Neuroscience Research 37: 515-528. Copyrighted © 1994 by Wiley-Liss. Text is used with the permission of Wiley-Liss, a division of John Wiley & Sons, Inc.

CHAPTER 5

IDENTIFICATION OF CANDIDATE NEUROFILAMENT BINDING PROTEINS

Introduction

NFs are abundant proteins within the nervous system, however, the role of these proteins is not well defined. Protein sequence information has given insight to the protein structure of the NF subunits and how NF may interact with each other. NFs have been shown to bind to cytoskeletal elements directly as in the case of tubulin (Minami et al., 1983) and microtubules (MTs) (Hisanaga and Hirokawa, 1990) or indirectly by the cross-linking ability of MAP2 to both MTs and NFs (ie. Leterrier et al., 1982; Flynn et al., 1987). Various other proteins such as brain spectrin (fodrin) (Frappier et al., 1987), plectin (Foisner et al., 1988) and synapsin I (Steiner et al., 1987) have been shown to bind to various forms of NFs *in vitro.*

Previous studies utilizing affinity columns to identify actin (Miller et al., 1989) and microtubule binding proteins (Kellog et al., 1989) were successful in identifying cytoskeletal associated proteins. Here, NF affinity columns were employed to test the hypothesis that soluble proteins bind to NF subunits, and were used as a way to identify candidate cytosolic NF associated proteins in a partially purified form.

Methods

Pig Spinal Cord Cytosolic Preparation

The pig spinal cord was obtained from a slaughterhouse within an hour after the pigs were killed. The connective tissue and blood vessels were removed and the spinal cord was placed on ice. The spinal cord was homogenized at 4°C in a Sears blender in 50 mM MES pH 6.5, 5 mM $MgCl_2$, 1 mM DTT, 1 mM PMSF and 1 mM TAME. The tissue was homogenized with three 5 second pulses on low speed and three 5 second pulses on high speed. The crude homogenate was centrifuged at 9240xg for 30 minutes at 4°C in a SS34 Sorvall rotor. The supernatant was filtered through gauze sponge type VII (8 ply). The supernatant was re-centrifuged at 147,000xg for 1 hour at 4°C in a T865 Sorvall rotor. The final supernatant was filtered through a Whatmann #1 filter and was referred to as pig cytosol. The cytosol was used immediately for affinity column binding.

Affinity Column Preparation

Affinity columns were made using Affi-Gel 10 resin (Bio-Rad). The Affi-Gel beads offer high stability bonds, high coupling efficiency and rapid coupling of proteins to the gel support. The Affi-Gel 10 support is composed of a 10 atom spacer arm that is linked through ether bonds to chemically cross-linked agarose gel beads (Bio-Gel A-5m gel). The protein ligand forms a stable amide bond with the Affi-Gel's terminal carboxyl of the spacer arm by displacing N-hydroxysuccinimide. Seven different types of affinity columns were made: crude IF preparation, NF triplet proteins purified using ion exchange chromatography, purified subunits (NF-H, NF-M and NF-L), and control columns with either BSA or no protein bound. The protein ligands were coupled to the gel support using 0.1 M MES pH 6.5, 5 mM $MgCl_2$, and 1 mM DTT. The coupling reaction occurred at 4°C for at least 12 hours. The remaining active ester groups were blocked with 0.1 ml 1 M ethanolamine-HCl (pH 8) per ml of gel at 4°C for 2 hours. The columns were then washed with coupling buffer followed by a wash with coupling buffer containing 1 M KCl. The column was ready to use, after a final wash with coupling buffer. Columns were stored at 4°C and used 4 to 5 times before a new column was made.

Binding of Cytosolic Proteins to Affinity Columns

An overview of the procedure to bind cytosolic proteins to the affinity columns is shown in schematic form in Figure 5-1. The affinity column to be used was equilibrated with 50 mM MES pH 6.5, 5 mM MgCl, and 1 mM DTT (Binding Buffer). Approximately 20 ml of pig spinal cord cytosol (2.5 mg/ml) was cycled through a particular NF affinity column at a rate of 0.5 ml/minute for 2 hours at 4°C. The column flow through was collected and saved. The column was washed with 50 ml of binding buffer to remove any unbound protein. To make sure no more unbound protein was being eluted, the optical density at 280nm was measured using the last milliliter of eluted wash buffer. Proteins that bound to the affinity column were eluted using a 30 ml salt gradient; 0 to 0.5 M KCl in binding buffer. Column fractions were precipitated with trichloro-acetic acid and precipitated proteins were brought up in 25 µl of 1 M Tris and 25 µl of 2X sample

Figure 5-1. Outline of the method used for identifying candidate NF binding proteins.

The top gel shows the purity of the different NF proteins used in making the affinity columns. The purified NF triplet affinity column is a mixture of the three purified NF triplet subunits. As an example, the bottom gel shows the cytosol preparation before it is cycled through a column (C) and with a representative gel of the proteins which bound to the NF-L affinity column. The horizontal markers between the cytosol lane and the candidate NF binding protein gel represents the relative positions of the molecular weight standards.

NF Affinity Columns

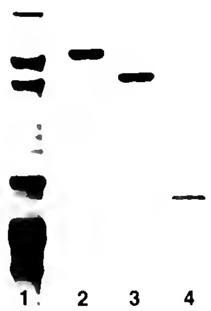

1 Crude IF
2 Purified NF-H
3 Purified NF-M
4 Purified NF-L

Preparation of Pig S.C. Cytosol

5 g Pig Spinal Cord

homogenize in 50mM MES pH=6.5 containing 5mM MgCl , 1mM DTT, proteases inhibitors

Centrifuge

10,000xg
150,000xg

Cycle 20ml Cytosol (2-3mg/ml) through Column for 2 hours

Flow Rate 0.5ml/min.

Wash Column

to remove unbound protein

Elute Bound Protein with 30ml Salt Gradient (0-0.5M NaCl)

collect 1ml fractions
concentrate samples

Separate with SDS PAGE

Measure Relative MW of Unknown Proteins

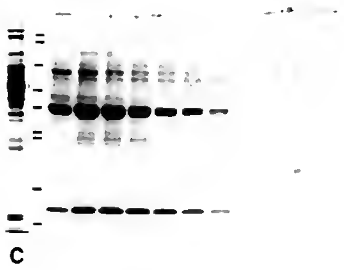

buffer. A sample (10 µl) of each precipitated fraction was separated on either a 10% or 12% SDS polyacrylamide gel. Proteins were visualized using the method described in Chapter 2.

Production of Polyclonal and Monoclonal Antibodies

Polyclonal antibodies to GAPDH were produced in male Balb-C mice (n=2). The mice initially received an intraperitoneal injection with 0.4 ml solution containing 50% GAPDH (Sigma; 2 mg/ml) and 50% Freund's complete adjuvant. Two weeks following the first injection the mice received a second injection consisting of 50% GAPDH (2mg/ml) and 50% Freund's incomplete adjuvant. All subsequent immunogen injections used this solution. The third injection followed a week later where a test bleed was done to determine the antibody titre. Weekly injections of the immunogen solution followed with test bleeds until an appropriate titre level was reached (total of 4 injections). In addition, both mice were producing fluid in the peritoneal cavity. This fluid was drained using a 16 gauge needle inserted into the cavity and tested for presence of antibodies to GAPDH. The titre was determined using a immuno-blot of the candidate NFL-38 protein and purified GAPDH (Sigma). The mouse with the higher antibody titre was then used to make monoclonal antibodies. This mouse was injected with 0.1 ml of a 1 mg/ml solution of GAPDH five days before the mouse was brought to the hybridoma core facility for the monoclonal antibody fusion procedure. ELISA positive clones were tested by immunoblot analysis to determine if GAPDH was recognized.

Results

A number of proteins bound to the various NF affinity columns with different specificity. Table 5-1 shows the relative molecular weight of proteins from the pig cytosol preparation which bound consistently to the different NF affinity columns. None of these proteins bound to control columns containing either BSA or no protein. The individual NF columns bound the following proteins, based on relative molecular weight, consistently and exclusively: NF-H bound 70 kD and 49 kD proteins; NF-M bound 87 kD, 66 kD and 46 kD proteins; and NF-L bound 84 kD and 55 kD proteins. Some of these proteins bound to the crude IF and purified NF columns which was expected since these columns contain all 3 NF subunits. In contrast not all the proteins which bound to the purified NF columns (84, 66 and 15 kD) bound to the crude IF affinity column. A possible reason for this selectivity is that the binding site on the individual subunit columns may be blocked with another protein in the crude IF affinity column. All the NF columns bound the following proteins: 20, 29, and 38 kD. The most prominent protein band present was a 38 kD protein which bound to all NF affinity columns, but seemed to bind to the NF-L affinity column particularly well. The 38 kD band eluted from the various NF affinity columns at KCl salt concentrations in the range of 0.1 M - 0.2 M, with the salt concentrations being slightly different for each column.

The characterization of the 38 kD protein began with testing the hypothesis that the 38 kD protein could be a degradation product of intermediate filaments (IFs) since the α-helical rod domain of IFs is approximately 39 kD. To examine

Table 5-1. Relative molecular weight (kD) of candidate proteins which bound to the five different types of NF affinity columns.

Crude IF	Purified NF	Purified NF-H	Purified NF-M	Purified NF-L
88	87	----	87	----
----	----	----	----	84
68	----	70	----	----
----	65	----	66	----
60	59	60	----	61
54	----	----	----	55
50	----	49	----	----
45	----	----	46	----
38	37	38	40	39
29	28	30	29	29
19	21	19	20	20
----	16	----	----	15

this possibility, an immunoblot of 38 kD protein from each of the affinity columns was done using Pruss monoclonal antibody which labels a common epitope in the rod domain of all IFs (Pruss et al., 1981). Only the 38 kD protein which bound to the crude IF affinity column (IF-38) labeled with the Pruss antibody (Figure 5-2a; lane 1, lower band). The other proteins which weakly labeled with Pruss antibody at ~50 kD were most likely keratin contamination from skin. To further examine if the IF-38 was the rod domain of IF protein, the amino acid composition of IF-38 was compared to that of the rod domain of NF-L which demonstrated that these proteins were not related (Figure 5-2b). This conclusion was based primarily on the difference in leucine content which is characteristically high in the α-helical rod domain of all IFs (10.84% for NF-L) but was low in the IF-38 candidate protein (5.78%). This suggests that IF-38 would not form the typical IF type coiled-coil structure.

In addition, the differential antibody staining with the Pruss antibody between IF-38 and the other 38 kD NF binding proteins from the other NF affinity columns was not supported by the amino acid profiles (Table 5-2; Figure 5-3) and chemical cleavage studies (data not shown) done on IF-38 and the 38 kD protein that bound to the NF-L affinity column (NFL-38). These results showed that these two proteins were very similar if not identical. One plausible explanation for this was that there were two proteins at the same relative molecular weight (38 kD) binding to the crude IF affinity column, and the one which labeled with the Pruss antibody was at such a low concentration that it did not make a significant contribution to

Figure 5-2. Comparison of candidate 38 kD NF binding protein to rod domain of IF proteins.

(A) Immunoblot using Pruss antibody (anti-IFA) to examine if the 38 kD protein is a degradation product of IF rod domain. Lanes 1-5 contain fractions with the 38 kD protein from crude IF, purified NF, purified NF-H, NF-M and NF-L affinity columns. Only the 38 kD protein which bound to crude IF column (IF-38) labels with anti-IFA. The minor bands labelling at ~50 kD are probably due to keratin contamination.

(B) Comparison of amino acid composition for the IF-38 to that of the rod domain of NF-M. The spokes in the wheel represent the percent nanomole for each particular amino acid. The values for NF-L rod domain were determined from rat sequence. The prominent difference exists in leucine content which is low in IF-38 (5.78%) but high for rod domains in general (10.84% for NF-L).

A
1
2
3
4
5

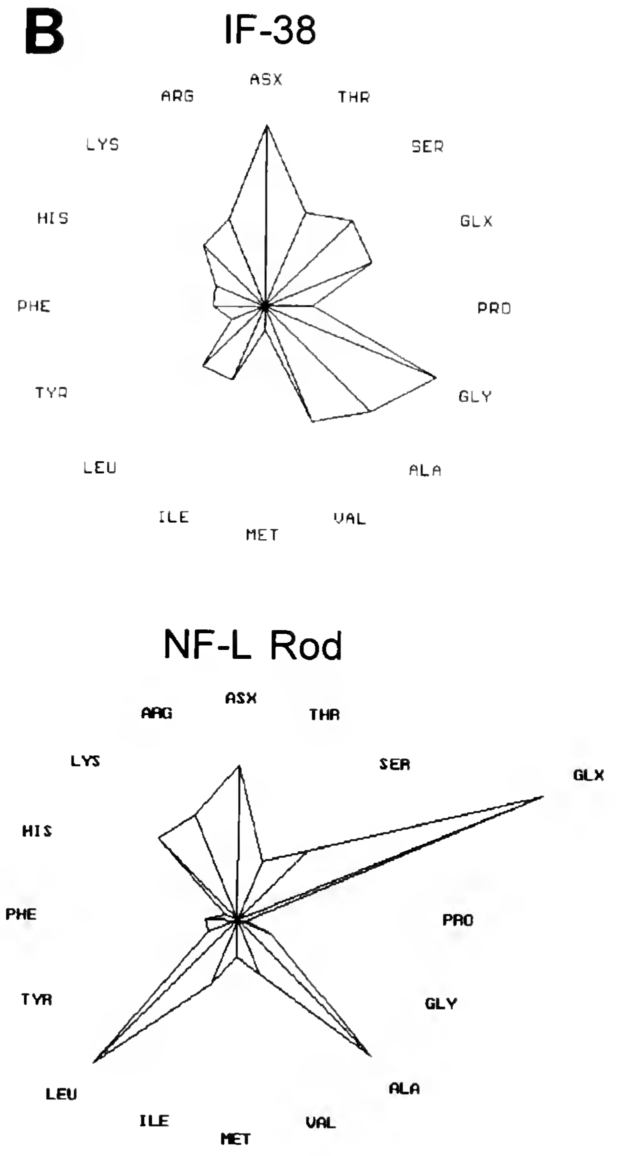
B
IF-38
ASX
THR
SER
GLX
PRO
GLY
ALA
VAL
MET
ILE
LEU
TYR
PHE
HIS
LYS
ARG
NF-L Rod
ASX
THR
SER
GLX
PRO
GLY
ALA
VAL
MET
ILE
LEU
TYR
PHE
HIS
LYS
ARG

Table 5-2. Amino acid composition for candidate neurofilament binding proteins with the data represented as nanomole percent.

	NFL-38			IF-38	NFL-16	NFL-62
Amino Acid	Result #1	Result #2	Average	Result	Result	Result
ASX	12.72	11.08	11.90	11.85	10.16	8.46
THR	7.06	5.70	6.38	6.64	7.49	3.94
SER	6.48	4.35	5.42	7.36	5.68	5.16
GLX	6.87	6.83	6.85	7.71	11.24	11.86
PRO	3.88	3.41	3.65	3.56	0.00	0.00
GLY	11.72	9.97	10.85	13.15	10.98	19.51
ALA	10.47	8.95	9.71	9.99	4.69	8.66
VAL	6.38	13.97	10.18	7.02	9.86	9.01
MET	0.86	1.97	1.41	1.03	1.52	1.63
ILE	5.38	5.84	5.61	4.75	5.24	4.92
LEU	6.04	5.97	6.00	5.78	7.67	7.17
TYR	2.65	3.44	3.04	2.50	1.56	0.00
PHE	3.93	4.99	4.46	3.27	3.81	3.33
HIS	3.51	3.49	3.50	2.74	1.81	3.24
LYS	7.75	6.99	7.37	6.70	13.04	7.83
ARG	4.29	3.06	3.67	5.92	5.26	5.27

the amino acid analysis. The amino acid composition for IF-38 and NFL-38 was compared to the average amino acid composition of all the entries in Genbank in order to determine if these proteins were high or low in any particular amino acid. The amino acid data is graphically represented in Figure 5-3 in which the circle represents the average nanomole percent for each amino acid and the spokes represent the IF-38 and NFL-38 data normalized to the average amino acid profile of all entries in Genbank. Spokes outside the circle show that the 38 kD protein has more of that particular amino acid than the average amino acid, whereas, spokes inside the circle indicate that a particular amino acid is present in a lower concentration than that observed for the average amino acid in Genbank. The amino acid composition of IF-38 and NFL-38 is similar to the average protein but overall these proteins appear to be low in hydrophobic amino acids, and a little above average for glycine and alanine. In addition, NFL-38 protein is shown to be slightly higher in histidine content.

Preliminary identification of the 38 kD protein was accomplished using a computer program, FINDER, which searches the protein database for proteins of similar amino acid composition to that of an unknown protein (Shaw, 1993). The output data from the FINDER program gave the calculated molecular weight, isoelectric point and accession number for the known protein, as well as an amino acid match score. The amino acid match score is a representation of how similar the amino acid composition is between the candidate protein and a protein in the database. The highest possible match score is 32 and a close match is 22 or

Figure 5-3. Comparison of amino acid composition data between the NFL-38 and IF-38, and to that of the average amino acid composition in Genbank.

A) The diagrams represent the amino acid composition of NFL-38 in which the top figure represents nanomole percent for each amino acid. The bottom figure depicts the same values normalized to the average protein in Genbank.

B) The diagrams represent the amino acid composition of IF-38 in which the top figure represents nanomole percent of each amino acid. The bottom figure depicts the same values normalized to the average protein in Genbank.

Overall, there are no significant differences reflected in the amino acid composition between IF-38 and NFL-38 proteins. There does not appear to be any significant high or low concentration of any particular amino acid when compared to the average amino acid in Genbank. The actual nanomole percent for each amino acid for the 38 kD protein is given in Table 5-2.

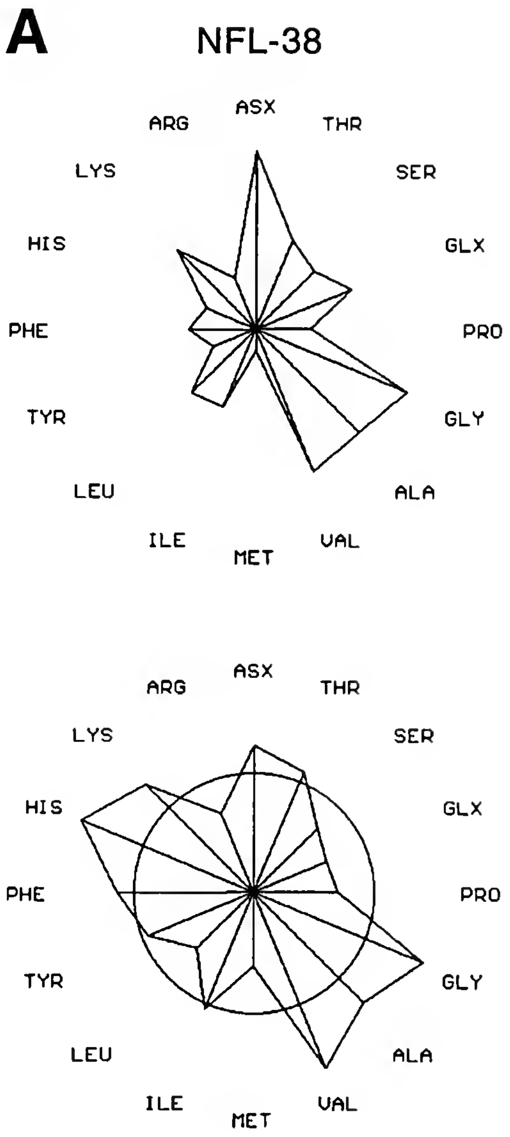
A
NFL-38
ASX
THR
SER
GLX
PRO
GLY
ALA
VAL
MET
ILE
LEU
TYR
PHE
HIS
LYS
ARG
ASX
THR
SER
GLX
PRO
GLY
ALA
VAL
MET
ILE
LEU
TYR
PHE
HIS
LYS
ARG

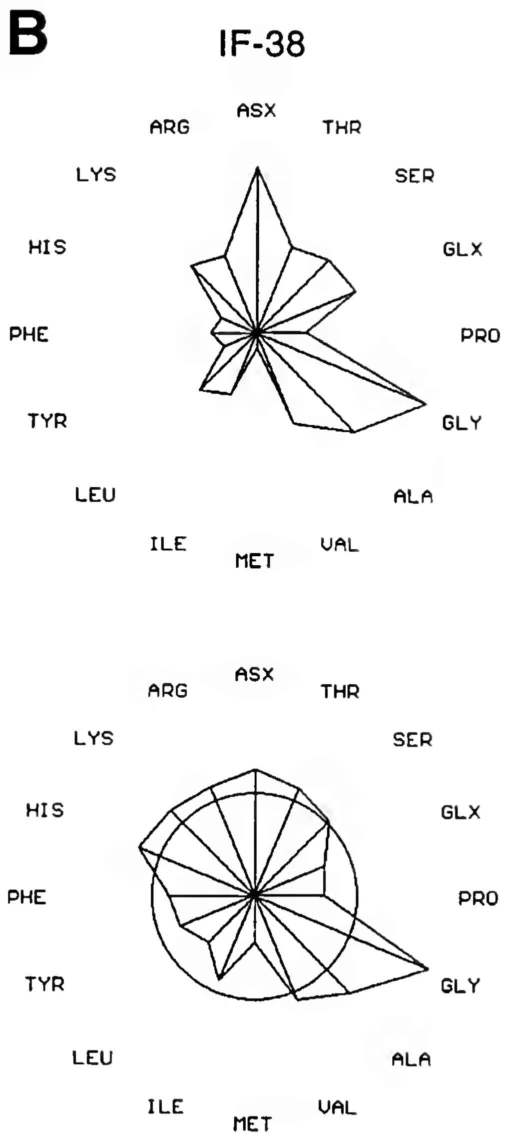
B
IF-38
ASX
THR
SER
GLX
PRO
GLY
ALA
VAL
MET
ILE
LEU
TYR
PHE
HIS
LYS
ARG
ASX
THR
SER
GLX
PRO
GLY
ALA
VAL
MET
ILE
LEU
TYR
PHE
HIS
LYS
ARG

Table 5-3. Results from the FINDER program to identify NFL-38.

Best Candidates	Score	MW* (kD)	IEP[¶]	Accession Number
GAPDH[§]; human	24	36.0	7.8	DEHUGL
GAPDH; chicken	24	35.7	8.0	A22035
GAPDH; human	24	36.0	7.9	A21939
GAPDH; human	24	36.0	7.9	A31988
GAPDH; human	24	35.9	7.9	B22939
GAPDH; human	23	35.8	6.7	DEHUG3
GAPDH; chicken	23	35.7	7.9	DECHG3
GAPDH; chicken	23	35.7	7.9	A32737
GAPDH; pig	22	35.6	6.9	DEPGG3
GAPDH; hamster	22	35.7	7.9	DEHYG
GAPDH; petunia	22	36.5	6.8	DEPJG
GAPDH; mouse-ear cress	22	36.9	6.4	JQ1287

MW: molecular weight (calculated)
IEP: isoelectric point (calculated)
GAPDH: glyceraldehyde-3-phosphate dehydrogenase

Table 5-4. Comparison of NFL-38 to GAPDH with data represented as nanomole percent for each amino acid.

Amino Acid	NFL-38 Average†	NFL-38 Corrected‡	GAPDH (human¶)	NFL-38 ± 1.5 SD Adjusted§	GAPDH Adjusted	Score¥
ASX	11.90	11.78	11.85	16.10 ± 1.36	16.12	2
THR	6.38	6.32	6.38	8.63 ± 0.35	8.68	2
SER	5.42	5.77	6.38	7.88 ± 0.90	8.68	2
GLX	6.85	6.59	6.08	9.00 ± 0.71	8.26	1
PRO	3.65	3.17	3.65	4.34 ± 1.99	4.96	2
GLY	10.85	9.86	10.03	13.48 ± 1.98	13.64	2
ALA	9.71	9.34	9.42	12.76 ± 0.33	12.81	2
VAL	10.18	11.70	9.73	15.99 ± 1.51	13.22	1
MET	1.41	2.07	3.04	2.83 ± 2.19	4.13	2
ILE	5.61	6.16	6.69	8.42 ± 0.58	9.09	1
LEU	6.00	5.77	5.78	7.88 ± 0.42	7.85	2
TYR	3.04	2.76	2.74	3.78 ± 0.22	3.72	2
PHE	4.46	4.46	4.26	6.09 ± 0.44	5.79	2
HIS	3.50	4.37	3.04	5.98 ± 0.70	4.13	0
LYS	7.37	6.09	7.90	8.32 ± 0.82	10.74	0
ARG	3.67	3.78	3.04	5.17 ± 0.61	4.13	1

†: data represents the average of two amino acid analysis

‡: data was multiplied by a correction factor which corrects for amino acid quantitation errors

¶: data for GAPDH was derived from human sequence (DEHUGL)

§: data is based on calculation initially excluding PRO, GLY, VAL and MET then calculating these four relative to 100% for the other 12 amino acids

¥: a score of 2 is given if the nanomole percent is within 1.5 SD and a score of 1 if it is within 3 SD (SD: standard deviation) above. The 12 closest matches were all forms of the same protein isolated from different species, glyceraldehyde-3-phosphate dehydrogenase (GAPDH) (Table 5-3). Comparison of the amino acid profile from 38 kD protein and GAPDH shows that the two proteins are similar with only a slight variation in the nanomole percent for any particular amino acid (Table 5-4).

Although the evidence presented above suggest that NFL-38 is GAPDH by computer analysis, further biochemical characterization was necessary. Cyanogen bromide cleavage experiments using NFL-38 and GAPDH from pig muscle (purchased from Sigma) demonstrated that the two proteins had the same cleavage fragment pattern (fingerprint) although the intensity of the silver stained bands varied somewhat (Figure 5-4). Subsequently, a polyclonal antibody was made in mouse to GAPDH using purified GAPDH from pig muscle. Figure 5-5a demonstrates that the polyclonal antibody to GAPDH labeled both GAPDH and NFL-38, and that the two proteins co-migrated at the same relative molecular weight on SDS polyacrylamide gel. In addition, we made a monoclonal antibody (mouse) to GAPDH and showed that it labelled the 38 kD protein which bound to all NF affinity columns (Figure 5-5b).

Other candidate cytosolic NF proteins have been initially characterized; however, identification of these proteins have met with little success. The amino acid composition for NFL-16 protein is given in Table 5-2 and graphically represented in Figure 5-6a. This data was then put through the FINDER program. Three close matches were found with a score of 22/32. These proteins, myelin

Figure 5-4. Comparison of CNBr cleavage fragments of NFL-38 and GAPDH.

The silver stained gel shows that GAPDH (lane 1) and NFL-38 (Lane 2) have similar cleavage fragments although the intensity of staining of individual bands was slightly different.

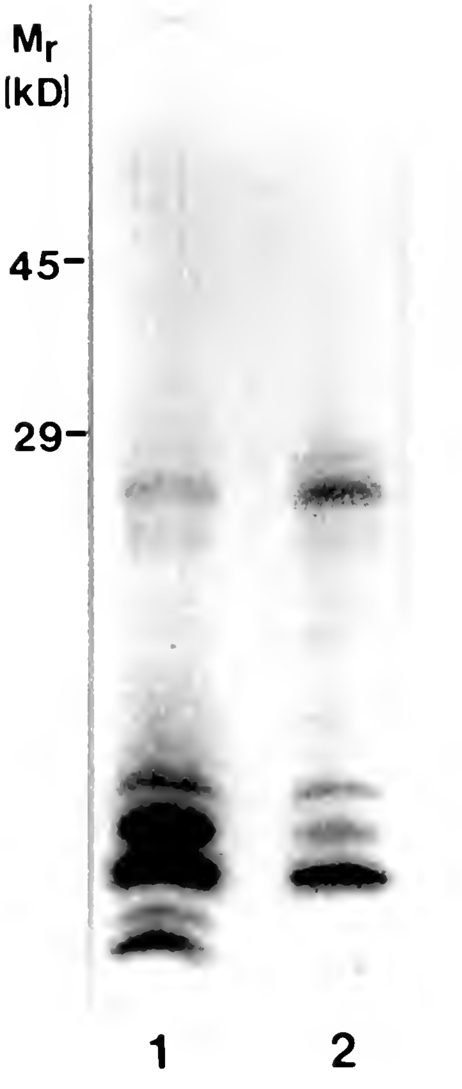
M_r
(kD)
45
29
1
2

Figure 5-5. Immunoblot analysis using antibodies to GAPDH to determine if the 38 kD proteins binding to various NF affinity columns is GAPDH

(A) Immunoblot demonstrates that the polyclonal antibody to GAPDH labels the 38 kD protein which bound to NF-L affinity column (lane 2). In addition, NFL-38 co-migrates with GAPDH (lane 1) which provides further evidence that these two proteins are similar.

(B) Immunoblot shows that the monoclonal antibody to GAPDH (1D4) labels the 38 kD protein which bound to all NF affinity columns. Lane 1-5 are fractions containing the 38 kD protein which bound to the different affinity columns; crude IF, NF-purified, NF-H, NF-M, and NF-L, respectively.

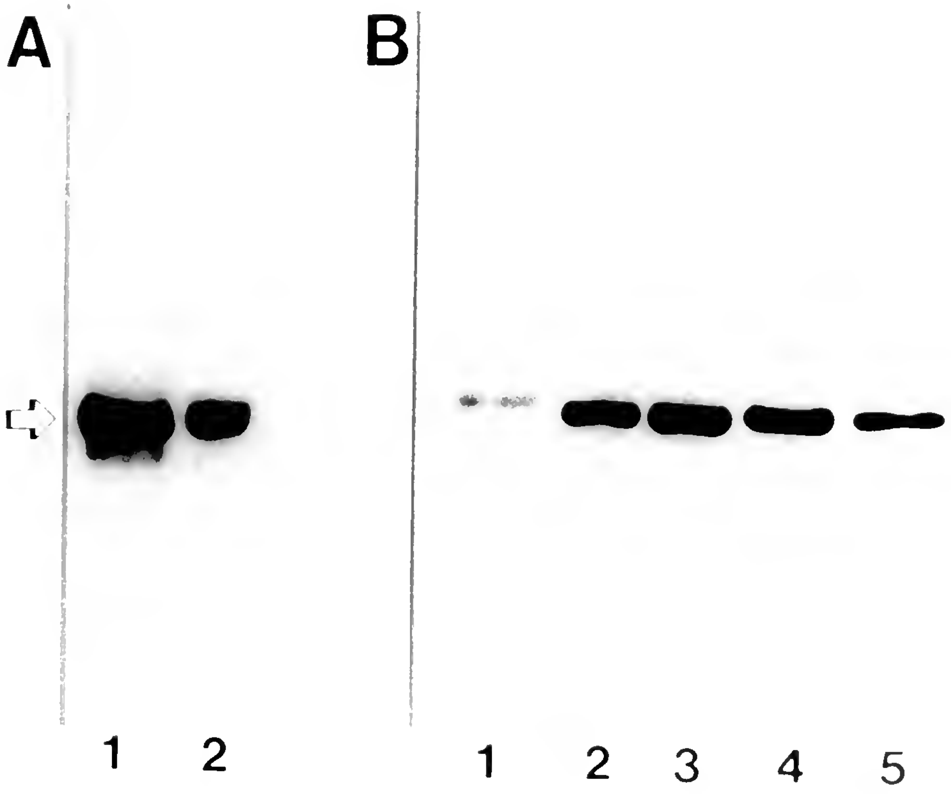
A
B
1
2
1
2
3
4
5

P2, fatty acid binding protein and phosphotransferase system II enzyme, are graphically represented in Figure 5-6a, and all have a similar molecular weight to that of NFL-16. However, on closer inspection these proteins may not be good matches since significant amounts of a particular amino acid is present in NFL-16 but not in the possible protein matches. This NFL-16 amino acid profile was compared to that of the average protein in Genbank and showed a very high concentration of lysine which is a basic amino acid (Figure 5-6b).

A similar analysis was performed on NFL-62 but no close matches were found using the FINDER program. The amino acid profile is given in Table 5-2 and graphically represented in Figure 5-6a. In addition, the amino acid composition was compared to the average protein in Genbank and showed a high concentration of glycine (Figure 5-6b). A potential and major problem to identify a protein is that one needs enough protein (at least 10 nmole) to get an accurate amino acid profile. In the case of NFL-16 and NFL-62, the amount of protein used for the analysis was 6.65 and 3.71 nmole, respectively. This may have resulted in no detectable amounts of proline in both NFL-16 and NFL-62, and no dectable amounts of tyrosine in NFL-62. In these cases, the insufficient amount of protein may have resulted in inaccurate estimates of the percent for each amino acid.

Discussion

This research represents a first attempt at identifying soluble candidate NF binding proteins using affinity chromatography. A number of proteins, based on relative molecular weights, were shown to bind to the various NF columns. In the

Figure 5-6. Graphical representions of the amino acid composition data for NFL-16, and possible matches as determined by the FINDER program.

(A) NFL-16 amino acid composition values (see Table 5-2) were put throught the FINDER program. Three protein closely matched with a score of 22/32: myelin P2, fatty acid binding protein, and phosphotransferase enzyme. However, these three proteins had significant differences with NFL-16 amino acid composition data which suggest that none of these proteins may be good matches.

(B) The NFL-16 protein was compared to the average protein in Genbank and the prominent feature that was shown is a high lysine content.

A

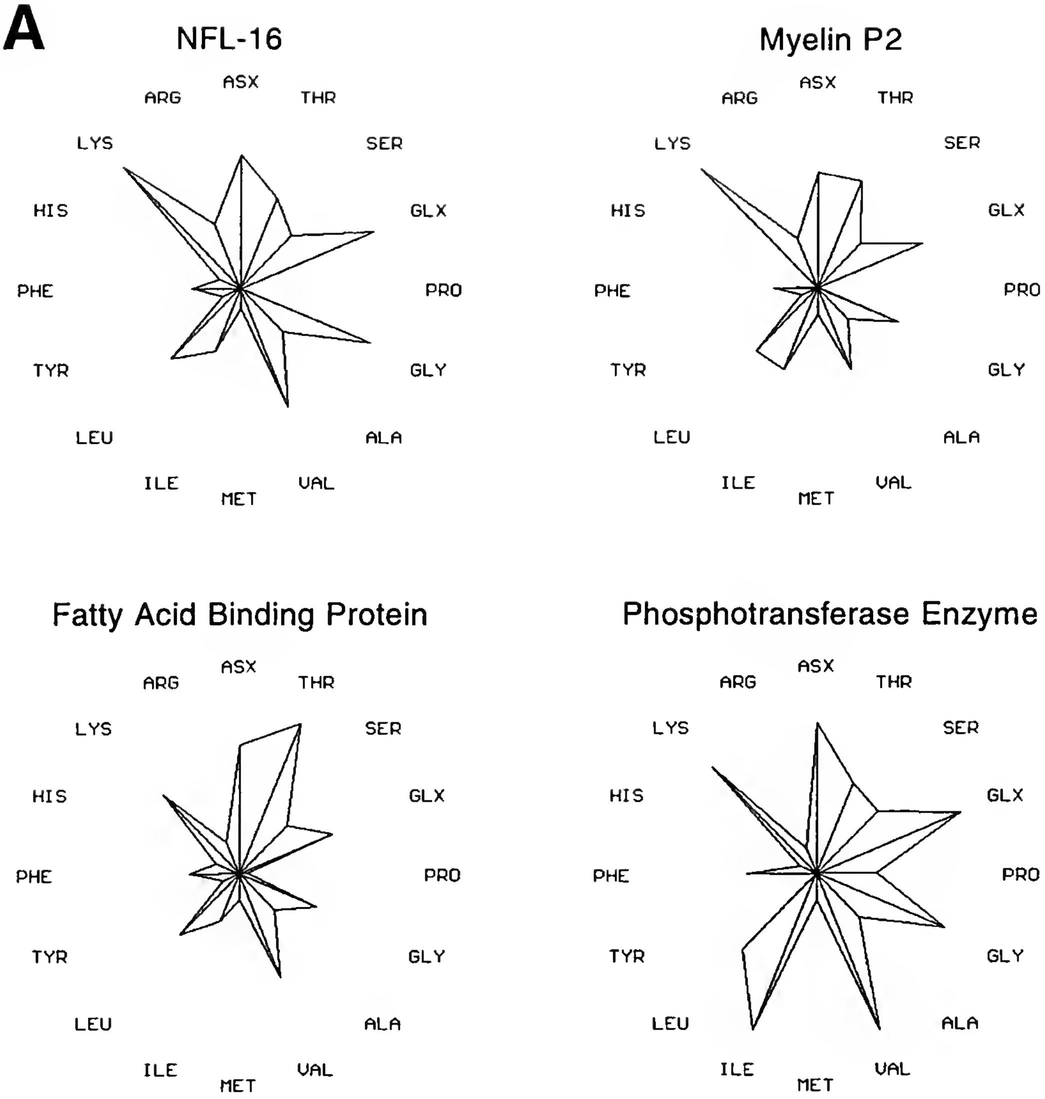

NFL-16

Myelin P2

Fatty Acid Binding Protein

Phosphotransferase Enzyme

B

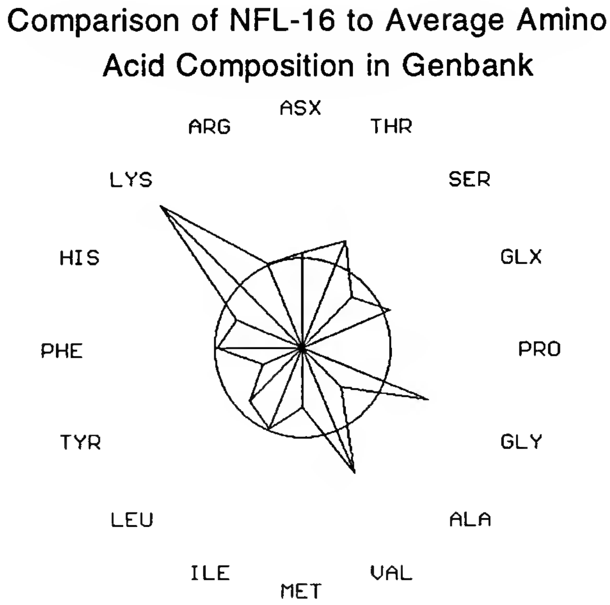

Comparison of NFL-16 to Average Amino Acid Composition in Genbank

Figure 5-7. Graphical represention of the amino acid composition data for NFL-62, and to that of the average amino acid composition in Genbank.

The top figure is a graphical representation of NFL-62 protein amino acid data (see Table 5-2). There was no percent nanomole given for either proline or tyrosine. Since proline and tyrosine are normally low in most proteins, the absence of these two amino acids may reflect the low amount of protein used in the quantitative amino acid analysis. In comparing this protein with the average amino acid composition of all proteins in Genbank shows that NFL-62 is particularly high in glycine. The amino acid composition for NFL-62 was put through the FINDER program; however, there were no close matches to help identify this protein.

NFL-62

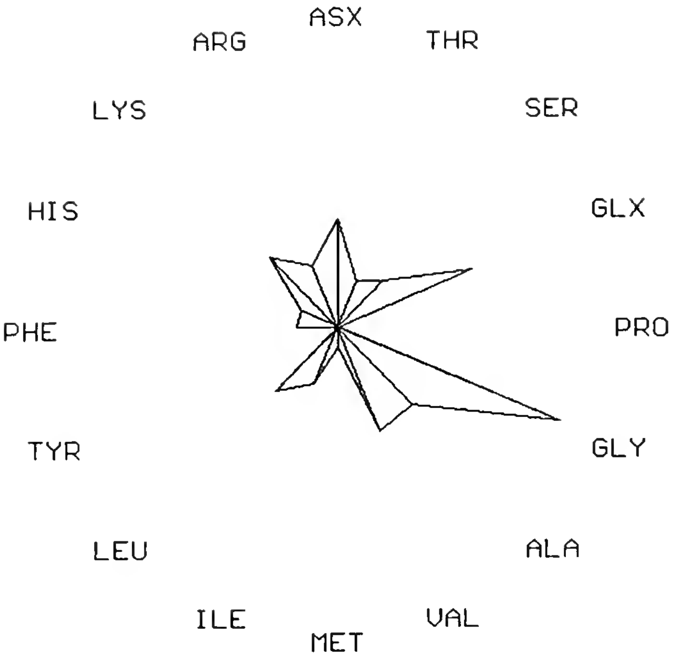

Comparison of NFL-62 to the Average Amino Acid Compostion in Genbank

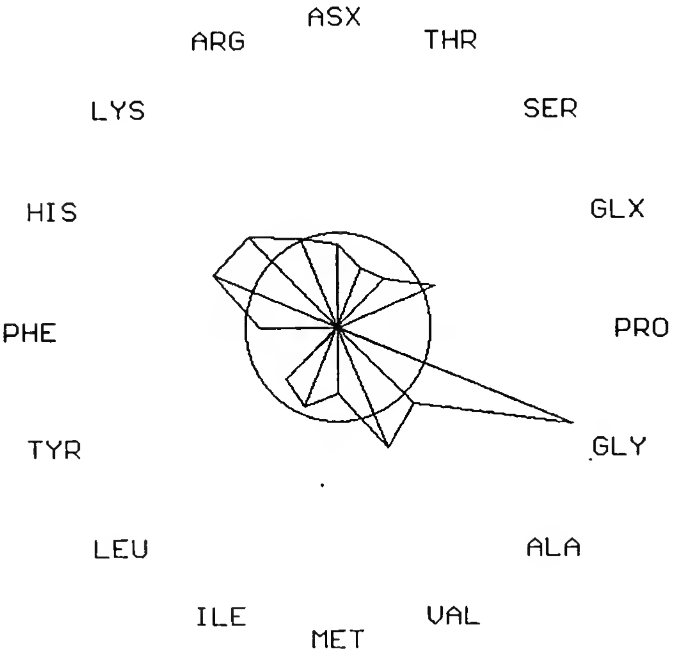

attempt to identify three of these proteins based on amino acid composition and the FINDER program (Shaw, 1993), only the 38 kD protein was identified.

The present work firmly identifies GAPDH as an *in vitro* NF binding protein, with the ability to stick to all three NF triplet proteins, although NF-L appears to have the largest binding capacity. GAPDH is a glycolytic enzyme which catalyzes the oxidative phosphorylation of D-glyceraldehyde 3-phosphate as well as other aldehydes (Lehninger, 1982). Most of the research relating to GAPDH has focused on bacterial systems and skeletal muscle, where glycolysis is an important mechanism (Opperdoes, 1988). In contrast, only a few papers describe a possible role for GAPDH in the nervous system. GAPDH is found in high abundance in the brain (Reid and Masters, 1986; Slagboom et al., 1990), presumably reflecting the almost absolute requirement for glucose as a substrate for oxidative metabolism in this organ. In relation to cytoskeletal elements *in vitro*, GAPDH has been shown to bind to and bundle MTs (Durrieu et al., 1987; Somers et al., 1990) and bind to actin filaments forming a gel-like, three dimensional filament network (Clarke and Morton, 1982; Clarke et al., 1986). These interactions with MTs and actin suggest an additional structural function for GAPDH.

GAPDH may bind to NFs to play a similar structural role as observed for the other cytoskeletal proteins. The crucial question that remains is whether NFs and GAPDH have the potential for interacting *in vivo*. The next chapter will focus on the strength of interaction between GAPDH and NF triplet proteins, and examine if this *in vitro* interaction may be relevant *in vivo*.

CHAPTER 6

CHARACTERIZATION OF GLYCERALDEHYDE-3-PHOSPHATE DEHYDROGENASE BINDING TO NEUROFILAMENTS IN VITRO

Introduction

GAPDH is a soluble glycolytic enzyme that is localized to subcellular structures in muscle (Masters, 1981; Bronstein and Knull, 1981) and particulate fractions of whole brain homogenates (Clarke and Morton, 1982). In the adult mouse brain the distribution between soluble and particulate GAPDH activity is roughly equal; however, the developmental ontogeny shows that bound GAPDH activity constantly increases from the prenatal period to adulthood, whereas, the soluble form is high prenatally and rapidly decreases during the first postnatal week. The soluble form then increases to a level similar to bound GAPDH activity in the adult mouse (Reid and Masters, 1986). GAPDH is present in brain tissue in higher amounts than the other glycolytic enzymes, and most other proteins with the exception of the cytoskeletal proteins. This suggests a possible structural role for GAPDH. Immunocytochemical analysis has demonstrated the presence of GAPDH in the cytoplasm of neurons (Morgenegg et al, 1986). In additon, GAPDH activity was shown to associate with the membrane fractions of a synaptosomal preparation (Knull, 1978; 1980).

In the previous chapter, an *in vitro* interaction between NF triplet proteins and GAPDH was demonstrated. However, before one could ask questions about the functional role of this interaction, the potential for *in vivo* interaction between NFs and GAPDH was examined.

Methods

Co-sedimentation Experiments

GAPDH from pig muscle was purchased from Sigma as a crystalline suspension in 3.2 M ammonium sulfate solution (500 units). GAPDH was centrifuged at 150,000xg for 15 minutes at 4°C in a Beckman TL-45 rotor and buffer exchanged with Centricon 30 microdialysis centrifuge tubes (Fisher Scientific) following manufacturers instructions. Purified NF subunits were prepared using the method described in Chapter 2 and dialyzed against 50 mM MES (pH 6.8) containing 3.4 M glycerol. Protein concentrations were determined for the dialyzed GAPDH and purified NF subunits using the Pierce microassay as described in Chapter 2.

GAPDH at a final concentration of 0.7 μM was incubated with NF-L (1.4 μM), NFM (1.0 μM), and NF-H (0.95 μM) for 1 hour at room temperature. The molar ratio of GAPDH to NF-L was varied to determine the total of amount of GAPDH that would bind to NF-L. Additionally, the NF-L concentration was held constant while the concentration of GAPDH was varied (0.35, 0.7, 1.4 and 2.8 μM). The strength of the interaction between GAPDH and NF-L subunit was examined by adding sodium chloride (0 M - 0.3 M) to the incubation mixture. The incubation mixture was centrifuge at 150,000xg for 1 hour at 25°C in a Beckman TL-45 rotor.

The supernatant was removed and added to SDS sample buffer. The pellet was then resuspended in 50 mM MES buffer (pH 6.8) and SDS sample buffer. Both the pellet and supernatant were separated on a 10% SDS polyacrylamide gel and proteins were visualized with Serva Blue G method (see Chapter 2).

Immunofluorescence Studies

DRG cultures were performed as described in Chapter 2. In addition to using post-natal day 1 rat pups, embryonic day 21 rat pups were used; however, no differences in the antibody staining patterns of DRG cells were observed between these two ages. Cells were fixed in methanol (-20°C) for 5 minutes or extracted with 0.1% Triton-X 100 for 1 minute. Immunocytochemical procedures were as described in Chapter 2 with the following exception, a 50 mM MES buffer (pH 6.8) was used to make all dilutions and for rinsing in between incubation steps.

PC12 cell cultures were prepared as described in Chapter 2 and fixation was the same as described above for the DRG cell cultures.

Antibodies

GAPDH monoclonal antibody, ID4 (undiluted), was characterized in Chapter 5. NF-H polyclonal rabbit serum (R14; dilution 1:200) to the KSP region of NF-H was made using NF fusion protein RH:559-794; NF-M polyclonal rabbit serum (R9; dilution 1:200) to the KE region of NF-M was made using NF fusion protein RM:677-845 (Harris et al., 1991). The polyclonal antibody to actin (dilution 1:25) was purchased from Sigma.

Results

Co-sedimentation Experiments

Without NFs in the co-sedimentation experiments, the majority of GAPDH remained in the supernatant fraction after a high speed centrifugation (Figure 6-1). In contrast , in the presence of NF-L, most of GAPDH was found in the pellet fraction with a ratio of 0.7 nM GAPDH to 1.4 nM NF-L subunit (Figure 6-1). The data were not as clear for NF-H and NF-M (Figure 6-1). The reason may be that NF-M and NF-H do not form a normal homopolymer like NF-L *in vitro* (Geisler and Weber, 1981; Liem and Hutchison, 1982) and thus do not pellet well even under high speed centrifugation conditions. In the case of NF-M, one observes more co-pelleting of GAPDH than with NF-H (Figure 6-1).

The maximum amount of GAPDH that would bind to NF-L was examined. NF-L concentration was kept constant at 1.4 μM while GAPDH concentration varied from 0.35 μM to 2.8 μM (Figure 6-2). These results demonstate qualitatively that GAPDH binds to NF-L in a 1 to 2 molar ratio.

In the presence of sodium chloride, the interaction of NF-L with GAPDH is dramatically affected. At low sodium chloride concentration (0.05 M), the amount of GAPDH that pellets with NF-L decreases approximately 50% (Figure 6-3). The interaction between NF-L and GAPDH is almost eliminated in the presence of 0.1 M sodium chloride (Figure 6-3). This interaction appears much weaker than observed during the elution of GAPDH from the NF-L affinity column where the eluting salt concentration ranged from 0.1 to 0.2 M potassium chloride (see

Figure 6-1. Co-sedimentation experiment with GAPDH and NF subunits.

GAPDH remains in the supernatant (S) fraction after high speed centrifugation. In the presence of the purified NF-L subunit, the majority of GAPDH is found in the pellet (P) fraction and not in the supernatant fraction. In the presence of NF-M, only some of GAPDH is localized to the pellet fraction, while in the presence of NF-H, most of the GAPDH is localized in the supernatant.

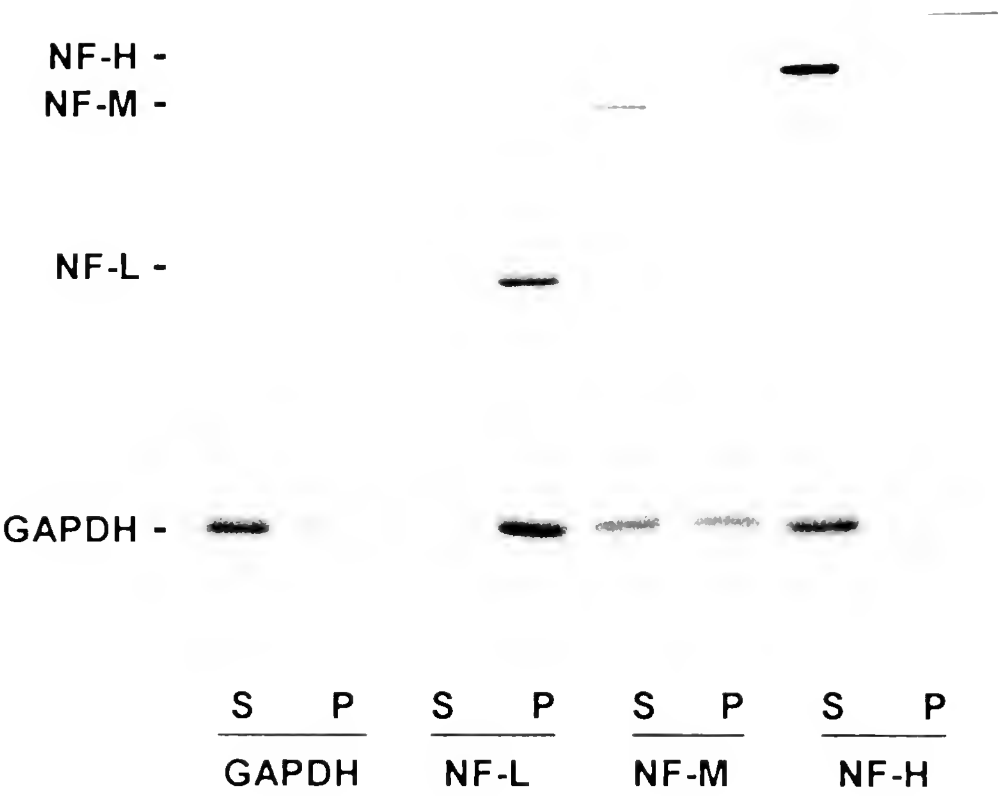
NF-H
NF-M
NF-L
GAPDH
S
P
S
P
S
P
S
P
GAPDH
NF-L
NF-M
NF-H

Figure 6-2. Co-sedimentation of GAPDH and NF-L with different concentrations of GAPDH.

The NF-L concentration was kept constant at 1.4 μM while GAPDH concentration varied from 0.35 to 2.8 μM. These results demonstrate that maximum binding of GAPDH occurs at approximately a 1 to 2 molar ratio of GAPDH to NF-L.

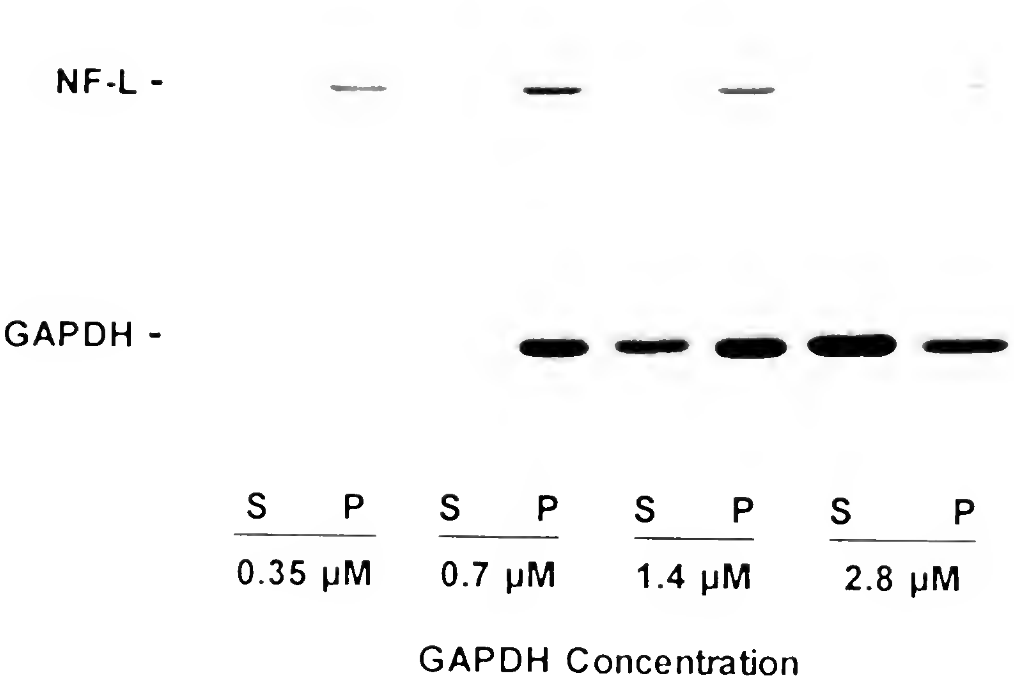
NF-L -
GAPDH -
S P S P S P S P
0.35 μM
0.7 μM
1.4 μM
2.8 μM
GAPDH Concentration

Figure 6-3. Co-sedimentation of GAPDH and NF-L with different concentrations of sodium chloride.

The addition of sodium chloride results in a dramatic decrease in binding of GAPDH to NF-L at 0.05M sodium chloride concentration, where much of the GAPDH is found in the supernatant (S). P: pellet fraction.

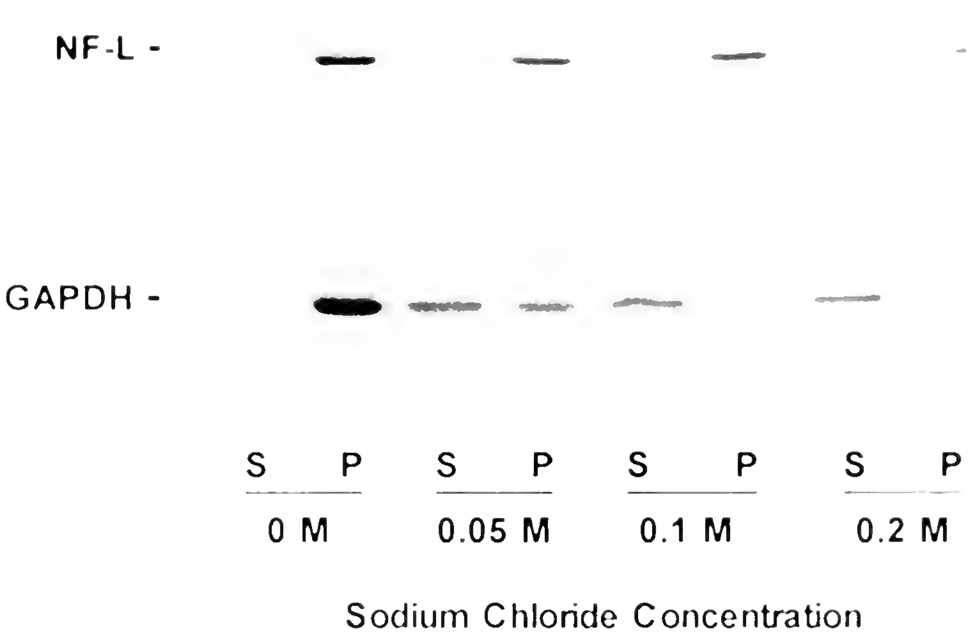
NF-L -
GAPDH -
S P S P S P S P
0 M
0.05 M
0.1 M
0.2 M
Sodium Chloride Concentration

Chapter 5). These results suggest that the NF-L subunit and GAPDH bind by means of a weak electrostatic interaction.

Immunofluorescence Studies in Cultured Cells

Single labelling of DRG cells with GAPDH monoclonal antibody (ID4) demonstrated that GAPDH was localized in the soma, neurites, and growth cones (Figure 6-4, arrows). The labelling along the neuritic processes had a patchy distribution. ID4 antibody appeared to label the neuritic branch points more intensely than the neurite itself (Figure 6-4, arrowheads).

Double-labelling of DRG cell cultures with ID4 and NF-H antibody (R14) resulted in an overlap in labelling between the two antibodies in the soma and along the neurites of these cells (Figure 6-5 a,b; arrowhead). However, the GAPDH antibody distribution was more extensive than the NF labelling pattern in the growth cone where ID4 labelling extended into the growth cone and labeled the filopodia (Figure 6-5 c,d). In addition, ID4 did not label the entire extent of the neurite as seen with NF antibodies but labeled along the neurite in a punctate distribution with increased labelling at neuritic branch points. In NGF differentiated PC12 cells, the GAPDH antibody labeling pattern was similar to that observed in DRG cells. Double-label experiments with NGF differentiated PC12 cell cultures showed that GAPDH appeared to be associated more with the membranous compartment of the neuron especially in the growth cone (arrow). This suggests a complementary distribution between NF subunits and GAPDH antibodies (Figure 6-6).

Figure 6-4. Composite of GAPDH antibody labelling (ID4) of a DRG cultured neuron.

GAPDH antibody staining pattern is localized throughout the cell body and into the neurites and growth cones (arrows). The labelling along the neurite appears patchy with intense labelling at neuritic branch points (arrowheads). s: satellite cells or non-neuronal cells. Scale bar: 25 μm.

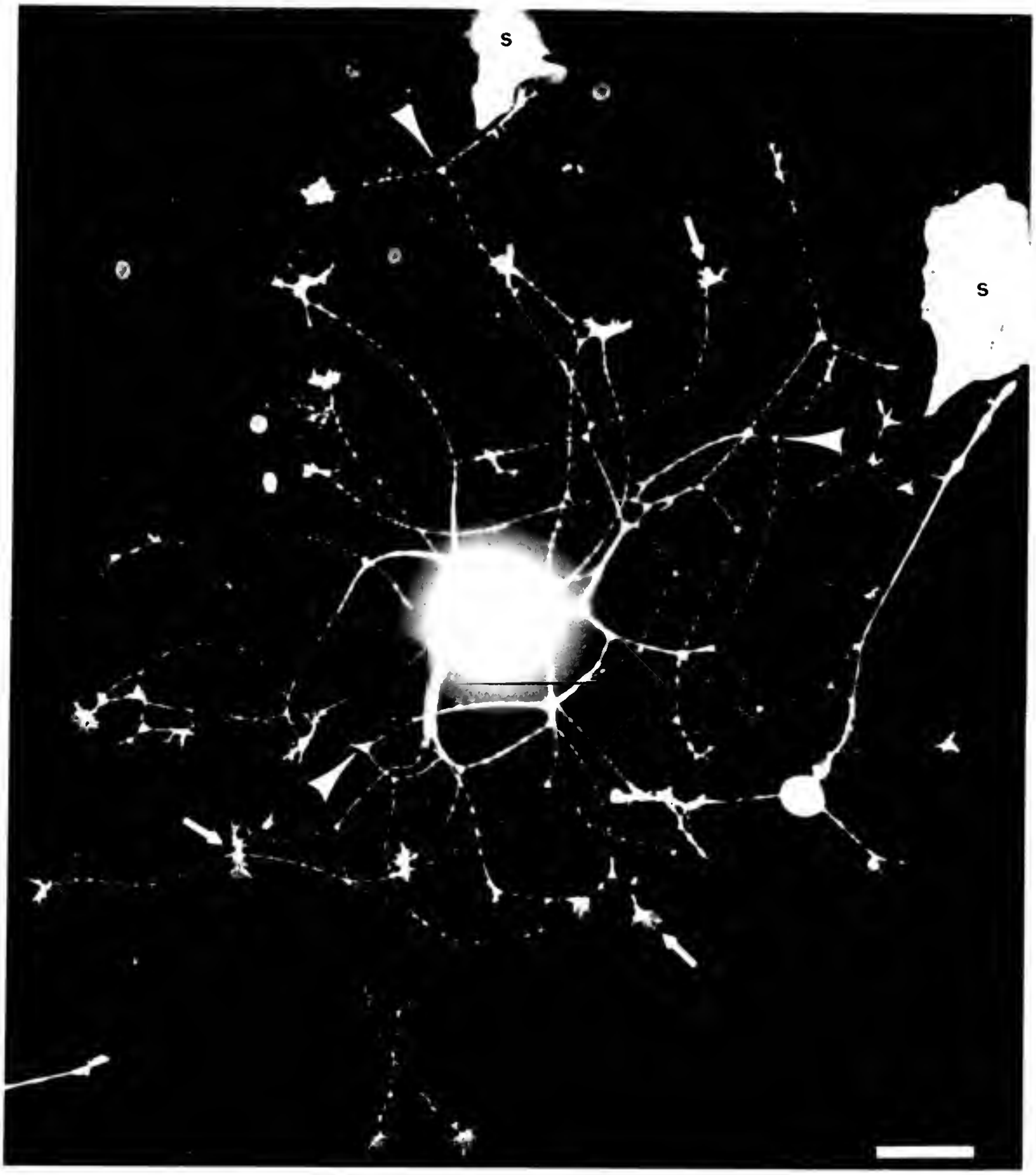
s
s

Figure 6-5. Co-localization experiment in DRG cell cultures with antibodies to GAPDH (ID4) (A,C) and NF-H (R14) (B,D).

(A,B) Double-labelling of DRG cells demonstrates that the GAPDH labelling pattern (A) overlaps with the NF labelling pattern (B) in the cell body and along the neurites, particularly at branch points (arrowheads). In contrast, in growth cones GAPDH labels throughout the growth cone and into the filopodia (A, arrows), whereas, NF proteins are localized only at the base of the growth cone (B). Scale bar: 25 µm.

(C,D) A high power view of growth cones shown in (A and B) demonstrates that GAPDH (C) and NF (D) antibody labelling patterns overlap along the neurite and into the base of the growth cone; however, GAPDH labelling extends well into the growth cone and filopodia (arrow). Scale bar: 12.5 µm.

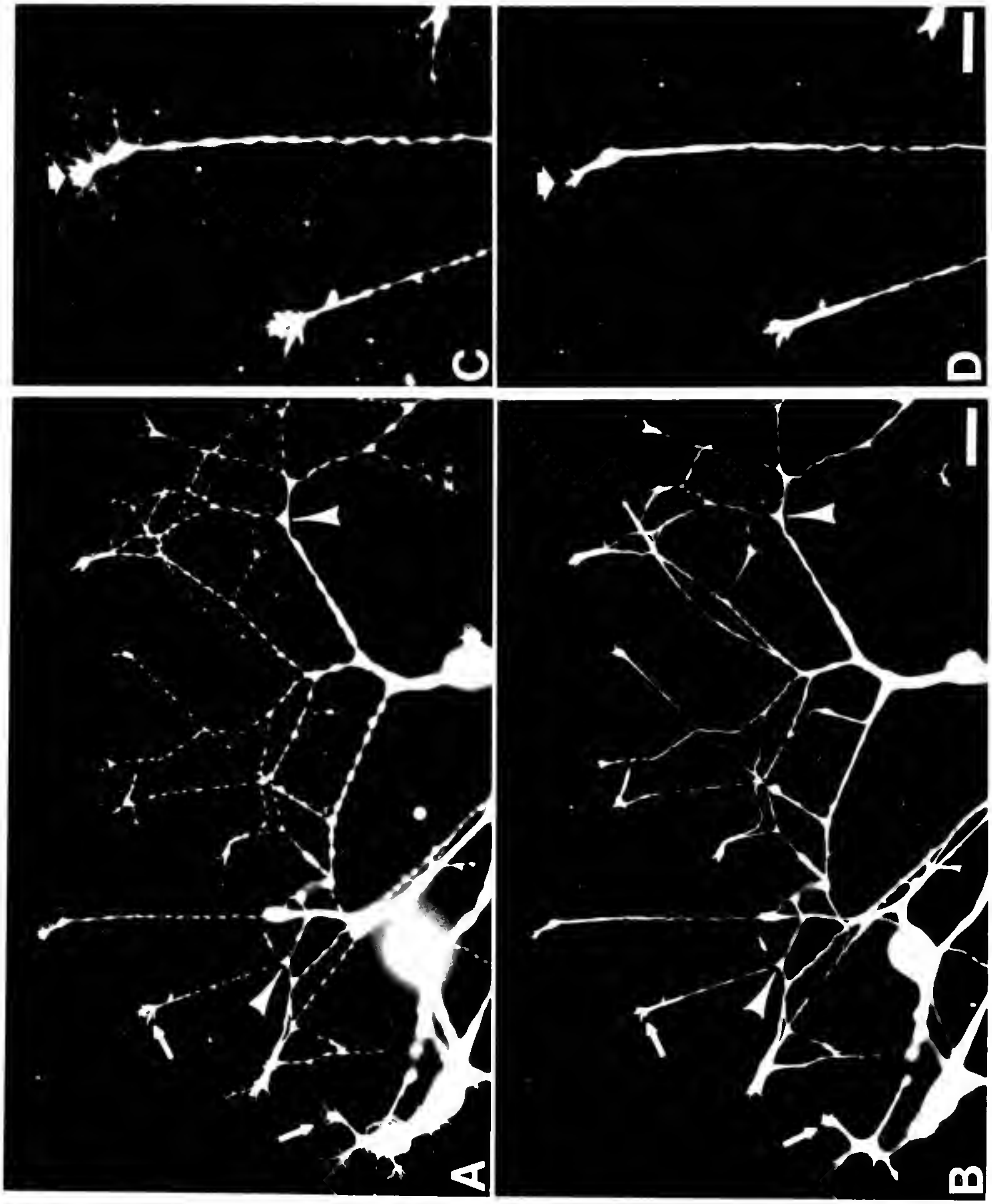
A
B
C
D

Figure 6-6. Co-localization experiment in differentiated PC12 cell cultures with antibodies to GAPDH (ID4) (A,B) and NF-M (R9) (C).

(A) GAPDH immunoreactivity is observed throughout the NGF-differentiated PC12 cell. The strongest labelling was associated with the cell body and growth cone (arrow). In addition, GAPDH antibody labels the neurite in discrete patches (asterisks). Scale bar: 25 μm.

(B,C) Double-labelling of NGF-differentiated PC12 cells demonstrate that the GAPDH labelling pattern (B) overlaps with the NF labelling pattern (C). GAPDH immunoreactivity was observed in the filopodia and the labelling appeared to be associated with the plasma membrane. In contrast, NF-M immunoreactivity was observed labelling a distinct fiber bundle at the base of the growth cone (wide arrow) but no labelling was observed in the filopodia. Scale bar: 25 μm.

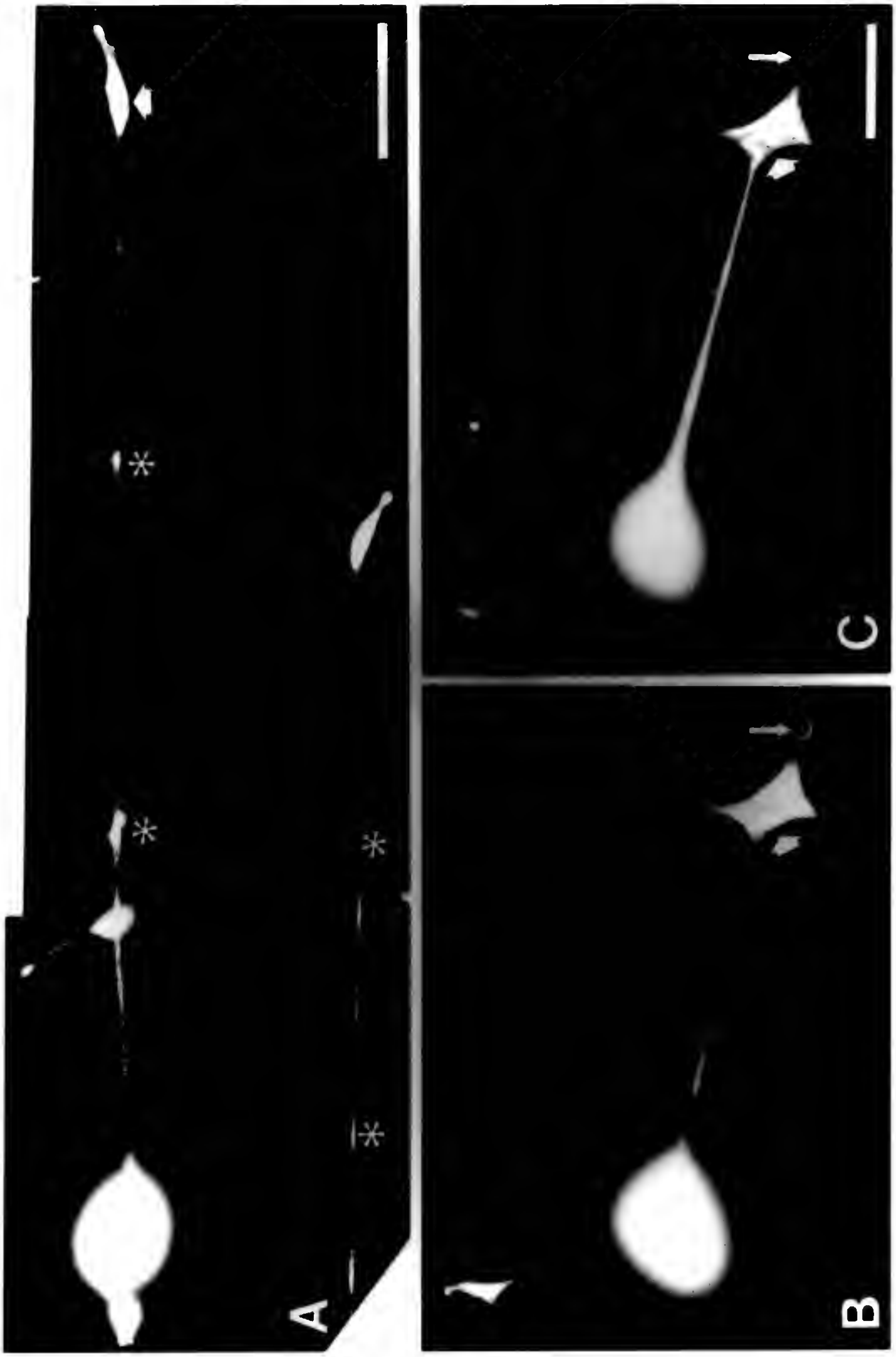
A
B
C

Since GAPDH antibody labelling pattern was found to label the growth cone, including the filopodia, double labelling of GAPDH with actin antibodies was examined in DRG cell cultures. Figure 6-7 demonstrates that GAPDH co-localized with actin throughout the soma and neurites, as well as in the growth cone.

Discussion

GAPDH was shown to co-sediment with purified NF-L subunit *in vitro*. These data confirmed the results of GAPDH binding to the NF-L affinity column (Chapter 5). The binding of GAPDH to NF-L appeared to be weak with a 50% decrease in binding of GAPDH to the NF-L subunit when only 0.05 M sodium chloride in 50 mM MES buffer was added to the incubation mixture. Although this interaction between GAPDH and NF-L subunit is weak, previous research showed that the bound form of GAPDH is released from particulate fraction of lysed nerve endings at a 0.1 M sodium chloride concentration (Knull, 1978). This suggests that overall there is a weak interaction between GAPDH and insoluble brain material.

Immunofluorescent studies of DRG cultured cells demonstrated the presence of GAPDH throughout the cell body and neuritic processes. However, GAPDH was not exclusively co-localized with NFs in DRG cells. This result was not unexpected given that previously GAPDH was shown to bind to both MFs and MTs *in vitro* (Clarke and Morton, 1982; Clarke et al., 1986; Durrieu et al., 1987; Somers et al., 1990).

The data presented here suggest that some neuronal GAPDH could be

Figure 6-7. Co-localization experiment in DRG cell cultures with antibodies to GAPDH (ID4) (A) and actin (polyclonal) (B).

(A,B) Double-labelling of DRG cells demonstrated that the GAPDH labelling pattern (A) overlaps completely with the actin labelling pattern (B) in the cell body, along the neurites and in the growth cones (arrow). Scale bar: 25 μm.

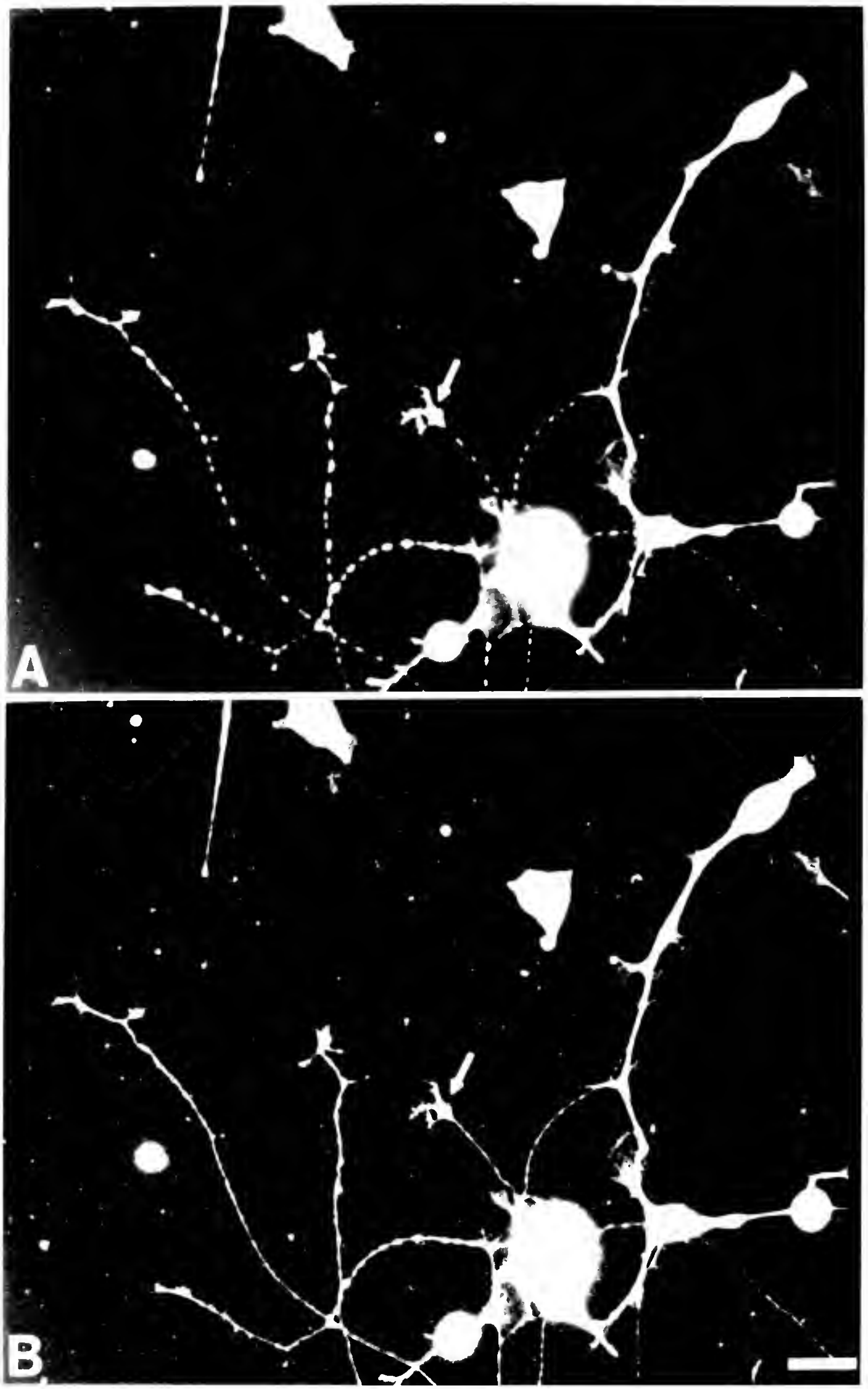
A
B

associated with NF *in vivo*. However, additional results suggest that GAPDH may be more closely associate with the actin network than the NF network. In muscle cells, a number of glycolytic enzymes bind to the actin network which allows for a close physical association between the energy pathway and the contractile machinery (Clarke et al., 1985). A similar mechanism in neurons would in turn suggest that one of the functions of NF proteins may be to act as docking substrates for the localization of GAPDH and possibly other enzymes *in vivo*. Future electron microscopical studies that examine the question of the exact localization of GAPDH *in vivo* may give a better idea of how GAPDH interacts with cytoskeletal structures.

If GAPDH and NFs are shown to interact *in vivo*, the next step would be to determine which part of the NF subunit is interacting with GAPDH. The NF binding site for GAPDH may be represented by one of the homologous sequences found in NF triplet proteins, such as the α-helical rod regions or the glutamic acid rich segments in the carboxyl terminal. It is interesting to note that GAPDH is mildly basic and that tubulins, which also bind GAPDH, also contain a glutamic acid rich region. This suggests that the glutamic rich region in the carboxyl-terminal domain of NFs may be a candidate binding site.

CHAPTER 7

OVERALL DISCUSSION

General Considerations

This dissertation research took two different approaches to identify candidate NF binding proteins. The first approach focused on insoluble proteins that co-purify with NFs in a salt and detergent preparation from spinal cord. This resulted in the identification of plectin, a known IFAP characterized in non-neural tissues which was previously shown to bind to NF triplet proteins *in vitro* (Foisner et al., 1988). The second approach used different NF affinity columns to identify candidate soluble NF binding proteins based on relative mobility on SDS polyacrylamide gels. Although a number of proteins were found to bind with varying specificity to the different NF affinity columns, this work focused on a 38 kD protein which was identified as glyceraldehyde-3-phosphate dehydrogenase (GAPDH). The potential *in vivo* interaction was examined for both of these *in vitro* NF binding proteins.

Criteria for Classifying IF Binding Proteins

A number of lines of evidence are required to classify a protein as a protein binding to a specific target protein. Depending on the knowledge of the target protein, this evidence will vary from weak to strong criteria. It is important to establish an overall criteria, as well as a minimal criteria to judge your candidate binding protein. The following represents criteria by which one can use in identifying and classifying candidate binding proteins: (1) co-purification or co-sedimentation of the candidate binding protein to the target protein; (2) colocalization of both the candidate binding protein and target protein in the same cell types; (3) ultrastructural localization of the candidate binding protein to the target protein; (4) an affinity or dissociation constant of the candidate protein to the target protein, and how sensitive this interaction is to the addition of salt; (5) stoichiometry of this interaction; and (6) functionality of the interaction between the candidate binding protein and target protein.

In the case of IFAP a very loose criteria has been used in identifying a protein as an IF binding protein in which only one of the above criteria needs to shown (Foisner and Wiche, 1991). One reason for this is that not much is understood about the function of IF proteins in general, and it is therefore difficult to design a functional assay to determine a possible relationship between the candidate binding protein and the target protein. The hope of research is that by defining what proteins bind to and interact with IF proteins one will be able to assign more functions to IF proteins.

Relationship between Plectin and NF Proteins

Based on the above criteria, plectin has been firmly established as an IFAP. Plectin co-purifies with a number of IF proteins, and co-localizes with IF proteins at both the light and ultrastructural level. The stoichiometry of this interaction is 1 plectin per 20 vimentin polypeptide chains, where plectin is thought to cross-link IF proteins, at least in cultured cells (for review: Wiche, 1989).

One of the original reasons for examining the relationship between plectin and NFs was to determine whether the proposed cross-linking function of plectin could account for the marked stability of NF bundles *in vitro* (Shaw and Hou, 1990). Although plectin was localized to the cytoplasm of select neurons, the distribution of plectin more closely reflected that of vimentin in non-neuronal cells in the nervous system. In addition, the submembranous localization of plectin observed in neurons, especially in the mesencephalic nucleus of V and in the axonal bundles in both the CNS and PNS suggests that plectin does not contributes to the marked stability of NF bundles. Pilot experiments that examined crude IF bundles isolated from spinal cord found that the NF bundles were not labeled by plectin antibodies (data not shown). Rather, plectin immunoreactivity was associated with small punctate structures which may have been derived from the submembranous cytoskeleton. Therefore it seems that plectin is not responsible for a significant amount of NF cross-linking; instead, plectin may be responsible for the interaction between NF network and plasma membrane in select neurons.

One interesting feature of plectin's anatomical distribution was the expression of plectin in moderate amounts in select motoneurons in the brainstem and spinal cord. These cells were also labeled with antibodies to NF triplet proteins and peripherin. To determine whether plectin expression corresponded more closely with NF triplet proteins or peripherin, facial nerve lesions were performed. An interesting feature after a peripheral nerve lesion is that the mRNA of NF triplet proteins is down-regulated (Hoffman et al., 1987; Wong and Oblinger, 1987; Goldstein et al., 1988; Tetzlaff et al., 1988); whereas, peripherin mRNA is upregulated in axotomized motoneurons (Oblinger et al., 1989; Wong and Oblinger, 1990). This upregulation is reflected in an increase in peripherin immunoreactivity in motoneurons. After peripheral nerve transection, plectin and peripherin immunoreactivity increased in axotomized motoneurons. This suggests that plectin may more closely be associated with the class III neural IF proteins, peripherin and vimentin, than with the class IV neural IF proteins *in vivo*.

Finally, the types of motoneurons that express plectin are similar to the motoneurons which contain abnormal NF accumulations that degenerate in motoneuron diseases. This occurrence taken together with the dramatic increase in plectin immunoreactivity in motoneurons after axonal injury suggest that the high level of this known IF cross-linker may play some role in the NF accumulations seen in some motoneuron diseases.

The Role of GAPDH in the Nervous System

A known role of GAPDH in the nervous system is its function in glucose metabolism, an essential component of cellular energy production. GAPDH is found in high abundance in brain, more than any other enzyme, and is present at comparable levels, although in lower amounts, to the cytoskeletal proteins. This suggests that GAPDH may perform a dual function in the CNS.

This research demonstrated that GAPDH is a protein that binds *in vitro* to NFs. Additionally, previous research has shown that GAPDH binds *in vitro* with actin and tubulin. These results taken together suggest that GAPDH may also function in a structural role in the CNS.

In muscle cells, GAPDH is one of a number of glycolytic enzymes that binds to the actin network. This allows for a close association between the energy pathway and contractile machinery. In the case of developing neurons, GAPDH was shown to co-localize with actin in the growth cone. Since growth cones are pathfinding structures and actin assemblies generate the movements of growth cones, localization of GAPDH to actin network may be an important theme in linking energy pathways to contractile machinery in a number of cell types. In addition, GAPDH has been shown to assembly actin monomers *in vitro* to form a gel-like matrix. This suggests that *in vivo* GAPDH may be structurally important in stabilizing the newly formed actin network at the leading edge of the growth cone, as well as acting in the same fashion in synaptic plasticity in the adult nervous system. Finally, the intense labelling of GAPDH antibodies at neuritic branch points may reflect GAPDH's role in structural stability, since this enzyme was shown to bundle microtubules *in vitro*, in addition to assembling actin monomers.

Immunofluorescent studies suggest a potential *in vivo* interaction of GAPDH and NFs; however, in some areas GAPDH appeared more closely associated to the plasma membrane. If the interaction between GAPDH and NFs is physiological, then a potential role for GAPDH may be to allow energy production near proteins that are heavily phosphorylated in the axon. The punctate labelling of GAPDH along the developing neurite may correspond to docking sites for this enzyme, as well as other glycolytic enzymes, where NF phosphorylation may be taking place along the neurite.

Based on the criteria for characterizing a protein as a binding protein, GAPDH can be defined as an *in vitro* NF binding protein. GAPDH bound to the different NF affinity columns and co-sedimented with NF-L subunit with an approximate ratio of 1 mole of GAPDH (tetramer form) to 2 mole of NF-L subunit. Although this interaction was shown to be relatively weak with the addition of salt, the *in vivo* interaction between GAPDH and NFs may only be a transient event where a tight interaction is not necessary. In addition, the potential for an *in vivo* interaction is shown in the co-localization of GAPDH with NFs at the light level.

Future Directions

Other NF Binding Assays

In addition to the approaches taken in this dissertation to identify and characterize IFAPs, other strategies are also available.

NF Fusion Proteins. Molecular biology techniques have allowed for high level of protein expression which results in a higher yield of protein and easier purification methods. One such protein expression system, glutathione S-transferase (GST) gene fusion system, allows for rapid purification of the GST fusion protein by taking advantage of the binding of GST to Glutathione Sepharose 4B (Kaelin et al., 1991). The GST fusion protein can be eluted from Glutathione

Sepharose 4B by using reduced glutathione or by cleaving the clone portion of the GST fusion protein using site-specific proteases. This rapid and simple purification procedure has the advantage over other fusion protein systems (ie. trpE bacterial system) because the purification methodology is performed under non-denaturing conditions.

In addition, one could take advantage of the tight interaction between GST fusion protein and Glutathione Sepharose 4B and directly make an affinity column to examine the interactions between a specific region of the protein of interest with other proteins. This minimizes the need to utilize harsh methods used in protein purification procedures as well as the problem of knowing whether the region of interest is available for binding since the GST portion of the fusion protein is binding to the immobilized matrix.

Competition Experiments. These experiments use known proteins, fusion proteins or peptide sequences which are known to bind to NFs *in vitro* to determine if your candidate NF binding protein has a similar binding domain to that of the known NF binding protein. In addition, these types of experiments can be used to examine the effects of co-factors such as ATP or calcium to determine if they have any effect on the ability of proteins to bind. For example, the addition of co-factors could induce binding of proteins to NFs or decrease the affinity of a particular protein to NFs.

Bio-Sensor. For studying molecular interactions in real time, the biosensor-based technology employs a surface plasmon resonance system (Jönsson et al., 1991). To covalently immobilize a protein, the amine groups of the protein are reacted with the active esters of a polymer consisting of a carboxymethylated dextran matrix plated on a sensor chip (a glass surface covered with gold film). To examine the possible interaction of a particular protein or a mixture of proteins with that of an immobilized protein, proteins are allowed to flow across the immobilized protein complex. Interactions are measured by using polarized light from a light-emitting diode, which is reflected by the gold film where the reflected light is detected by a photo detector array. Changes in the refractive index, as measured by this optical technique are directly proportional to the change in adsorbed mass of the protein complex. The advantages of using the Biosensor system is that allows for the detection of an interaction of a protein, normally found in such low concentration that it would be missed in a SDS polyacrylamide gel when using affinity chromatogaphy techniques. In addition, the binding constants of most interactions can be determined.

The two-hybrid system. The two-hybrid system takes advantage of molecular biology techniques to detect protein-protein interactions *in vivo* (Fields and Song, 1989; Guarente, 1993) and is available commercially from Clontech. This system uses two reporter genes HIS3 and lacZ which are under the control of the GAL4 responsive sequences in yeast host cells. The clone gene for the protein of interest is put into a DNA-binding domain vector, pGBT9, which also contains the TRP1 gene necessary for tryptophan biosynthesis, whereas, a cDNA library or select clone genes for candidate binding proteins are placed into the activation domain vector, pGAD424, which contains a gene encoding for LEU2 necessary for leucine biosynthesis. These two vectors are co-transformed into the HF7c yeast host strain and plated on synthetic medium without tryptophan, leucine or histidine, to select for co-transformants which contain two interacting hybrid proteins. If the target protein interacts with a library-encoded protein then the functional GAL4 activator is reconstituted by the interaction of the two proteins, and HIS3 reporter gene is activated which allows for the selection of histidine producing yeast cells. A secondary screen of the histidine positive transformants is tested by the expression of the second reporter gene using ß-galactosidase activity.

The advantages of this system are that weak or transient interactions are readily observed, that the experiment is performed *in vivo* and thus proteins are more likely to be in their native conformation, and once the interacting protein has been identified, the gene is already cloned.

Conclusions

A great deal of work remains to fully understand the potential interaction of plectin and GAPDH to neural IF proteins, as well as the roles of all of these proteins in the nervous system. One step would be to examine more closely the distribution of GAPDH and plectin within the neuron using electron microscopy. If these *in vitro* interactions between NFs with plectin and GAPDH prove to be physiologically relevant, then NF proteins will be shown to be as functionally diverse as the other cytoskeletal elements.

REFERENCES

Aamodt, E.J. and Williams, R.C.Jr. (1984) Microtubule-associated proteins connect microtubules and neurofilaments in vitro. Biochem. 23: 6023-6031.

Abercrombie, R.F., Al-Baldawi, N.F., and Jackson, J. (1990) Ca2+ binding by Myxicola neurofilament proteins. Cell Calcium 11: 361-370.

Aletta, J.M., Shelanski, M.L., and Greene, L.A. (1989) Phosphorylation of the peripherin 58-kDa neuronal intermediate filament protein. J. Biol. Chem. 264: 4619-4627.

Bamburg, JR. and Bernstein, B.W. Actin and actin-binding proteins in neurons. In: *The neuronal cytoskeleton*, edited by R. D. Burgoyne. New York: Wiley-Liss, 1991, p. 121-160.

Berthold, C. Some aspects of the ultrastructural organization of peripheral myelinated axons in the cat. In: *Axoplasmic Transport*, edited by D. Weiss. New York: Springer-Verlag, 1982, p. 40-54.

Bertowitz, S.A., Katagiri, J., Binder, H.K., and Williams, R.C. (1977) Separation and characterization of microtubule proteins from brain. Biochem. 16: 5610-5617.

Brady, S.T. (1993) Motor neurons and neurofilaments in sickness and in health. Cell 73: 1-3.

Brody, B.A., Ley, C.A., and Parysek, L.M. (1989) Selective distribution of the 57 kDa neural intermediate filament protein in the rat CNS. J. Neurosci. 9: 2391-2401.

Bronstein, W.W. and Knull, H.R. (1981) Interaction of muscle glycolytic enzymes with thin filament proteins. Can. J. Biochem. 59: 494-499.

Burgoyne, R.D. High molecular weight microtubule-associated proteins of brain.In *The neuronal cytoskeleton*, edited by R. D. Burgoyne. New York: Wiley-Liss, 1991, p. 75-92.

Burton, P.R. and Fernandez, H.L. (1973) Delineation by lanthanum staining of filamentous elements associated with the surfaces of axonal microtubles. J. Cell Sci. 127: 567-583.

Chiu, R.-C., Barnes, E.A., Das, K., Haley, J., Socolow, P., Macaluso, F.P., and Fant, J. (1989) Characterization of a novel 66 kd subunit of mammalian neurofilaments. Neuron 2: 1435-1445.

Ciment, G. (1990) Precocious expression of NAPA-73, an intermediate filament-associated protein, during nervous system and heart development in the chicken embryo. Annals New York Academy of Sciences 588: 225-235.

Ciment, G., Ressler, A., Letourneau, P.C., and Weston, J.A. (1986) A novel intermediate filament-associated protein, NAPA-73, that binds to different filament types at different stages of nervous system development. J. Cell Biol. 102: 246-251.

Clark, A.W., Griffin, J.W., and Price, D.L. (1980) The axonal pathology in chronic IDPN intoxication. J. Neuropathol. Exp. Neurol. 39: 42-55.

Clarke, F.M. and Morton, D.J. (1982) Glycolytic enzyme binding in fetal brain - the role of actin. Biochem. Biophys. Res. Commun. 109: 388-393.

Clarke, F.M., Morton, D.J., Stephan, P., and Wiedmann, J. The functional duality of glycolytic enzymes: potential integrators of cytoplasmic structure and function. In: *Cell motility: mechanisms and regulation*, edited by H. Ishikawa, S. Hatano and H. Sato. New York: Alan R. Liss, 1986, p. 235-250.

Clarke, F.M., Stephan, P., and Morton, D.J. Glycolytic enzyme organization via the cytoskeleton and its role in metabolic regulation. In: *Regulation of Carbohydrate Metabolism*, edited by R. Beitner. New York: CRC Press, 1985, p. 1-30.

Coulombe, P.A. and Fuchs, E. (1990) Elucidating the early stages of keratin filament assembly. J. Cell Biol. 111: 153-169.

Côté, F., Collard, J.-F., and Julien, J.-P. (1993) Progressive neuonopathy in transgenic mice expressing the human neurofilament heavy gene: a mouse model of amyotrophic lateral sclerosis. Cell 73: 35-46.

de Waegh, S.M., Lee, V.M.-Y., and Brady, S.T. (1992) Local modulation of neurofilament phosphorylation, axonal caliber, and slow axonal transport by myelinating Schwann cells. Cell 68: 451-463.

Debus, E., Weber, K., and Osborn, M. (1983) Monoclonal antibodies specific for glial fibrillary acidic (GFA) protein and for each of neurofilament triplet polypeptides. Differentiation 25: 193-203.

Delacourte, A., Filliatreau, G., Boutteau, F., Bisterte, G., and Schrevel, J. (1980) Study of the 10-nm-filament fraction isolated during the standard microtubule preparation. Biochem. J. 191: 543-546.

Dosemeci, A., Floyd, C.C., and Pant, H.C. (1990) Characterization of neurofilament-associated protein kinase activities from bovine spinal cord. Cell. Molec. Neurobiol. 10: 369-381.

Draeger, U. (1983) Coexistance of neurofilaments and vimentin in a neurone of adult mouse retina. Nature 303: 169-172.

Dräger, U.C. and Hofbauer, A. (1984) Antibodies to heavy neurofilament subunit detect a subpopulation of damaged ganglion cells in retina. Nature 309: 624-626.

Durrieu, C., Bernier-Valentin, F., and Rousset, B. (1987) Microtubules bind glyceraldehyde 3-phosphate dehydrogenase and modulate its enzyme activity and quaternary structure. Arch. Biochem. Biophys. 252: 32-40.

Eyer, J. and Leterrier, J.-F. (1988) Influence of the phosphorylation state of neurofilament proteins on the interactions between purified filaments in vitro. Biochem. J. 252: 655-660.

Ferri, G.-L., Sabani, A., Abelli, L., Polak, J.M., Dahl, D., and Portier, M.-M. (1990) Neuronal intermediate filaments in rat dorsal root ganglia: differential distribution of peripherin and neurofilament protein immunoreactivity and effect of capsaicin. Brain Res. 515: 331-335.

Fields, S. and Song, O. (1989) A novel genetic system to detect protein-protein interactions. Nature 340: 245-246.

Fliegner, K.H. and Liem, R.K.H. (1991) Cellular and molecular biology of neuronal intermediate filaments. Int. Rev. Cytol. 131: 109-167.

Floyd, C.C., Grant, P., Gallant, P.E., and Pant, H.C. (1991) Principal neurofilament-associated protein kinase in squid axoplasm is related to casein kinase I. J. Biol. Chem. 266: 4987-4994.

Flynn, G., Joly, J.C., and Purich, D.L. (1987) The 28,000 Mr microtubule-binding domain of microtubule-associated protein-2 also contains a neurofilament -binding site. Biochem. Biophys. Res. Commun. 148: 1453-1459.

Foisner, R., Feldman, B., Sander, L., and Wiche, G. (1991) Monoclonal antibody mapping of structural and functional plectin epitopes. J. Cell Biol. 112: 397-405.

Foisner, R., Leichtfried, F.E., Herrmann, H., Small, J.V., Lawson, D., and Wiche, G. (1988) Cytoskeleton-associated plectin: in situ localization, in vitro reconstruction, and binding to immobilized intermediate filament proteins. J. Cell Biol. 106: 723-733.

Foisner, R. and Wiche, G. (1991) Intermediate filament-associated proteins. Curr. Opinion Cell Bio. 3: 75-81.

Frappier, T., Regnouf, F., and Pradel, L.A. (1987) Binding of brain spectrin to the 70-kDa neurofilament subunit protein. Eur. J. Biochem. 169: 651-657.

Frappier, T., Stetzkowski-Marden, F., and Pradel, L.-A. (1991) Interaction domains of neurofilament light chain and brain spectrin. Biochem. J. 275: 521-527.

Frederiksen, K. and McKay, R.D.G. (1988) Proliferation and differentiation of rat neuroepithelial precursor cells in vivo. J. Neurosci. 8: 1144-1151.

Geisler, N., Kaufmann, E., Fischer, E., Plessmann, U., and Weber, K. (1983) Neurofilament architecture combines structural principles of intermediate filaments with carboxy-terminal extensions of increasing size between triplet proteins. EMBO J. 2: 1295-1302.

Geisler, N., Kaufmann, E., and Weber, K. (1985) Antiparallel orientation of the double-stranded coiled coils in the tetrameric protofilament unit of intermediate filaments. J. Mol. Biol. 182: 173-177.

Geisler, N., Plessmann, U., and Weber, K. (1985) The complete amino acid sequence of the major mammalian neurofilament protein (NF-L). FEBS letters 182: 475-478.

Geisler, N. and Weber, K. (1981) Self-assembly in vitro of the 68,000 molecular weight component of the mammalian neurofilament triplet proteins into intermediate sized filaments. J. Mol. Biol. 151: 565-571.

Gill, S.R., Wong, P.C., Monteiro, M.J., and Cleveland, D.W. (1990) Assembly properties of dominant and recessive mutations in the small mouse neurofilament (NF-L) subunit. J. Cell Biol. 111: 2005-2019.

Gold, B.G., Griffin, J.W., and Price, D.L. (1985) Slow axonal transport in acrylamide neuropathy: different abnormalities produced by single-dose and continuous administration. J. Neurosci. 5: 1755-1768.

Goldman, J.E. and Yen, S.-H. (1986) Cytoskeletal protein abnormalities in neurodegenerative diseases. Ann. Neurol. 19: 209-223.

Goldstein, M.E., Cooper, H.S., Bruce, J., Carden, M.J., Lee, V.M.-Y., and Schlaepfer, W.W. (1987) Phosphorylation of neurofilament proteins and chromatolysis following transection of rat sciatic nerve. J. Neurosci. 7: 1586-1594.

Goldstein, M.E., House, S.B., and Gainer, H. (1991) NF-L and peripherin immunoreactivities define distinct classes of rat sensory ganglion cells. J. Neurosci. Res. 30: 92-104.

Goldstein, M.E., Weiss, S.R., Lazzarini, R.A., Shneidman, P.S., Lees, J.F., and Schlaepfer, W.W. (1988) mRNA levels of all three neurofilament proteins decline following nerve transection. Mol. Brain Res. 3: 287-291.

Gonda, Y., Nishizawa, K., Ando, S., Kitamura, S., Minoura, Y., Nishi, Y., and Inagaki, M. (1990) Involvement of protein kinase C in the regulation of assembly-disassembly of neurofilaments in vitro. Biochem. Biophys. Res. Commun. 167: 1316-1325.

Gorham, J.D., Baker, H., Kegler, D., and Ziff, E.D. (1990) The expression of the neuronal intermediate filament protein peripherin in the rat embryo. Dev. Brain Res. 57: 235-248.

Greene, L.A., Sobeih, M.M., and Teng, K.K. Methodologies for the culture and experimental use of the PC12 rat pheochromocytoma cell line. In: *Culturing nerve cells*, edited by G. Banker and K. Goslin. Cambridge, MA: MIT Press, 1991, p. 207-226.

Griffin, J.W., Hoffman, P.N., Clark, A.W., Carroll, P.T., and Price, D.L. (1978) Slow axonal transport of neruofilament proteins: impairment by β,β'-iminodipropionitrile administration. Science 202: 633-635.

Griffin, J.W. and Watson, D.F. (1988) Axonal transport in neurological disease. Ann. Neurol. 23: 3-13.

Guan, R.J., Hall, F.L., and Cohlberg, J.A. (1992) Proline-directed protein kinase (p34cdc2/p58cyclinA) phosphorylates bovine neurofilaments. J. Neurochem. 58: 1365-1371.

Guarente,L. (1993) Strategies for the identification of interacting proteins. Proc. Natl. Acad. Sci. USA 90: 1639-1641.

Harris, J., Ayyub, C., and Shaw, G. (1991) A molecular dissection of the carboxyterminal tails of the major neurofilament subunits NF-M and NF-H. J. Neurosci. Res. 30: 47-62.

Hathaway, G.M. and Traugh, J.A. (1982) Casein kinase- multipotential protein-kinases. Curr. Top. Cell. Regul. 21: 101-127.

Heimann, R., Shelanski, M.L., and Liem, R.K.H. (1985) Microtubule-associated proteins bind specifically to the 70-kDa neurofilament protein. J. Biol. Chem. 260: 12160-12166.

Herrmann, H. and Wiche, G. (1987) Plectin and IFAP-300K are homologous proteins binding to microtubule-associated proteins 1 and 2 and to the 240-kilodalton subunit of spectrin. J. Biol. Chem. 262: 1320-1325.

Hirano, A. Cytopathology of amyotrophic lateral sclerosis. In: *Amyotrophic lateral sclerosis and other motor neuron diseases*, edited by L. P. Rowland. New York: Raven Press, 1991, p. 91-101.

Hirokawa, N. (1982) The crosslinker system between neurofilaments, microtubules and membranous organelles in frog axons revealed by quick freeze, freeze-fracture, deep-etching method. J. Cell Biol. 94: 129-142.

Hirokawa, N. (1989) The arrangement of actin filaments in the postsynaptic cytoplasm of the cerebellar cortex revealed by quick-freeze deep-etch electron microscopy. Neurosci. Res. 6: 269-275.

Hirokawa, N., Glicksman, M.A., and Willard, M.B. (1984) Organization of mammalian neurofilament polypeptides within the neuronal cytoskeleton. J. Cell Biol. 98: 1523-1536.

Hirokawa, N., Sobue, K., Kanda, K., Harada, A., and Yorifuji, H. (1989) The cytoskeletal architecture of the presynaptic terminal and molecular structure of synapsin I. J. Cell Biol. 108: 111-126.

Hisanaga, S. and Hirokawa, N. (1989) The effects of dephosphorylation on the structure of the projections of neurofilament. J. Neurosci. 9: 959-966.

Hisanaga, S. and Hirokawa, N. (1990a) Dephosphorylation-induced interactions of neurofilaments with microtubules. J. Biol. Chem. 265: 21852-21858.

Hisanaga, S. and Hirokawa, N. (1990b) Molecular architecture of the neurofilament: II. reassembly process of neurofilament L. protein in vitro. J. Mol. Biol. 211: 871-882.

Hisanaga, S., Ikai, A., and Hirokawa, N. (1990) Molecular architecture of the neurofilament: I. Subunit arrangement of neurofilament L protein in the intemediate-sized filament. J. Mol. Biol. 211: 857-869.

Hisanaga, S., Kusubata, M., Okumura, E., and Kishimoto, T. (1991) Phosphorylation of neurofilament H subunit at the tail domain by CDC2 kinase dissociates the association to microtubules. J. Biol. Chem. 266: 21798-21803.

Hisanaga, S.-H. and Hirokawa, N. (1988) Structure of the periperal domains of neurofilaments revealed by low angle rotary shadowing. J. Mol. Biol. 202: 297-305.

Hockfield, S. and McKay, R.D.G. (1985) Identification of major cell classes in the developing mammalian nervous system. J. Neurosci. 5: 3310-3328.

Hoffman, P.N., Cleveland, D.W., Griffin, J.W., Landes, P.W., Cowan, N.J., and Price, D.L. (1987) Neurofilament gene expression: a major determinant of axonal caliber. Proc. Natl. Acad. Sci. USA 84: 3472-3476.

Hoffman, P.N., Griffin, J.W., and Price, D.L. (1984) Control of axonal caliber by neruofilament transport. J. Cell Biol. 99: 705-714.

Hoffman, P.N. and Lasek, R. (1975) The slow component of axonal transport. Identification of major structural polypeptides of the axon and their generality among mammalian neurons. J. Cell Biol. 66: 351-366.

Hoffman, P.N., Thompson, G.W., Griffin, J.W., and Price, D.L. (1985) Changes in neruofilament transport coincide temporally with alterations in the caliber of axons in regenerating motor fibers. J. Cell Biol. 101: 1332-1340.

Huiatt, T.W., Robson, R.M., Arakawa, N., and Stromer, M.H. (1980) Desmin from Avian Smooth Muscle. J. Biol. Chem. 255: 6981-6989.

Huitorel, P. and Pantaloni, D. (1985) Bundling of microtubules by glyceraldehyde-3-phosphate dehydrogenase and its modulation by actin. Eur. J. Biochem. 150: 265-269.

Ip, W. (1988) Modulation of desmin intermediate filament assembly by a monoclonal antibody. J. Cell Biol. 106: 735-745.

Ip, W., Hartzer, M.K., Pang, Y.-Y., and Robson, R.M. (1985) Assembly of vimentin in vitro and its implications concerning the structure of intermediate filaments. J. Mol. Biol. 183: 365-375.

Jönsson, U., Fägerstam, L., Ivarsson, B., Johnsson, B., Karlsson, R., Lundh, K., Löfås, S., Persson, B., Roos, H., Rönnberg, I., Sjökander, S., Stenberg, E., Ståhlberg, R., Urbaniczky, C., Östlin, H., and Malmqvist, M. (1991) Real-time biospecific interaction analysis using surface plasmon resonance and a sensor chip technology. BioTechniques 11: 620-627.

Julien, J.-P. and Mushynski, W.E. (1981) A comparison of in vitro- and in vivo-phosphorylated neurofilament polypeptides. J. Neurochem. 37: 1579-1585.

Julien, J.-P. and Mushynski, W.E. (1982) Multiple phosphorylation sites in mammalian neurofilament polypeptides. J. Biol. Chem. 257: 10467-10470.

Julien, J.-P. and Mushynski, W.E. (1983) The distribution of phosphorylation sites among identified proteolytic fragments of mammalian neurofilaments. J. Biol. Chem. 258: 4019-4025.

Kaelin, W.G., Pallas, D.C., DeCaprio, J.A., Kaye, F.J., and Livingston, D.M. (1991) Cell 64: 521-532.

Kaplan, M.P., Chin, S.S.M., Fliegner, K.H., and Liem, R.K.H. (1990) α-Internexin, a novel neuronal intermediate filament protein, precedes the low molecular weight neurofilament protein (NF-L) in the developing rat brain. J. Neurosci. 10: 2735-2748.

Kellogg, D.R., Field, C.M., and Alberts, B.M. (1989) Identification of microtubule-associated proteins in the centrosome, spindle, and kenetochore of the early dosophila enbryo. J. Cell Biol. 109: 2977-2991.

Kilhoffer, M.-C., Haiech, J., and Demaille, J.G. (1983) Ion binding to calmodulin. Mol. Cell. Biochem. 51: 33-54.

Knull, H.R. (1978) Associations of glycolytic enzymes with particulate fractions from nerve endings. Biochim. Biophys. Acta 522: 1-9.

Knull, H.R. (1980) Compartmentation of glycolytic enzymes in nerve ending as determined by glutaraldehyde fixation. J. Biol. Chem. 255: 6439-6444.

Koerner, T.J., Hill, J.E., Myers, A.M., and Tzagoloff, A. (1991) High-expression vectors with multiple cloning sites for construction of trpE fusion genes: pATH vectors. Mets. Enzymol. 194: 477-490.

Koszka, C., Leichtfried, F.E., and Wiche, G. (1985) Identification and spatial arrangement of high molecular weight proteins (M_r 300,000-330,000) co-assembly with microtubules from a cultured cell line (rat glioma C6). Eur. J. Cell Biol. 38: 149-156.

Kreutzberg, G.W., Graeber, M.B., Raivich, G., and Streit, W.J. Neuron-glial relationship suring regeneration of motoneurons. In: *Regulation of Gene Expression in the Nervous System*, New York: Wiley-Liss, Inc., 1990, p. 333-341.

Laemmli, U.K. (1970) Cleavage of structural proteins during the assembly of the head of bacteriophage T4. Nature 227: 680-685.

Lee, V.M.-Y., Otvos, L.,Jr., Carden, M.J., Hollosi, M., Dietzschold, B., and Lazzarini, R.A. (1988) Identification of the major multiphosphorylation site in mammalian neurofilaments. Proc. Natl. Acad. Sci. USA 85: 1998-2002.

Lefebvre, S. and Mushynski, W.E. (1988) Characterization of the cation-binding properties of porcine neurofilaments. Biochem. 27: 8503-8508.

Lehninger, A.L. Glycolysis: a central pathway of glucose catabolism. In: *Principles of Biochemistry*, New York: Worth Publishers, Inc., 1982, p. 397-434.

Lendahl, U., Zimmerman, L.B., and McKay, R.D.G. (1990) CNS stem cells express a new class of intermediate filament protein. Cell 60: 585-595.

Leterrier, J.F. and Eyer, J. (1987) Properties of highly viscous gels formed by neurofilaments in vitro. A possible consequence of a specific inter-filament cross-bridging. Biochem. J. 245: 93-101.

Leterrier, J.F., Liem, R.K.H., and Shelanski, M.L. (1982) Interactions between neurofilaments and microtubule-associated proteins: a possible mechanism for intraorganellar bridging. J. Cell Biol. 95: 982-986.

Levine, J. and Willard, M. (1981) Fodrin: axonally transported polypeptides associated with the internal periphery of many cells. J. Cell Biol. 90: 631-643.

Lew, J., Beaudette, K., Litwin, C.M., and Wang, J.H. (1992a) Purification and characterization of a novel proline-directed protein kinase from bovine brain. J. Biol. Chem. 267: 13383-13390.

Lew, J., Winkfein, R.J., Paudel, H.K., and Wang, J.H. (1992b) Brain proline-directed protein kinase is a neurofilament kinase which displays high sequence homology to p34cdc2. J. Biol. Chem. 267: 25922-25926.

Liem, R.K.H. and Hutchinson, S.B. (1982) Purification of individual components of the neurofilament triplet: Filament assembly from the 70,000-Dalton subunit. Biochem. 21: 3221-3226.

Liem, R.K.H., Solomon, G.D., and Shelanski, M.L. (1978) Intermediate filaments in nervous tissue. J. Cell Biol. 79: 637-645.

Lieska, N., Yang, H.-Y., and Goldman, D. (1985) Purification of the 300K intermediate filament-associated protein and its in vitro recombination with intermediate filaments. J. Cell Biol. 101: 802-813.

Llinas, R.T., McGuinness, T.L., Leonard, C.S., Sugimori, M., and Greengard, P. (1985) Intraterminal injection of synapsin I or calcium/calmodulin dependent protein kinase II alters neurotransmitter release at the squid giant synapse. Proc. Natl. Acad. Sci. USA 82: 3035-3039.

Lowry, O.H., Rosebrough, N.J., Farr, A.L., and Randall, R.J. (1951) Protein measurement with the folin phenol reagent. J. Biol. Chem. 193: 265-275.

Martenson, R.E., Deibler, G.E., and Kramer, A.J. (1977) Reaction of peptide 89-169 of bovine myelin basic protein with 2-(2-nitrophenylsulfenyl)-3-methyl -3'-bromoindolenine. Biochem. 16: 216-221.

Master, C.J. (1981) Interactions between soluble enzymes and subcellular structures. CRC Crit. Rev. Biochem. 11: 105-143.

Merdes, A., Brunkener, M., Horstmann, H., and Georgatos, S.D. (1991) Filensin: a new vimentin-binding, polymerization-competant, and membrane-associated protein of the lens fiber cell. J. Cell Biol. 115: 397-410.

Miller, K.G., Field, C.M., and Alberts, B.M. (1989) Actin-binding proteins from drosophila embryos: a complex network of interacting proteins detected by F-actin affinity chromatography. J. Cell Biol. 109: 2963-2975.

Minami, Y., Murofushi, H., and Sakai, H. (1982) Interaction of tubulin with neurofilaments: formation of networks by neurofilament-dependent tubulin polymerization. J. Biochem. 92: 889-898.

Minami, Y. and Sakai, H. (1983) Network formation by neurofilament-induced polymerization of tubulin: 200K subunit of neurofilament triplet promotes nucleation of tubulin polymerization and enhances microtubule assembly. J. Biochem. 94: 2023-2033.

Miyata, Y., Hoshi, M., Nishida, E., Minami, Y., and Sakai, H. (1986) Binding of microtubule-associated protein 2 and tau to the intermediate filament reassembled from the neurofilament 70-kDa subunit protein. J. Biol. Chem. 261: 13026-13030.

Monaco, S., Autilio-Gambetti, L., Zabel, D., and Gambetti, P. (1985) Giant axonal neuropathy: acceleration of neurofilament transport in optic axons. Proc. Natl. Acad. Sci. USA 82: 920-924.

Monaco, S., Jacob, J., Jenich, H., Patton, A., Autilio-Gambetti, L., and Gambetti, P. (1989) Axonal transport of neurofilament is accelerated in peripheral nerve during 2,5-hexanedione intoxication. Brain Res. 491: 328-334.

Morgenegg, G., Winkler, G.C., Hübscher, U., Heizmann, C.W., Mous, J., and Kuenzle, C.C. (1986) Glyceraldehyde-3-phosphate dehydrogenase is a nonhistone protein and a possible activator of transcription in neurons. J. Neurochem. 47: 54-62.

Mulligan, L., Balin, B.J., Lee, V.M.-Y., and Ip, W. (1991) Antibody labeling of bovine neurofilaments: implications on the structure of neurofilament sidearms. J. Struct. Biol. 106: 145-160.

Nakamura, Y., Takeda, M., Angelides, K.J., Tanaka, T., Tada, K., and Nishimura, T. (1990) Effect of phosphorylation on 68 KDa neurofilament subunit protein assembly by the cyclic AMP dependent protein kinase in vitro. Biochem. Biophys. Res. Commun. 169: 744-750.

Nixon, R.A. and Lewis, S.E. (1986) Differential turnover of phosphate groups on neurofilament subunits in mammalian neurons in vivo. J. Biol. Chem. 261: 16298-16301.

Nixon, R.A. and Logvinenko, K.B. (1986) Multiple fates of newly synthesized neurofilament proteins: evidence for a stationary neurofilament network distributed nonuniformly along axons of retinal ganglion cell neurons. J. Cell Biol. 102: 647-659.

Nixon, R.A. and Sihag, R.K. (1991) Neurofilament phosphorylation: a new look at regulation and function. TINS 14: 501-506.

Oblinger, M.M. and Lasek, R.J. (1988) Axotomy-induced alterations in the synthesis and transport of neurofilaments and microtubules in the dorsal root ganglion cells. J. Neurosci. 8: 1747-1758.

Oblinger, M.M., Wong, J., and Parysek, L.M. (1989) Axotomy-induced changes in the expression of a type III neuronal intermediate filament gene. J. Neurosci. 9: 3766-3775.

Opperdoes, F.R. (1988) Glycosomes may provide clues to the import of peroxisomal proteins. TIBS 13: 255-260.

Osborn, M.O., Debus, E., and Weber, K. (1984) Monoclonal antibodies to vimentin: immunological recognition of only a single intermediate filament protein. Eur. J. Cell Biol. 34: 137-143.

Pachter, J.S. and Liem, R.K.H. (1985) α-Internexin, a 66-kD intermediate filament-binding protein from mammalian central nervous tissues. J. Cell Biol. 101: 1316-1322.

Palay, S.L. and Chan-Palay, V. The neuroglial cells of the cerebellar cortex. In: *Cerebellar cortex cytology and organization*, edited by S. L. Palay and V. Chan-Palay. New York: Springer-Verlag, 1974, p. 288-321.

Pallen, C.J. and Wang, J.H. (1983) Calmodulin-stimulated dephosphorylation of p-nitrophenyl phosphate and free phosphotyrosine by calcineurin. J. Biol. Chem. 258: 8550-8553.

Papasozomenos, S.C., Binder, L.I., Bender, P.K., and Payne, M.R. (1985) Microtubule-associated protein 2 within axons of spinal motor neurons: associations with microtubules and neurofilaments in normal and β,β'-iminodipropionitrile-treated axons. J. Cell Biol. 100: 74-85.

Parry, D.A. (1982) Coiled-coils in alpha-helix-containing proteins: analysis of the residue types within the heptad repeat and the use of these data in the prediction of coiled-coils in other proteins. Biosci-Rep. 2: 1017-1024.

Parysek, L.M. and Goldman, R.D. (1988) Distribution of a novel 57 kDa intermediate filament (IF) protein in the nervous system. J. Neurosci. 8: 555-563.

Parysek, L.M., McReynolds, M.A., Goldman, R.D., and Ley, C.A. (1991) Some neural intermediate filaments contain both peripherin and the neurofilament proteins. J. Neurosci. Res. 30: 80-91.

Peters, A. , Palay, S. L. , and Webster, H. deF. *The Fine Structure of the Nervous System*. New York: Oxford University Press, 1991.

Pixley, S.R., Kobayashi, Y., and de Vellis, J. (1981) A monoclonal antibody against vimentin: characterization. Dev. Brain Res. 15: 185-199.

Portier, M.M., Brachet, P., Croizat, B., and Gros, F. (1984a) Regulation of peripherin in mouse neuroblastoma and rat PC12 pheochromocytoma cell lines. Dev. Neurosci. 6: 215-226.

Portier, M.M., Nechaud, B., and Gros, F. (1984b) Periperin, a new member of the intermediate filament protein family. Dev. Neurosci. 6: 335-344.

Price, R.L., Paggi, P., Lasek, R.J., and Katz, M.J. (1988) Neurofilaments are spaced randomly in the radial dimension of axons. J. Neurocytol. 17: 55-62.

Pruss, R.M., Mirsky, R., and Raff, M.C. (1981) All classes of intermediate filaments share a common antigenic determinant defined by a monoclonal antibody. Cell 27: 419-428.

Pytela, R. and Wiche, G. (1980) High molecular weight polypeptides (270,000-340,000) from cultured cells are related to hog brain microtublue-associated proteins but copurify with intermediate filaments. Proc. Natl. Acad. Sci. USA 77: 4808-4812.

Reid, S. and Masters, C. (1986) On the ontogeny and interactions of glyceraldehyde-3-phosphate dehydrogenase. Mech. Ageing Dev. 35: 209-219.

Rice, R.V., Roslansky, P.F., Pascoe, N., and Houghton, S.M. (1980) Bridges between microtubles and neurofilaments visualized by stereoelectron microscopy. J. Ultrastruct. Res. 71: 303-310.

Saier, M.H.,Jr., Wu, L.-F., and Reizer, J. (1990) Regulation of bacterial physiological processes by three types of protein phosphorylating systems. TIBS 15: 391-395.

Scharp, G.A., Shaw, G., and Weber, K. (1982) Immunoelectron microscopical localization of the three neurofilament triplet proteins along neurofilaments of cultured dorsal root ganglion neurons. Exp. Cell Res. 137: 403-413.

Schlaepfer, W.W. (1985) An immunoblot study of neurofilament degradation in situ and during calcium-activated proteolysis. J. Neurochem. 44: 502-509.

Schlaepfer, W.W. (1987) Neurofilaments: structure, metabolism and implications in disease. J. Neuropathol. Exp. Neurol. 46: 117-129.

Schwob, J.E., Farber, N.B., and Gottlieb, D.I. (1986) Neurons of the olfactory epithelium in adult rats contain vimentin. J. Neurosci. 6: 208-217.

Semple-Rowland, S.L. (1989) Two-dimensional gel electrophoresis analysis of proteins in the rd chick retina. Prog. Clin. Biol. Res. 314: 455-465.

Shaw, G. (1989) Identification of previously unrecognized sequence motifs at the extreme carboxyterminus of the neurofilament subunit NF-M. Biochem. Biophys. Res. Commun. 162: 294-299.

Shaw, G. Neurofilament proteins. In: *The neuronal cytoskeleton*, edited by R. D. Burgoyne. New York: Wiley-Liss, Inc., 1991, p. 185-214.

Shaw, G. (1992) Convenient methods for display, comparison and interpretation of amino acid composition data. Biotechniques 12: 886-891.

Shaw, G. (1993) Rapid indentification of blotted proteins. Proc. Natl. Acad. Sci. USA 90: 5138-5142.

Shaw, G. and Hou, Z.-C. (1990) Bundling and cross-linking of intermediate filaments of the nervous system. J. Neurosci. Res. 25: 561-568.

Shaw, G., Osborn, M.O., and Weber, K. (1981) An immunofluorescence microscopical study of the distribution of the neurofilament triplet proteins, vimentin and glial fibrillary acidic protein in the adult rat brain. Eur. J. Cell Biol. 26: 68-82.

Shaw, G. and Weber, K. (1981) The distribution of the neurofilament triplet proteins within individual neurons. Exp. Cell Res. 136: 119-125.

Shaw, G., Winialski, D., and Reier, P. (1988) The effect of axotomy and deafferentation on phosphorylation dependent antigenicity of neurofilaments in rat superior cervical ganglion neurons. Brain Res. 460: 227-234.

Shelanski, M.L., Albert, S., Devries, G.H., and Norton, W.T. (1971) Isolation of filaments from brain. Science 174: 1242-1245.

Sihag, R.K., Jeng, A.Y., and Nixon, R.A. (1988) Phosphorylation of neurofilament proteins by protein kinase C. FEBS letters 233: 181-185.

Sihag, R.K. and Nixon, R.A. (1989) In vivo phosphorylation of distinct domains of the 70-kilodalton neurofilament subunit involves different protein kinases. J. Biol. Chem. 264: 457-464.

Slagboom, P.E., de Leeuw, W.J.F., and Vijg, J. (1990) Messenger RNA levels and methylation patterns of GAPDH and β-actin genes in rat liver, spleen and brain in relation to aging. Mech. Ageing Dev. 53: 243-257.

Sokolov, B.P., Sher, B.M., and Kalinin, V.N. (1989) Modified method for peptide mapping of collagen chains using cyanogen bromide-cleavage of protein within polyacrylamide gels. Anal. Biochem. 176: 365-367.

Somers, M., Engelborghs, Y., and Baert, J. (1990) Analysis of the binding of glyceraldehyde-3-phosphate dehydrogenase to microtubules, the mechanism of bundle formation and the linkage effect. Eur. J. Biochem. 193: 437-444.

Steiner, J.P., Ling, E., and Bennett, V. (1987) Neariest neighbor analysis for brain synapsin I. J. Biol. Chem. 262: 905-914.

Steinert, P.M. and Liem, R.K.H. (1990) Intermediate filament dynamics. Cell 60: 521-523.

Steinert, P.M. and Roop, D.R. (1988) Molecular and cellular biology of intermediate filaments. Ann. Rev. Biochem. 57: 593-625.

Sternberger, L.A. and Sternberger, N.H. (1983) Monoclonal antibodies distinguish phosphorylated and nonphosphorylated forms of neurofilaments in situ. Proc. Natl. Acad. Sci. USA 80: 6126-6130.

Stewart, M., Quinlan, R.A., and Moir, R.D. (1989) Molecular interactions in paracrystals of a fragment corresponding to the α-helical coiled-coil rod portion of glial fibrillary acidic protein: evidence for an antiparallel packing of molecules and polymorphism related to intermediate filament structure. J. Cell Biol. 109: 225-234.

Szaro, B.G., Grant, P., Lee, V.M.-Y., and Gainer, H. (1991) Inhibition of axonal development after injection of neurofilament antibodies into a Xenopus laevis embryo. J. Comp. Neurol. 308: 576-585.

Szaro, B.G., Whitnall, M.H., and Gainer, H. (1990) Phosphorylation-dependent epitopes on neurofilament proteins and neurofilament densities differ in axons in the corticospinal and primary sensory dorsal column tracts in the rat spinal cord. J. Comp. Neurol. 302: 220-235.

Tanaka, E., Miyamoto, E., Tashiro, T., Komiya, Y., and Kurokawa, M. (1984) Ca2+-calmodulin-dependent and cyclic AMP-dependent phosphorylation of neurofilaments and glial fibrillary acidic protein. Biomed. Res. 5: 239-244.

Tetzlaff, W., Bisby, M.A., and Kreutzberg, G.W. (1988) Changes in cytoskeletal proteins in the rat facial nucleus following axotomy. J. Neurosci. 8: 3181-3189.

Tokutake, S. (1984) Complete separation of the triplet components of neurofilament by DE-52 column chromatography depends on urea concentration. Anal. Biochem. 140: 203-207.

Toru-Delbauffe, D. and Pierre, M. (1983) A rat brain kinase phosphorylation specifically neurofilaments. FEBS letters 162: 230-234.

Toru-Delbauffe, D., Pierre, M., Osty, J., Chantoux, F., and Francon, J. (1986) Properties of neurofilament protein kinase. Biochem. J. 235: 283-289.

Traub, P. *Intermediate filaments: a review.* Germany : Springer-Verlag, 1985.

Troy, C.M., Muma, N.A., Greene, L.A., Price, D.L., and Shelanski, M.L. (1990) Regulation of peripherin and neurofilament expression in regenerating rat motor neurons. Brain Res. 529: 232-238.

Vallano, M.L., Buckolz, T.M., and DeLorenzo, R.J. (1985) Phosphorylation of neurofilament proteins by endogenous calcium/calmodulin-dependent protein kinase. Biochem. Biophys. Res. Commun. 130: 957-963.

Wible, B.A., Smith, K.E., and Angelides, K.J. (1989) Resolution and purification of a neurofilament-specific kinase. Proc. Natl. Acad. Sci. USA 86: 720-724.

Wiche, G. (1989) Plectin: general overview and appraisal of its potential role as a subunit protein of the cytomatrix. Crit. Rev. Biochem. Mol. Biol. 24: 41-67.

Wiche, G. and Baker, M.A. (1982) Cytoplasmic network arrays demonstrated by immunolocalization using antibodies to a high molecular weight protein present in cytoskeletal preparations from cultured cells. Exp. Cell Res. 138: 15-29.

Wiche, G., Becker, B., Luber, K., Weitzer, G., Castañon, M.J., Hauptmann, R., Stratowa, C., and Stewart, M. (1991) Cloning and sequencing of rat plectin indicates a 466-kD polypeptide chain with a three-domain structure based on a central alpha-helical coiled coil. J. Cell Biol. 114: 83-99.

Wiche, G., Krepler, R., Artlieb, U., Pytela, R., and Denk, H. (1983) Occurrence and immunolocalization of plectin in tissues. J. Cell Biol. 97: 887-901.

Wiche, G., Krepler, R., Artlieb, U., Pytela, R., and Aberer, W. (1984) Identification of plectin in different human cell types and immunolocalization at epithelial basa cell surface membranes. Exp. Cell Res. 155: 43-49.

Willard, M. and Simon, C. (1981) Antibody decoration of neurofilaments. J. Cell Biol. 89: 198-205.

Willard, M. and Simon, C. (1983) Modulations of neurofilament axonal transport during the development of rabbit retinal ganglion cells. Cell 35: 551-559.

Wong, J. and Oblinger, M.M. (1987) Changes in neurofilament gene expression occur after axotomy of dorsal root ganglion neurons: an in situ hybridization study. Metab. Brain Dis. 2: 291-303.

Wong, P.C. and Cleveland, D.W. (1990) Characterization of dominant and recessive assembly-defective mutations in mouse neurofilament NF-M. J. Cell Biol. 111: 1987-2003.

Wuerker, R.B. and Palay, S.L. (1969) Neurofilaments and microtubules in anterior horn cells of the rat. Tissue Cell 1: 387-402.

Xu, Z., Cork, L.C., Griffin, J.W., and Cleveland, D.W. (1993) Increased expression of neurofilament subunit NF-L produces morphological alterations that resemble the pathology of human motor neuron disease. Cell 73: 23-33.

Xu, Z.-S., Cheney, R., and Willard, M. (1989) Identification of six phosphorylation sites on the neurofilament polypeptide NF-M. J. Cell Biol. 109: 70a, #383.(Abstract)

Xu, Z.-S., Liu, W.S., and Willard, M. (1990) Identification of serine 473 as a major phosphorylation site in the neurofilament polypeptide NF-L. J. Neurosci. 10: 1838-1846.

Yen, S.-H. and Fields, K.L. (1981) Antibodies to neurofilament, glial filament, and fibroblast intermediate filament proteins bind to different cell types of the nervous system. J. Cell Biol. 88: 115-126.

BIOGRAPHICAL SKETCH

Laura Diane Errante was born on April 9, 1965, in Binghamton, New York. Being the youngest of 6 children, she was eager to go to school like her older brothers and sister and was always fascinated with nature and science. She entered SUNY Plattsburgh as a biochemistry major in 1982 and by the end of her freshman year, she knew that she wanted to attend graduate school, and thus began a research project with Dr. Roger Heintz which lasted until she graduated in 1986. Here she learned that although research can be difficult at times, it was always fascinating. Her interest in neuroscience was cultivated in an independent reading project in neuroscience with Dr. Henry Morlock, and after an attempt at sheep brain dissection (or mutilation?) under his guidance, Laura became intrigued with how the brain worked. After a stint as a lab technician determining amino acid composition of soil samples from Back Bay in Virginia, she entered the Neuroscience Department at the University of Florida College of Medicine in 1987. Determined to choose the best possible lab based on sound advice, she made that critical decision based on a short film on growth cone motility. Thus she entered the laboratory of Dr. Gerry Shaw. Although her research she conducted in his lab went in a different direction, she learned valuable techniques and knowledge which she will use during her postdoc on cellular mechanisms of neuronal growth cones.

I certify that I have read this study and that in my opinion it conforms to acceptable standards of scholarly presentation and is fully adequate, in scope and quality, as a dissertation for the degree of Doctor of Philosophy.

Gerard P. J. Shaw, Chairperson
Associate Professor of Neuroscience

I certify that I have read this study and that in my opinion it conforms to acceptable standards of scholarly presentation and is fully adequate, in scope and quality, as a dissertation for the degree of Doctor of Philosophy.

B-A. Battelle

Barbara-A. Battelle
Associate Professor of Neuroscience

I certify that I have read this study and that in my opinion it conforms to acceptable standards of scholarly presentation and is fully adequate, in scope and quality, as a dissertation for the degree of Doctor of Philosophy.

Kevin J. Anderson
Associate Professor of Neuroscience

I certify that I have read this study and that in my opinion it conforms to acceptable standards of scholarly presentation and is fully adequate, in scope and quality, as a dissertation for the degree of Doctor of Philosophy.

Daniel L Purich

Daniel L. Purich
Professor of Biochemistry and
Molecular Biology

This dissertation was submitted to the Graduate Faculty of the College of Medicine and to the Graduate School and was accepted as partial fulfillment of the requirements for the degree of Doctor of Philosophy.

April 1994

Mohan K Raizada

Dean, College of Medicine

Karen G. Holbrook

Dean, Graduate School

UNIVERSITY OF FLORIDA
3 1262 08554 3196